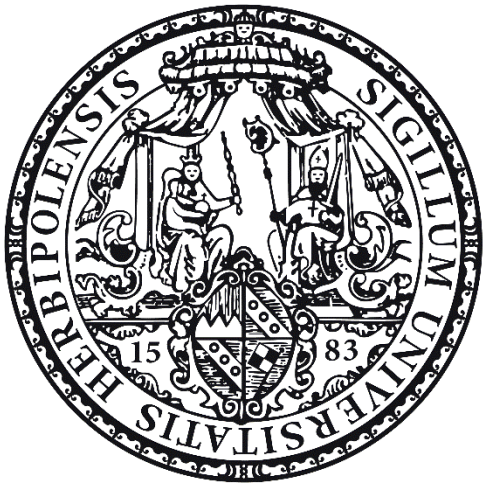

Exploration of proteasome interactions with human platelet function

Untersuchung von Proteasom-Wechselwirkungen mit der Funktion humaner Thrombozyten

Doctoral thesis for a doctoral degree
at the Graduate School of Life Sciences,
Julius-Maximilians-Universität Würzburg,
Section Biomedicine

submitted by

Philipp Klingler

from Bad Mergentheim, Germany

Würzburg, 2022

Submitted on: _____

Office stamp

Members of the Thesis Committee:

Chairperson:	Prof. Dr. Jürgen Seibel
Primary Supervisor:	Dr. Anna Kobsar
Supervisor (Second):	Prof. Dr. Alexander Buchberger
Supervisor (Third):	PD Dr. med. Jürgen Kößler
Supervisor (Fourth):	Dr. Ingolf Berberich

Date of Public Defense: _____

Date of Receipt of Certificates: _____

This thesis was drawn up at the Institute of Clinical Transfusion Medicine and Haemotherapy of the University Hospital of Würzburg in the period from August 2018 to April 2022.

It was drafted under the direction of Prof. Dr. Markus Böck and under supervision of Dr. Anna Kobsar and PD Dr. Jürgen Kößler using parts and excerpts from the following published article:

Klingler, P., Niklaus, M., Koessler, J.*, Weber, K., Koessler, A., Boeck, M., Kobsar, A. Influence of long-term proteasome inhibition on platelet responsiveness mediated by bortezomib. *Vascular Pharmacology.* **2021**, 138, 106830.

ScienceDirect-Link for the Published Journal Article (PJA):
https://www.sciencedirect.com/science/article/abs/pii/S1537189121000021?dgcid=rss_sd_all

The corresponding author is marked with *

For my wife, my daughter and my parents.

Table of contents

Summary

Platelets are anucleated cell fragments derived from megakaryocytes. They play a fundamental role in hemostasis, but there is rising evidence that they are also involved in immunological processes. Despite absence of a nucleus, human platelets are capable of *de novo* protein synthesis and contain a fully functional proteasome system, which is, in nucleated cells, involved in processes like cell cycle progression or apoptosis by its ability of protein degradation. The physiological significance of the proteasome system in human platelets is not yet fully understood and subject of ongoing research.

Therefore, this study was conducted with the intention to outline the role of the proteasome system for functional characteristics of human platelets. For experimentation, citrated whole blood from healthy donors was obtained and preincubated with proteasome inhibitors. In addition to the commonly used bortezomib, the potent and selective proteasome inhibitor carfilzomib was selected as a second inhibitor to rule out agent-specific effects and to confirm that observed changes are related to proteasome inhibition.

Irreversibly induced platelet activation and aggregation were not affected by proteasome blockade with bortezomib up to 24 hours. Conversely, proteasome inhibition led to enhanced threshold aggregation and agglutination up to 25 %, accompanied by partial alleviation of induced VASP phosphorylation of approximately 10-15 %. Expression of different receptors were almost unaffected. Instead, a significant increase of PP2A activity was observable in platelets after proteasome blockade, accompanied by facilitated platelet adhesion to coated surfaces in static experiments or flow chamber experiments.

Carfilzomib, used for the first time in functional experimentation with human platelets *in vitro,* led to a dose-dependent decrease of proteasome activity with accumulation of poly-ubiquitylated proteins. Like bortezomib, carfilzomib treatment resulted in enhanced threshold aggregation with attenuated VASP phosphorylation.

As the main conclusion of this thesis, proteasome inhibition enhances the responsiveness of human platelets, provided by an alleviation of platelet inhibitory pathways and by an additional increase of PP2A activity, resulting in facilitated platelet adhesion under static and flow conditions. The proteasome system appears to be involved in the promotion of inhibitory counterregulation in platelets. The potential of proteasome inhibitors for triggering thromboembolic adverse events in patients must be clarified in further studies, in addition to their possible use for targeting platelet function to improve the hemostatic reactivity of platelets.

Zusammenfassung

Thrombozyten sind kernlose Zellfragmente, welche aus Megakaryozyten gebildet werden. Sie spielen eine fundamentale Rolle in der Hämostase, aber es gibt immer mehr Hinweise, dass Thrombozyten auch in immunologischen Prozessen involviert sind. Trotz Fehlen eines Zellkerns haben humane Thrombozyten die Fähigkeit zur *de novo*-Proteinsynthese und besitzen außerdem ein voll funktionstüchtiges Proteasomsystem, welches in kernhaltigen Zellen über den Proteinabbau an Prozessen wie dem Fortschreiten des Zellzyklus oder der Apoptose beteiligt ist. Die physiologische Bedeutung des Proteasomsystems in humanen Thrombozyten ist nicht vollständig geklärt und ist aus diesem Grund Gegenstand aktueller Forschung.

Daher war es Ziel dieser Studie, die Rolle des Proteasomsystems für die funktionellen Eigenschaften humaner Thrombozyten zu erforschen. Für die Experimente wurde Citrat-Vollblut von gesunden Spendern gewonnen und mit Proteasom-Hemmstoffen vorinkubiert. Es wurde neben dem gängigen Bortezomib der potente und selektive Proteasom-Inhibitor Carfilzomib als zweiter Inhibitor eingesetzt, um substanzspezifische Effekte auszuschließen und zu bestätigen, dass die beobachteten Veränderungen auf der Proteasom-Inhibition beruhen.

Die irreversibel induzierte Thrombozytenaktivierung und -aggregation wurde durch die Hemmung des Proteasoms mit Bortezomib bis zu 24 Stunden nicht beeinflusst. Allerdings führte die Proteasom-Hemmung zu einer verstärkten Schwellenwertaggregation und -agglutination um bis zu 25 % sowie zu einer partiellen Abschwächung der induzierten VASP-Phosphorylierung um etwa 10-15 %. Die Expression verschiedener Rezeptoren blieb nahezu unbeeinflusst. Stattdessen konnte unter Proteasom-Inhibition eine erhöhte Enzymaktivität der PP2A beobachtet werden, begleitet von einer erleichterten Thrombozytenadhäsion an beschichteten Oberflächen bei statischen Versuchen ober bei Flusskammerversuchen.

Carfilzomib, welches erstmals für funktionelle Experimente mit menschlichen Thrombozyten *in vitro* eingesetzt wurde, führte zu einer dosisabhängigen Abnahme der Proteasom-Aktivität mit einer Akkumulation von poly-ubiquitylierten Proteinen. Wie Bortezomib mündete die Behandlung mit Carfilzomib in einer verstärkten Schwellenwertaggregation und abgeschwächter VASP-Phosphorylierung.

Die wichtigste Schlussfolgerung dieser Arbeit ist, dass die Inhibition des Proteasoms die Reaktivität humaner Thrombozyten erhöht, gekennzeichnet durch eine Abschwächung der hemmenden Signalwege der Thrombozyten und durch eine zusätzliche Erhöhung der PP2A-Enzymaktivität, was zu einer erleichterten Thrombozytenadhäsion unter statischen Verhältnissen und unter Flussbedingungen

führt. Das Proteasomsystem scheint an der Förderung der hemmenden Gegenregulation in Thrombozyten beteiligt zu sein. Das Potenzial von Proteasom-Inhibitoren, thromboembolische Nebenwirkungen bei Patienten auszulösen, muss in weiteren Studien geklärt werden, ebenso wie ihr möglicher Einsatz für die gezielte Beeinflussung der Thrombozytenfunktion zur Verbesserung der hämostatischen Reaktivität der Thrombozyten.

1. Introduction

1.1. Platelet physiology

Human platelets are small non-nucleated cells of the human blood system in addition to leukocytes and erythrocytes. They were first described by Schultze in 1865 [1], but their most prominent role as important mediators in maintaining hemostasis was not known until Bizzozero's investigations [2]. They are discoid shaped cells with a diameter of 2 to 4 µm in their resting, non-activated conformation, therefore being the smallest blood cells. Ranges from 150,000 to 400,000 platelets per µL of whole blood are defined as normal human platelet count [3]. They bear a relatively short life span of approximately up to 8 to 9 days in circulation [4]. To maintain sufficient platelet count, there is a platelet turnover of around 1×10^{11} platelets per day under steady-state conditions [5]. They get cleared via various mechanisms, by hepatocytes recognizing a change in glycoconjugates [6], via phagocytosis by macrophages [7] or as well by induction of apoptosis [8]. As mentioned, platelets play a major role in hemostasis, since they are responsible for the occlusion of vessel wall injuries to prevent blood loss by thrombus formation and initiation of wound healing. This is achieved by several consecutive mechanisms under physiological conditions, including platelet tethering, attachment and adhesion to the endothelial lesion [9], platelet activation, shape change, granule secretion, spreading and culminates in platelet aggregation to form a stable thrombus [10, 11]. The morphologic changes of a single platelet during activation are shown in **Figure 1.1**. Finally, platelets are also considered to be involved in inflammation and immunological processes of the innate immune system [12-15].

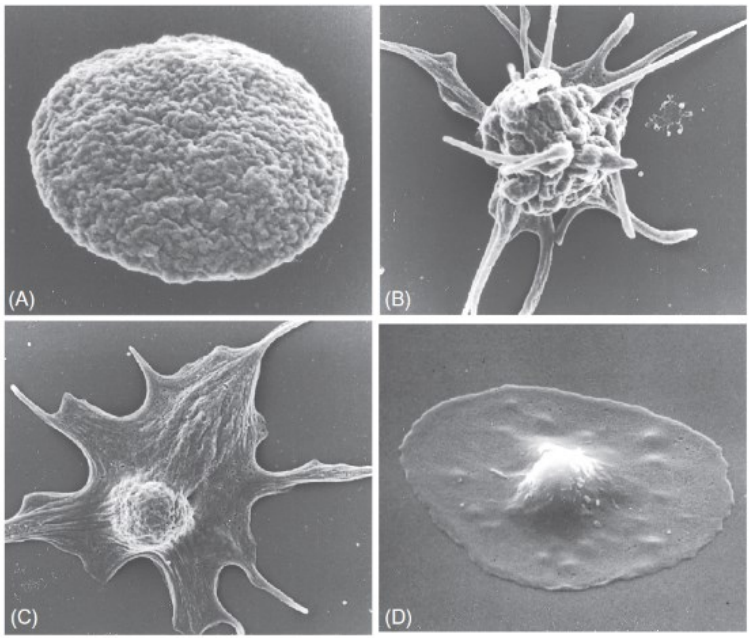

Figure 1.1: Morphology of resting and activated platelets.

(**A**) Resting platelet with typical discoid shape in x30,000 magnification. (**B**) Platelet developing filopodia during early stage of activation and spreading (x13,000 magnification). (**C**) Activated platelet spreading with formation of lamellipodia (x11,000 magnification). (**D**) Platelet in fully spread conformation (x9,000 magnification). From Thomas [16].

1.1.1. Platelet production

In 1906, Wright discovered that platelets originate from megakaryocytes (MKs) in the bone marrow [17]. Meanwhile, it has become evident that platelets can also be produced in MKs residing in the lung [18]. MKs develop from hematopoietic stem cells particularly under the influence of the hormone thrombopoietin in a process called megakaryopoiesis [19, 20]. During differentiation and proliferation into MKs, the hematopoietic stem cells undergo several developmental steps, namely common myeloid progenitor, megakaryocyte-erythroid progenitor, megakaryocyte progenitor, promegakaryoblast, megakaryoblast, promegakaryocyte and finally megakaryocyte [21-23]. While MK maturation, they undergo polyploidization and expand their cytoplasmic mass [24]. Furthermore, they produce plethora of proteins and molecules and prepare their cytoplasm and membrane systems for platelet biogenesis [25, 26], thereby reaching sizes from 50 to 120 µm in diameter accompanied by ploidy up top 128 N [27]. Proplatelets then get extended into sinusoidal vessels as protrusions from the MKs as depicted in **Figure 1.2** [28]. Shear flow finally leads to budding of platelets into the blood circulation. In this process,

2,000-5,000 platelets can be released from a single MK [29]. Thus, platelets are considered to be cell fragments and inherit their major receptors from the MKs [30, 31].

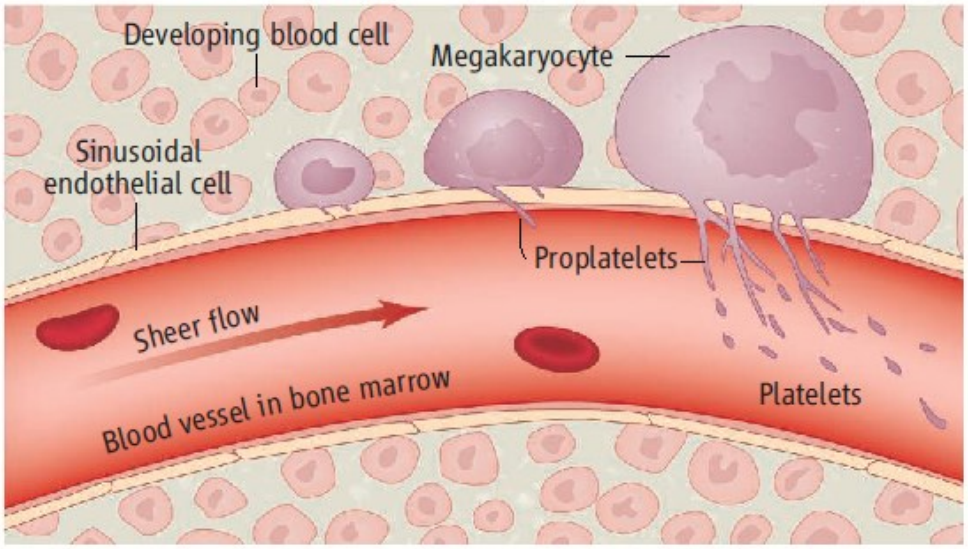

Figure 1.2: Platelet release from mature MKs into a sinusoidal blood vessel.

Mature MKs derive from hematopoietic stem cells predominantly in the bone marrow. After extension of proplatelets into sinusoidal blood vessels, platelets get budded by shear forces of the blood flow. From Geddis and Kaushansky [32].

1.1.2. Functional compartments of platelets

Platelets have an asymmetric phospholipid bilayer membrane enclosing the cytoplasm in analogue to most other human cell types [33]. Many different receptors are integrated into the plasma membrane, potentiating activating platelet signaling in response to agonists like adenosine diphosphate (ADP), adenosine triphosphate (ATP), fibrinogen, von Willebrand factor (vWF), thrombin, collagen, epinephrine, serotonin or thromboxane A_2 (TxA_2) [34, 35]. As well, receptors for platelet inhibition are available for the tight regulation of platelet activation. The most important ones are the prostaglandin receptor (EP receptor), mediating proteinkinase A (PKA) activity via increase of cyclic adenosine monophosphate (cAMP) and the soluble guanylyl cyclase (sGC) as receptor for nitric oxide (NO), leading to the generation of cyclic guanosine monophosphate (cGMP) with subsequent activation of proteinkinase G (PKG) [36]. Jointly, PKA and PKG phosphorylate predominantly the unique amino acids Ser^{157} and Ser^{239} of the vasodilator-stimulated phosphoprotein (VASP) [37, 38]. Phosphorylated VASP finally inhibits platelet activation by keeping the fibrinogen receptor in the resting conformation [39].

The activating receptors are of different nature. Recognition of fibrinogen, collagen and vWF is realized by integrins like $\alpha_{IIb}\beta_3$ (fibrinogen receptor) or $\alpha_2\beta_1$ (collagen receptor), whereas ADP or thrombin, among others, interact with G protein-coupled receptors (GPCR), predominantly the $P2Y_1$ and $P2Y_{12}$ receptor ($P2Y_1R$/$P2Y_{12}R$) for ADP or the protease-activated receptors (PAR) 1 and PAR4 for thrombin, respectively. ATP as agonist manipulates the activity of the ligand-gated ion channel $P2X_1$ receptor ($P2X_1R$) with preferential permeability for calcium (Ca^{2+}) [40]. There are also further receptors like the C-type lectin receptor P-selectin, which is able to bind the P-selectin glycoprotein ligand-1 and is responsible for the interaction of platelets with other cell types [41].

Moreover, it was found that platelets also bear distinct subtypes of toll-like receptors (TLR), for example TLR2 and TLR4 [42, 43], responsible for the detection of pathogen-associated molecular patterns like lipopolysaccharides from gram-negative bacteria or lipopeptides from gram-positive bacteria [44]. Occurrence of TLR on platelets emphasize evidence that platelets are, in addition to their well-known function in hemostasis, involved in immune response of the innate immune system [45]. Exact interactions and mechanisms of TLR in platelets are still subject of ongoing research, yet there are some studies investigating involvement of TLR signaling in classic platelet functions, as performed by Niklaus *et al.* [46].

Similar to other cell types, platelets possess the cell organelles Golgi apparatus, endoplasmic reticula (known as dense tubular system in platelets), mitochondria, peroxisomes, ribosomes, endosomes and, additionally, a proficient cytoskeleton as integral part for the hemostatic capacity [47], together with an open canalicular system [48].

1.1.2.1. Platelet granules

Supplementary to the aforementioned organelles, there are three major types of granules in platelets: dense granules, α-granules and lysosomal granules [49]. Small inorganic molecules like serotonin, ADP, ATP, Ca^{2+} and polyphosphates are stored in dense granules and derive from MKs. The secretion of dense granules support platelet aggregation. In contrast to dense granules, α-granules contain a myriad of proteins with different functions like hemostatic and adhesion factors (e.g. vWF, Factor V,

fibrinogen, P-selectin), growth factors, proteases, necrosis factors and other cytokines [50]. Some of these proteins are stored in MKs by endocytosis, as they cannot be synthesized by MKs themselves [51]. Platelets secrete the granule contents when they get activated. This leads to potentiation of activation and aggregation. Lysosomes are a storage pool for glycohydrolases in platelets, comparable to other cell types. Their content are also released upon platelet activation [52].

1.1.2.2. Collagen receptors

Collagen is the most abundant component of the extracellular matrix (ECM), whereby especially type I, III, IV, V and VI of at least 28 different types are present in the vessel walls [53-55]. When a vessel wall is injured, collagen from subendothelial matrix gets locally exposed, which is then recognized by circulating platelets with the glycoprotein (GP) Ib in complex with GPIX and GPV mediated via vWF in indirect manner as well as by direct interaction with the receptors GPVI and GPIa/IIa [56, 57].

The GPIb-IX-V receptor is composed of 4 distinct subunits, GPIbα, GPIbβ, GPV and GPIX, each containing leucine-rich repeats and is responsible for platelet tethering and primary adhesion [58, 59]. This means that its interaction with exposed collagen from the ECM, mediated by vWF, leads to slowing down of circulating platelets in the area of vessel injury and attachment for an initial, transient adhesion to it, thereby activating platelet signaling [60, 61]. To enable the interaction between the GPIbα subunit of the GPIb-IX-V receptor and vWF, it is necessary that the globular form of vWF gets unfolded by hydrodynamic forces into a stretched, linear conformation to expose the GPIb binding A1 domain [62, 63]. Ristocetin, a glycopeptide antibiotic, is able to promote interaction of vWF with the GPIb-IX-V receptor by interaction with the A1 domain of vWF supporting its unfolding independent of shear forces and is therefore used for investigations of GPIb [64]. Besides collagen, the GPIb-IX-V receptor complex bears binding sites for thrombin and other ligands [65, 66]. Signaling of activated GPIb-IX-V is associated with the scaffold protein 14-3-3ζ and phosphorylation by Src family tyrosine kinases (SFKs) with subsequent activation of the phosphoinositide 3-kinase (PI3K), leading to upregulated proteinkinase B (Akt) by phosphorylation of phosphatidylinositol 4,5-bisphsphate (PIP_2) into

phosphatidylinositol 3,4,5-trisphosphate (PIP_3) as well as activation of phospholipase C (PLC) γ2 and proteinkinase C (PKC) [67].

The first receptor directly recognizing collagen is the GPVI receptor and represents the most potent platelet signaling receptor for collagen [68]. Its extracellular domain is related to the immunoglobulin superfamily and is constitutively attached to a Fc receptor γ-chain (FcRγ) bearing immunoreceptor tyrosine-based activation motif, important for signal transduction [69]. Stimulation of the GPVI receptor with collagen leads to the phosphorylation of the FcRγ by Fyn and Lyn [70], driving recruitment of Syk with concomitant phosphorylation and activation of PLCγ2. This culminates in Ca^{2+} mobilization and activation of PKC by hydrolysis of PIP_2 into inositol 1,4,5-trisphosphate (IP_3) and diacylglycerol (DAG) [71]. Furthermore, arachidonic acid is released and PI3K is activated, leading to the phosphorylation of Akt, mediating collagen-induced effects [72, 73]. For sufficient signal transduction, the GPVI receptor has to build a dimeric cluster during activation [74].

GPIa/IIa (also known as integrin $\alpha_2\beta_1$) is the second receptor, which is able to directly bind collagen and is an integrin in a low-affinity conformation in quiescent platelets, comparable with the fibrinogen receptor as described in **1.1.2.5**. Therefore, initial platelet activation by "*inside-out signaling*" is required for conformation change of the GPIa/IIa receptor and its ability to bind exposed collagen with high affinity [75]. GPIa/IIa activation leads to signaling via SFKs and subsequent activation of the PLCγ2, resulting in intracellular Ca^{2+} mobilization with formation of filopodia and lamellipodia [76]. It was found that GPIa/IIa receptor stimulation also activates further kinases like the p38 mitogen-activated protein kinase [77]. Overall, current consent for the GPIa/IIa receptor is to strengthen platelet-collagen interactions and to reinforce stable thrombi production [78]. The activation cascade of the collagen receptors and crosstalk between them is shown in **Figure 1.3**.

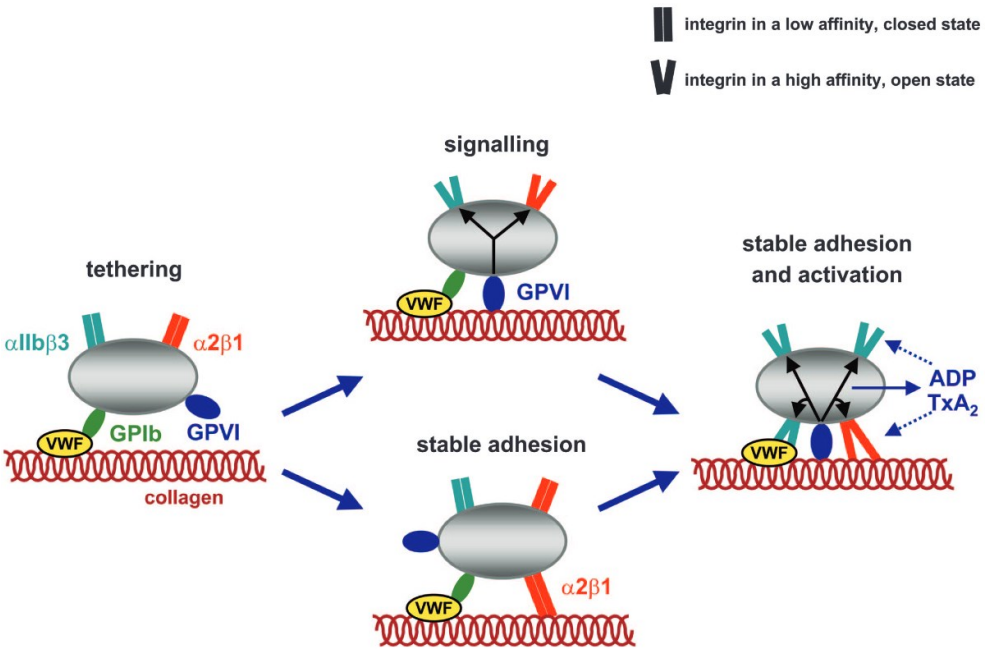

Figure 1.3: Model for proposed mechanisms of collagen-receptors for platelet tethering, signaling, adhesion and activation.

Platelets are initially tethering to exposed subendothelial collagen via vWF with GPIb of the GPIb-IX-V receptor complex (left). From here, two pathways are possible. The first way: Activation of the GPVI receptor (upper) leads to downstream signaling and subsequent activation of the integrin receptors $\alpha_{IIb}\beta_3$ (GPIIb/IIIa – fibrinogen receptor) and $\alpha_2\beta_1$ (GPIa/IIa – collagen receptor). Activated integrin receptors then attach to collagen directly ($\alpha_2\beta_1$) or via vWF ($\alpha_{IIb}\beta_3$). The second way (lower): Platelets adhere to collagen via $\alpha_2\beta_1$ prior to collagen-mediated activation of GPVI with concomitant platelet activation. The final stage for both pathways (right) consists of stable adhesion and full release of secondary mediators like ADP and TxA_2, further potentiating collagen-induced mechanisms. As well, both pathways may reinforce each other. From Auger *et al.* [79].

1.1.2.3. Thrombin receptors PAR1 and PAR4

Thrombin itself is a serine protease and, as clotting factor IIa, an integral part of the coagulation cascade, responsible for the conversion of fibrinogen into fibrin to form fibrin clots [80]. It also activates the GPCRs PAR1 and PAR4 by cleavage of a small extracellular N-terminal sequence to expose the tethered ligand for the receptor, resulting in its activation [81]. Upon binding of the tethered ligand, downstream signaling leads to activation of PLCβ mediated through the G protein $G\alpha_q$, accompanied by Ca^{2+} mobilization and activation of PKC [82]. Furthermore, PAR1 and PAR4 signaling can also be mediated by $G\alpha_{12/13}$, leading to the activation of the small G Protein RhoA with subsequent activation of the Rho-kinase (ROCK) [83]. These steps lead to platelet activation followed by platelet shape change, granule secretion and platelet aggregation [84]. Both receptors PAR1 and PAR4 can also be activated

by synthetic hexapeptides corresponding to the amino acid sequence of their tethered ligands. For PAR1, such specific hexapeptide is SFLLRN, also called thrombin receptor-activating peptide 6 (TRAP-6), which is frequently used for experimentation with platelets [85], especially in platelet-rich-plasma (PRP), avoiding activation of coagulation. The mechanisms of activation by tethered ligands or synthetic peptides are depicted in **Figure 1.4**.

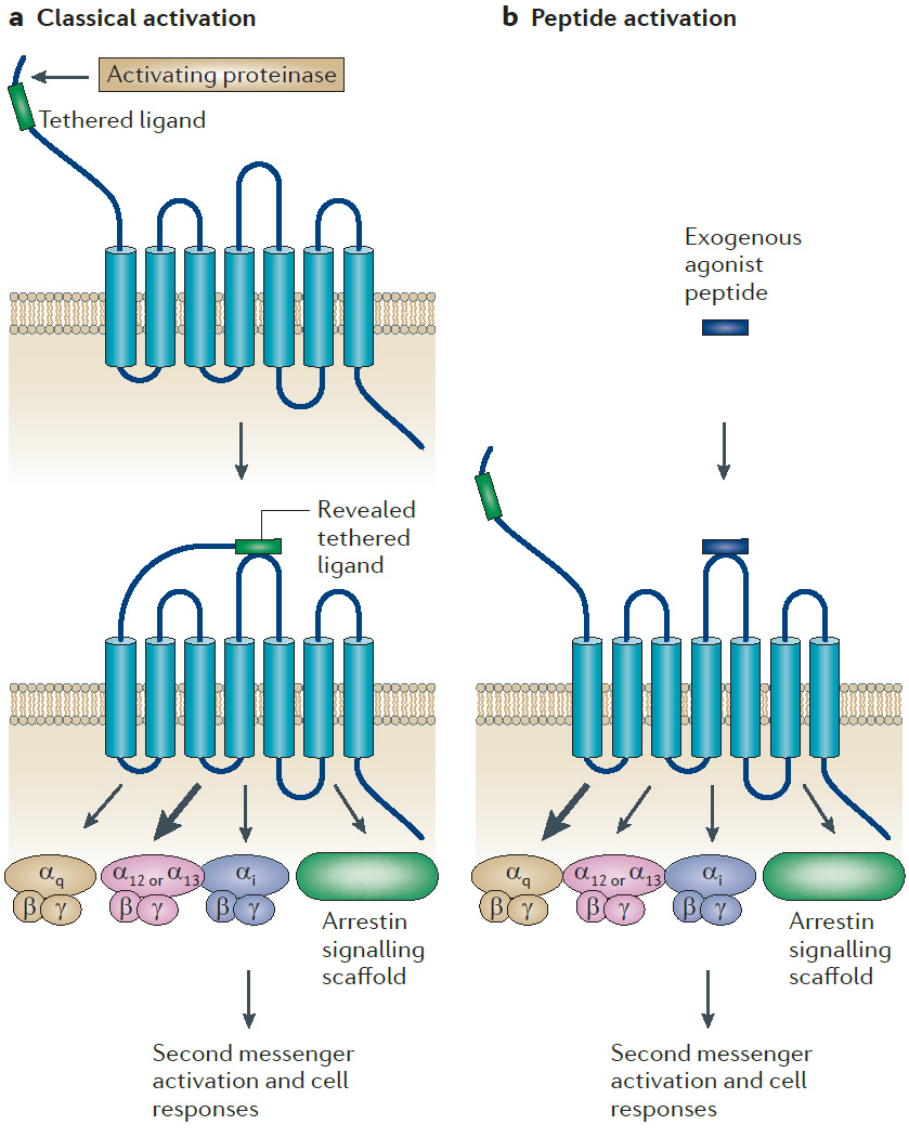

Figure 1.4: Mechanisms of activation for PAR1 and PAR4.

PARs are classically activated by cleavage at the N-terminus by the protease thrombin, which reveals the tethered ligand (**a**). Exogenous application of synthetic peptides like TRAP-6 can activate PARs without proteolytic unmasking the tethered ligand (**b**), leading to the stimulation of downstream signaling. Adapted from Ramachandran *et al.* [86].

Finally, platelet activation of PAR1 and PAR4 with thrombin is capable of inhibiting adenylyl cyclase activity (AC) directly by the receptor coupled G protein $G\alpha_i$ or in an indirect manner by released ADP [87, 88], as described in **1.1.2.4** for the signaling of the purinergic receptor for ADP, $P2Y_{12}R$.

1.1.2.4. Purinergic receptors $P2Y_1R$, $P2Y_{12}R$ and $P2X_1R$

As mentioned above in **1.1.2.1**, small molecules like adenine-containing nucleotides are stored in dense granules of platelets. Upon platelet activation, dense granules are released from platelets and the dense granule content, including ADP and ATP, can act on platelets in an autocrine and paracrine manner [89]. The receptors for ADP are the purinergic receptors $P2Y_1R$ and $P2Y_{12}R$. They are both GPCR, but they are coupled to different G proteins, linked with divergent downstream signals. $P2Y_{12}R$ is coupled to the G protein $G\alpha_i$, leading to the inhibition of the AC and activation of PI3K when the receptors get activated by ADP [90]. Hereafter, PI3K is responsible for activation of Akt and Ras-related protein Rap1b, finally leading to the conformational change of the fibrinogen receptor GPIIb/IIIa, indispensable for the initiation of platelet aggregation [91, 92]. Furthermore, ADP-induced activation of $P2Y_{12}R$, associated with inhibition of AC, reduces cAMP-mediated phosphorylation of VASP, which is known to inhibit the platelet fibrinogen receptor in its phosphorylated form [93]. The $P2Y_{12}R$ is an effective target of clinical antiplatelet therapy, for example for inhibitors like clopidogrel or ticagrelor [94]. $P2Y_1R$, however, is coupled to the G protein $G\alpha_q$. Stimulation of the receptor with ADP leads to the activation of PLCβ with subsequent activation of PKC and Ca^{2+} mobilization as well as platelet shape change, comparable to the mechanism for PAR1 [95]. ADP-induced signaling of the $P2Y_1R$ can be inhibited using the selective antagonist MRS2500, which acts competitively at the receptor [96]. For sufficient stimulation of ADP-induced platelet aggregation, it is essential that both G protein-coupled purinergic receptors are activated concomitantly [97]. The generation of procoagulant TxA_2 is also dependent on ADP-induced platelet activation [98].

The purinergic receptor $P2X_1R$ is a ligand-gated cation channel, which is activated by ATP with preferential permeability for Ca^{2+}. Therefore, activation of the $P2X_1R$ generates an increase in intracellular Ca^{2+} levels, leading to platelet shape change and

amplifies signaling of other receptors, thereby promoting platelet aggregation [99]. Signaling of these three purinergic receptors is shown in **Figure 1.5**.

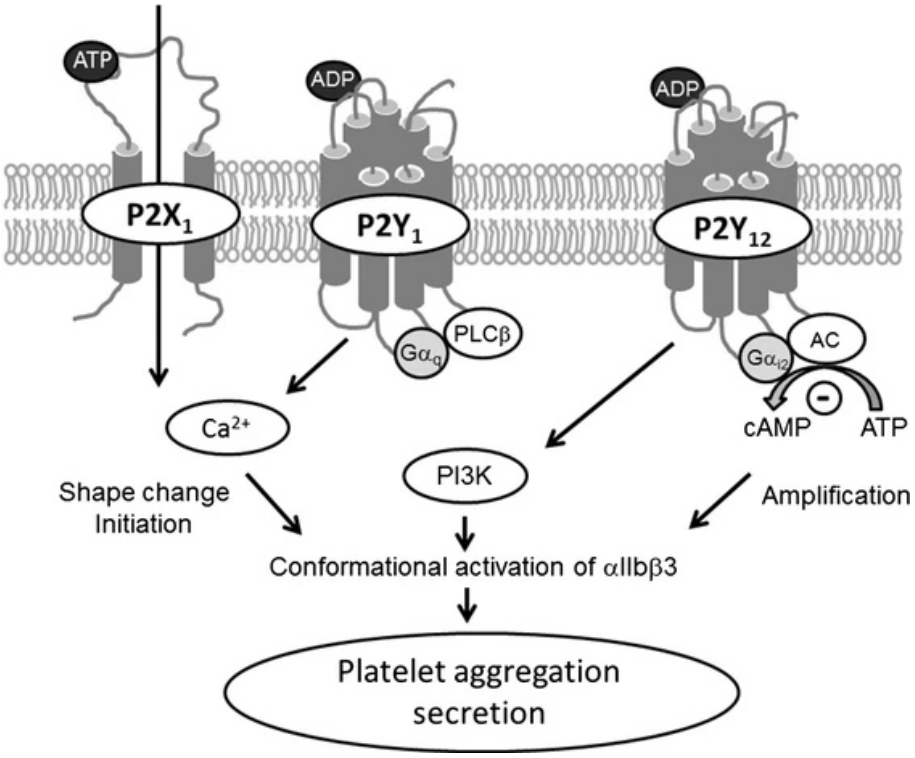

Figure 1.5: Signaling of the purinergic receptors $P2X_1$, $P2Y_1$ and $P2Y_{12}$ in platelets.

The $P2X_1R$ (left) is a ligand-gated cation channel activated by ATP and responsible for rapid Ca^{2+} influx. $P2Y_1R$ (middle) is activated by ADP, leading to the activation of the G protein $G\alpha_q$ with subsequent activation of PLCβ. $P2Y_{12}R$ (right) is the second purinergic receptor activated by ADP, leading to the inhibition of AC and activation of PI3K. Together, the activation of these receptors results in the initiation of platelet aggregation by activation of the fibrinogen receptor. From Ferri *et al.* [100].

1.1.2.5. Fibrinogen receptor (GPIIb/IIIa)

The fibrinogen receptor is built up of the GPs IIb and IIIa (GPIIb/IIIa) from the integrin family (integrin $\alpha_{IIb}\beta_3$). It is the most abundant receptor with approximately 80,000 copies on the platelet surface and is also found in internal pools [101, 102]. It is the common terminus of platelet pathways responsible for platelet activation, platelet adhesion and platelet aggregation and is itself involved in adhesion to the vessel wall, aggregation and bidirectional signaling [103]. In quiescent platelets, the fibrinogen receptor is resting in an inactive state with a bent closed, low-affinity conformation. Upon platelet activation, the fibrinogen receptor is subjected to conformational changes towards an extended open, high-affinity state [11, 104]. In this high-affinity state, the fibrinogen receptor is able to bind soluble fibrinogen and activates the

phosphoinositide metabolism as well as Ca^{2+} mobilization and cytoskeletal rearrangement by activation of Src tyrosine kinase within the framework of the fibrinogen "*outside-in signaling*" [105]. The two conformations of the fibrinogen receptor are illustrated in **Figure 1.6**. Noteworthy, GPIIb/IIIa is also able to bind collagen via vWF [106]. For the experimental detection of fibrinogen receptor activation, there is a specific monoclonal antibody, called "PAC-1", recognizing an epitope on the GPIIb/IIIa only in its activated conformation. Coupled to a fluorophore, with this antibody it is possible to quantitatively measure platelet fibrinogen receptor activation by flow cytometry [107].

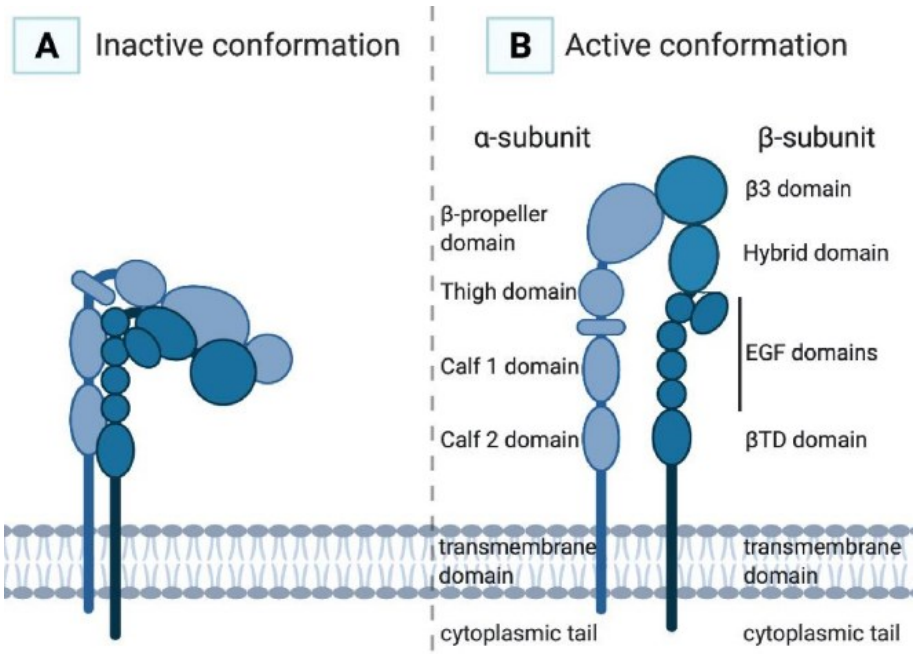

Figure 1.6: Fibrinogen receptor conformations.

The fibrinogen receptor occurs in two different conformations. In the inactive conformation (**A**), the receptor is bent closed with low binding affinity for its ligands, while in the active conformation (**B**), the receptor has an extended open form and is in a high-affinity state. From van den Kerkhof *et al.* [108].

Furthermore, platelet aggregation, which means crosslinking of platelets and following thrombus growth, is executed via the fibrinogen receptor. Platelet aggregation can be measured by light transmission aggregometry, which is also called Born aggregometry [109]. In light transmission aggregometry, transmission of light through a cuvette, filled with a platelet-containing suspension (*e.g.* PRP or washed platelets) is measured by a photocell. Without agonist-stimulation, the suspension has a high turbidity with low transmission of light. After stimulation with an agonist like ADP,

collagen or TRAP-6, platelets begin to aggregate and more light can pass through the suspension. Continuous measurement of light transmission after addition of an agonist finally creates an aggregation curve, which can be evaluated for example for their maximal aggregation, lag-time or occurrence of reversibility.

1.1.2.6. Inhibitory platelet signaling

As mentioned in **1.1.2**, there are two major pathways to ensure platelet inhibition with VASP as the common effector molecule. The sGC is activated by NO, which is produced by nitric oxide synthases (NOS) from L-arginine. There are different isoforms of NOS, for example the constitutively expressed isoform endothelial NOS (eNOS), producing NO in the vascular endothelium under physiological conditions *in vivo [110].* Another isoform, the inducible NOS (iNOS) is expressed upon stimulation of endothelial cells or macrophages with various cytokines or bacterial lipopolysaccharides [111]. Activated sGC triggers the production of cGMP from guanosine triphosphate, which subsequently activates PKG. Activated PKG is then able to phosphorylate Ser^{239} of VASP with high specificity, but also slightly phosphorylates VASP at Ser^{157} [112]. The second pathway is stimulated by prostaglandins, especially by prostacyclin I_2 released from vascular endothelial cells *in vivo* [113]. Prostaglandins stimulate the $G\alpha_s$-coupled EP receptor, which activates the AC to generate cAMP from ATP. Released cAMP from the AC activates PKA, which finally phosphorylates predominantly Ser^{157} of VASP, but also Ser^{239} in a lower extent [112]. Phosphorylated VASP is able to inhibit platelet activation and aggregation by blocking the activation of the receptor for fibrinogen and of cytoskeletal rearrangements via actin dynamics [114, 115]. Dephosphorylation of VASP as regulatory control of its activation is exerted by protein phosphatases like the protein phosphatase 2A (PP2A) [116].

For experimentation, synthetic substances are available to stimulate VASP phosphorylation. DEA/NO is used as NO donor to activate the sGC. Prostaglandin E_1 (PGE_1) stimulates VASP phosphorylation via activation of the EP receptor [117, 118]. The according signaling cascades are illustrated in **Figure 1.7**.

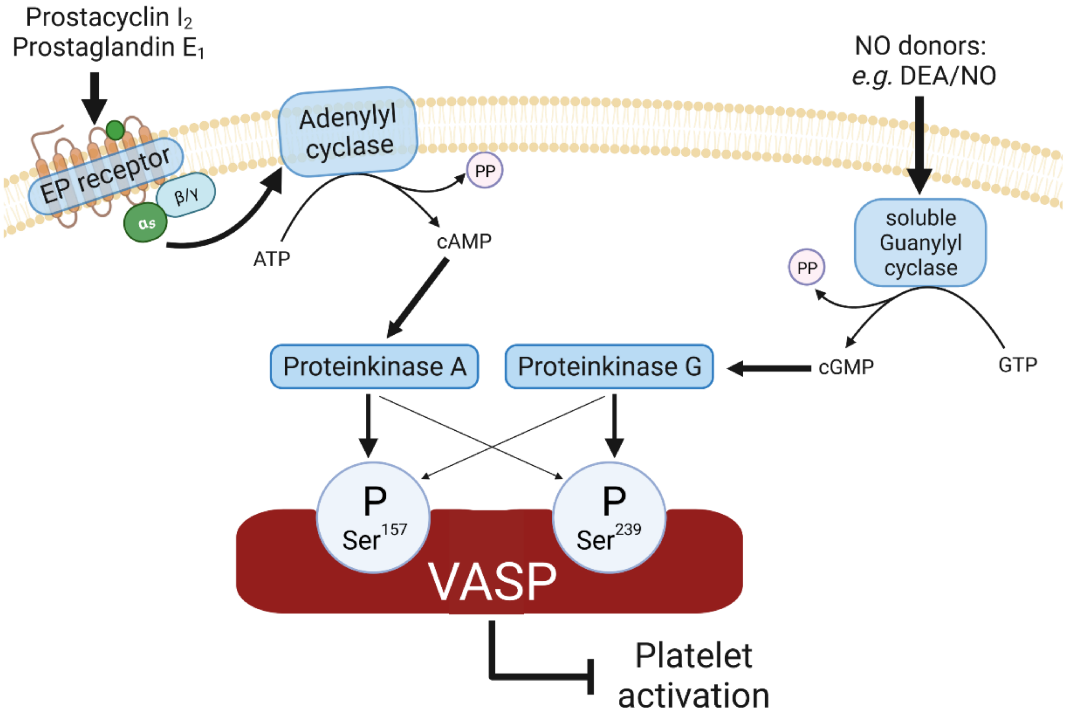

Figure 1.7: Regulation of the actin-binding protein VASP in platelet inhibition.

VASP bears two major phosphorylation sites. Ser^{157} is predominantly phosphorylated by the PKA after cAMP-dependent activation via signaling of the $G\alpha_s$-coupled EP receptor. Activation of sGC by NO donors leads to generation of cGMP with subsequent activation of PKG, which specifically phosphorylates Ser^{239} of VASP. Both kinases are also able to phosphorylate the other phosphorylation sites, but with lower affinity. Created with BioRender.com.

Taken together, many platelet receptor signaling pathways cross over and interact with each other, leading to a complex network of activating and inhibitory mechanisms as shown in **Figure 1.8**.

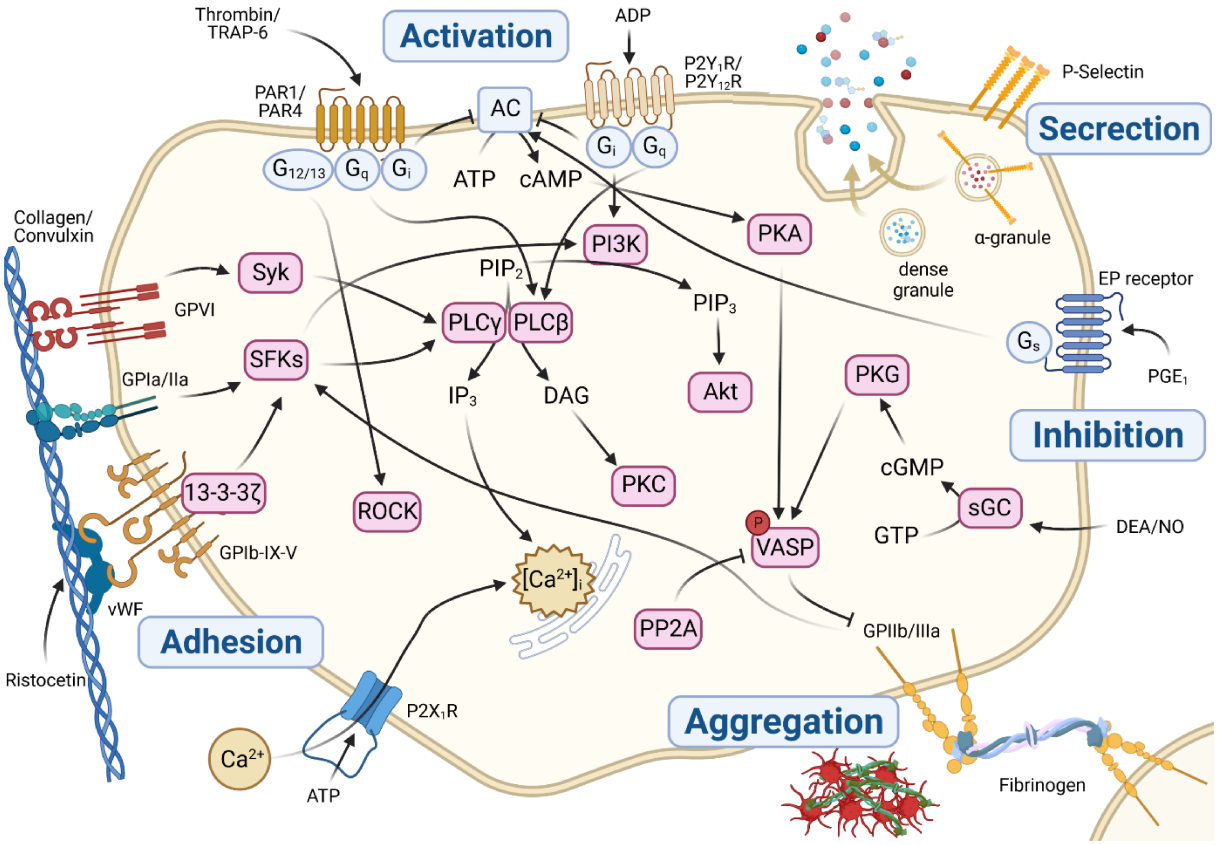

Figure 1.8: Overview of essential signaling pathways in human platelets.

Signal transduction in human platelets is executed through plenty of receptor systems with downstream kinase activities in response to various agonists. Created with BioRender.com.

1.1.3. Protein synthesis and protein degradation in platelets

In contrast to eukaryotic cells like lymphocytes, platelets do not contain a nucleus [2]. Therefore, *de novo* protein synthesis cannot be carried out by normal DNA transcription to messenger RNA (mRNA) and translation into proteins [119]. Nevertheless, there is residual potential of *de novo* protein synthesis in platelets [120], since they are equipped with mRNA and a translational machinery like ribosomes, derived from MKs during platelet production [121]. Furthermore, platelets are capable of splicing precursor mRNA into mature mRNA transcripts, for example the Interleukin-1β pre-mRNA, due to the fact that there is a spliceosome [122]. Several platelet proteins are synthesized in a signal-dependent manner upon platelet activation [123, 124]. To maintain protein homeostasis and to keep availability of free amino acids to synthesize new proteins, platelets also contain protein degrading

enzymes, *e.g.* the cysteine protease calpain with substrates like cytoskeletal proteins and the proteasome system [125], described in more detail in **1.3**.

1.2. The clinical significance of platelets in human medicine

The blockade of specific platelet activation mechanisms are useful tools to inhibit platelet aggregation and thrombus formation. For example, this is a major strategy in the prevention of ischemic stroke or acute myocardial infarction as consequence of arteriosclerotic plaque rupture causing thrombosis [126].

To achieve inhibition of platelet activation for therapeutic purposes, several pharmaceuticals, addressing different targets, are available for “antiplatelet therapy”. Acetylsalicylic acid (ASS, aspirin) is a well-known analgesic, which is, beyond that, an antiplatelet agent, irreversibly inhibiting the cyclooxygenases 1 and 2, resulting in decrease of prostaglandin-production from arachidonic acid as precursor for thromboxane A_2 [127]. There are number of antiplatelet drugs that have been developed, inhibiting the $P2Y_{12}R$ (clopidogrel), GPIIb/IIIa (tirofiban) or PAR1 (vorapaxar) [128]. In addition, compounds for the inhibition of plasmatic coagulation like heparin, phenprocoumon or rivaroxaban, preventing blood clotting, are available [129].

In contrast to the prevention of platelet activation, there are several hereditary diseases, affecting physiological platelet function. For example, Glanzmann’s thrombasthenia is a severe thrombocytopathy, in which the GPIIb/IIIa receptor is defective or totally missing, leading to significantly prolonged bleeding time caused by missing platelet aggregation [130]. Similarly, in Bernard-Soulier syndrome, the GPIb-IX-V complex is affected, while in von Willebrand disease, there is a qualitative or quantitative deficiency of vWF [131].

Finally, in case of low platelet count (thrombocytopenia), potentially resulting from various conditions like bone marrow suppression after radiochemotherapy, stem cell therapy, disseminated intravascular coagulopathy or massive blood loss, transfusion of platelet concentrates is indicated to increase platelet count and ensure sufficient coagulation capacity [132].

1.3. Ubiquitin-proteasome system

The proteasome system is a huge, multicatalytic protein complex and the major protein degrading machinery, located in the cytoplasm as well as in the nucleus of eukaryotic cells [133]. In nucleated cells, the proteasome system is responsible for the degradation of misfolded proteins and interacts with many regulatory cellular processes like cell cycle progression, antigen processing or transcription [134]. The degradation of proteins by the proteasome is determined by a sophisticated system of protein tagging with moieties of the small 76 amino acid protein ubiquitin (Ub), exerted by an ubiquitylation machinery.

1.3.1. Protein ubiquitylation

The machinery for protein ubiquitylation comprises ubiquitin-activating enzymes (E1), ubiquitin-conjugating enzymes (E2) and ubiquitin ligases (E3), coupling the C-terminal glycine 76 residue of Ub covalently to ε-amino groups of lysine residues of the target proteins [135, 136]. Together, ubiquitylation and proteasomal degradation build the ubiquitin-proteasome system (UPS). In the first step, Ub is activated by E1 in an ATP-dependent reaction, resulting in Ub-bound E1. Subsequently, activated Ub is transferred to E2. Finally, E3 and the target protein are recruited, building a complex to mediate the ligation of the target protein with the activated Ub. Repetition of these steps leads to poly-ubiquitylated proteins [137]. The mechanism of protein ubiquitylation is illustrated in **Figure 1.9A**. The fate of ubiquitylated proteins is dependent on the ubiquitylation pattern, Ub-chains linked over their lysine 48 are considered to be targeted for proteasomal degradation [138]. Other patterns of ubiquitylation can target proteins for lysosomal degradation, transport or endocytosis, for example [139].

1.3.2. Structure and function of the proteasome system

The proteasome system of eukaryotic cells comprises vast subunits, which can be divided in two major subassemblies, the 19S regulatory particle and the proteolytically active 20S core particle or 20S proteasome. The 20S proteasome in combination with two 19S regulatory particles form together the 26S proteasome [140].

The 20S proteasome is a barrel-shaped particle, composed of four stacked rings and a total weight of 700 kilodalton (kDa). The two outer rings are built up of seven different α-subunits (α1-α7), important as binding sites for the 19S regulatory subunits and necessary for the formation of the two inner rings in proteasome assembly [141], which are built up of seven different β-subunits each (β1-β7). Three of the β-subunits bear catalytic activity due to their N-terminal threonine residue in the active center. β1 has caspase-like activity (C-L), cutting peptides after acidic amino acid residues, β2 bears trypsin-like activity (T-L), cutting peptides after basic amino acid residues and β5 carries chymotrypsin-like activity (CT-L), cutting peptides after hydrophobic amino acid residues [142, 143].

The 19S regulatory particle is a complex of two structures, the base and the lid, with a total weight of approximately 700 kDa. The base of the 19S regulatory particle comprises six homologous AAA-ATPases (Regulatory Particle Triple A; Rpt1-Rpt6) and four non-ATPase subunits (Regulatory Particle Non-ATPase; Rpn1, Rpn2, Rpn10 and Rpn13). The lid of the 19S regulatory particle is composed of nine non-ATPase subunits (Rpn3, Rpn5-9, Rpn11, Rpn12 and Rpn15), whereby Rpn11 bears deubiquitylase activity [140].

With the base, the 19S regulatory particle is attached to the α-ring of the 20S core particle. Proteins, targeted for degradation by the proteasome are recognized by distinct subunits of the 19S regulatory subunit through their specific poly-ubiquitylation tag [144]. As well, deubiquitylation, unfolding of the protein and opening the gate in the α-ring of the 20S core particle are executed by the 19S regulatory subunit [145]. Entering the 20S proteasome, the unfolded protein gets degraded into peptide fragments by the aforementioned β-subunits, which can be further recycled into amino acids in the cytoplasm [146]. The degradation of poly-ubiquitylated proteins by the 26S proteasome is illustrated in **Figure 1.9B.**

There are also further structures in addition to the 19S regulatory subunit, forming different proteasome complexes, like the 200 kDa 11S particle, which acts independently of ATP or ubiquitin tags [147]. The 11S particle in combination with an alternative 20S core particle, in which the three constitutively active subunits β1, β2 and β5 are substituted by the inducible subunits β1i, β2i and β5i, shows higher chymotrypsin-like activity, favoring the production of MHC class I binding peptides and is therefore referred to as immunoproteasome [148].

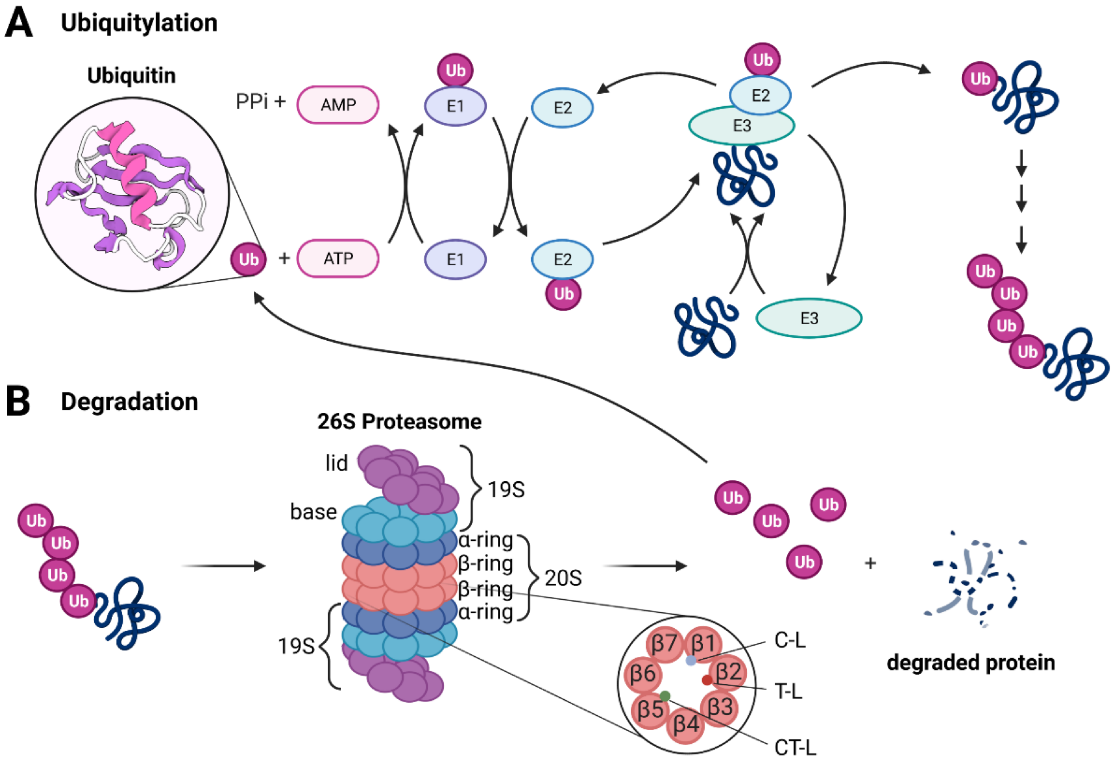

Figure 1.9: Protein degradation by the ubiquitin-proteasome system.

In the first step (**A**), proteins are tagged with ubiquitin via ubiquitin-activating, -conjugating and -ligating enzymes (E1-E3). Repeating this cycle leads to poly-ubiquitylated proteins, which are detected by the 26S proteasome system. In the second step (**B**), ubiquitin gets recycled, the protein unfolded and finally degraded. The 26S proteasome is built up of two 19S regulatory particles and the 20S core particle, which is composed of two α-rings and two β-rings. The β-subunits β1, β2 and β5 bear proteasomal activity. Adapted from "Ubiquitin Proteasome System", by BioRender.com (2022). Retrieved from https://apps.biorender.com/biorender-templates.

It was also found that particularly many malignant tumor types are accompanied by an elevated proteasomal activity which makes the proteasome an important pharmacological target for cancer treatment [149].

1.3.3. Bortezomib and other proteasome inhibitors

Bortezomib is a peptidyl boronic acid with a molecular weight of 384.24 g/mol, the chemical formula is $C_{19}H_{25}BN_4O_4$ and the chemical IUPAC name is [3-methyl-1-(3-phenyl-2-pyrazin-2-ylcarbonylamino-propanoyl) amino-butyl] boronic acid. It was first synthesized by the Myogenetics Company in 1995 and initially termed MG-341 and later PS-341 [150]. With its boronic acid as functional group it can

reversibly bind to the threonine of the β5- or the β1-subunit of the 20S proteasome, building a tetrahedral conformation at the boron atom [151], as shown in **Figure 1.10**.

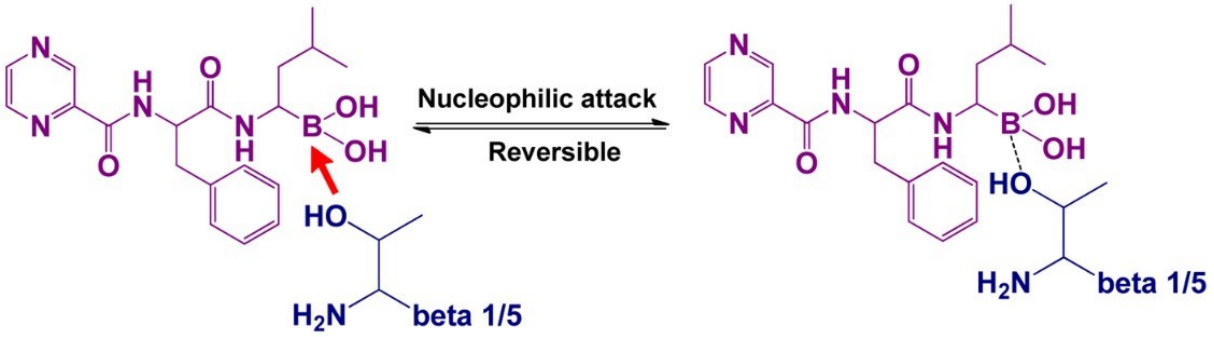

Figure 1.10: Reversible binding of bortezomib to β1/5 of the proteasome.

The proteasome inhibitor bortezomib (violet) with its boronic acid reversibly binds to a threonine residue of the β5- or β1-subunit in the active center of the proteasome (blue). Adapted from Shen *et al.* [152].

The highest binding affinity of bortezomib is shown for the β5-subunit (K_i=0.6 nM), followed by the β1-subunit and finally a relatively low affinity for the β2-subunit. Therefore, bortezomib inhibits the chymotrypsin-like activity most effectively [153]. Bortezomib has been successfully introduced into clinical practice for the treatment of patients suffering from multiple myeloma as first approved proteasome inhibitor by the FDA in 2003 [154]. Bortezomib-induced inhibition of proteasome activity recovers to normal in 48 to 72 h after *in vivo* application [155]. Treatment of multiple myeloma with proteasome inhibitors like bortezomib is effective, because of the high proliferation rate of tumor cells, dependent on high proteasome activity, compared to normal cells [156]. This leads to enhanced cytotoxicity of bortezomib for myeloma cells, caused by downstream inhibition of the nuclear factor kappa-light-chain-enhancer of activated B cells (NF-κB), accumulation of misfolded proteins, elevated endoplasmic reticulum stress and inhibition of angiogenesis, finally leading to apoptosis [157]. Common adverse effects of bortezomib are thrombocytopenia and neutropenia, associated with myelosuppresion and peripheral neuropathy, which has shown to be key dose-limiting adverse effect for bortezomib treatment [158, 159].

Meanwhile, proteasome inhibitors are an important part of the first line therapy in patients suffering from multiple myeloma [160, 161]. In addition to therapeutic applications, proteasome inhibitors like bortezomib are also important experimental

tools to evaluate the involvement of the proteasome system and its regulation in cellular processes of different cell types [151, 162-164].

Carfilzomib is another selective second-generation proteasome inhibitor approved for the treatment of multiple myeloma with higher binding affinity to the β5-subunit and lower extent of adverse effects, especially reduced peripheral neuropathy, compared to bortezomib. Carfilzomib contains an epoxyketone pharmacophore, mediating irreversible binding to the β5-subunit of the proteasome and leading to the inhibition of the chymotrypsin-like activity with high selectivity. Over and above, there are further novel proteasome inhibitors available like the orally available ixazomib [165].

1.3.4. Proteasome system in platelets

Despite absence of a nucleus and limited *de novo* protein synthesis, in 1991, the group around Yukawa was able to purify the proteasome from the cytosolic fraction of human platelets [166]. However, canonical functions of the proteasome like its role in cell cycle progression or in the regulation of transcription factors were unknown. Later, it could also be demonstrated by proteomic analysis that platelets express almost all subunits of the proteasome, including active subunits of the immunoproteasome [167]. Furthermore, they contain a complete ubiquitylation system [168], and possess several deubiquitylases [169]. Functionally, the platelet proteasome exerts chymotrypsin-like activity [170], and also trypsin-like activity or caspase-like activity [171].

In a recent study, we could show that platelet activation leads to elevated proteasome activity, emphasizing the importance of the proteasome system for platelet physiology [172]. Preincubation with the proteasome inhibitor bortezomib was able to block basal and collagen-stimulated proteasome activity in a dose-dependent manner [172]. This finding was accompanied by augmented levels of basal and collagen-induced poly-ubiquitylated proteins. Concentrations of 10 nM bortezomib showed already approximately 75 % inhibition of proteasome activity in washed platelets, whereas high concentrations above 10 µM bortezomib led to potentially toxic effects with reduced cell viability [173]. In contrast to platelets, myeloma cells displayed a stronger susceptibility to toxic effects of bortezomib with a drop of cell viability of > 80 % with 15 nM to 30 nM bortezomib [174], forcing bortezomib to be useful as pharmacological agent.

The working group around Nayak revealed that proteasome inhibition with 25 µM bortezomib leads to an increase in annexin V binding and decrease of mitochondrial membrane potential in platelets, implicating induction of apoptosis [175]. Therefore, they concluded that proteasome inhibition leads to decreased platelet life span in circulation *in vivo*. However, 25 µM bortezomib is a higher concentration than reached *in vivo* during clinical use, which is approximately 100 ng/mL (corresponding to 260 nM bortezomib) as average plasma concentration after intravenous injection of 1.3 mg per m^2 body surface of bortezomib [172, 176], potentially leading to cytotoxic effects.

2. Aim of the study

Despite absence of a nucleus, platelets possess a proteasome system, well characterized in nucleated cells as the major degradation machinery of proteins and indispensable for sufficient protein homeostasis. However, in anucleated platelets, the role of the proteasome system for platelet function is not fully understood.

Therefore, the aim of this study was to determine the interactions of the proteasome system with different functional characteristics of human platelets. Essential mechanisms of platelets, including activation, adhesion, secretion, aggregation and inhibition were investigated in dependence on proteasomal activity (as illustrated in **Figure 2.1**), achieved by blockade with the proteasome inhibitors bortezomib or carfilzomib.

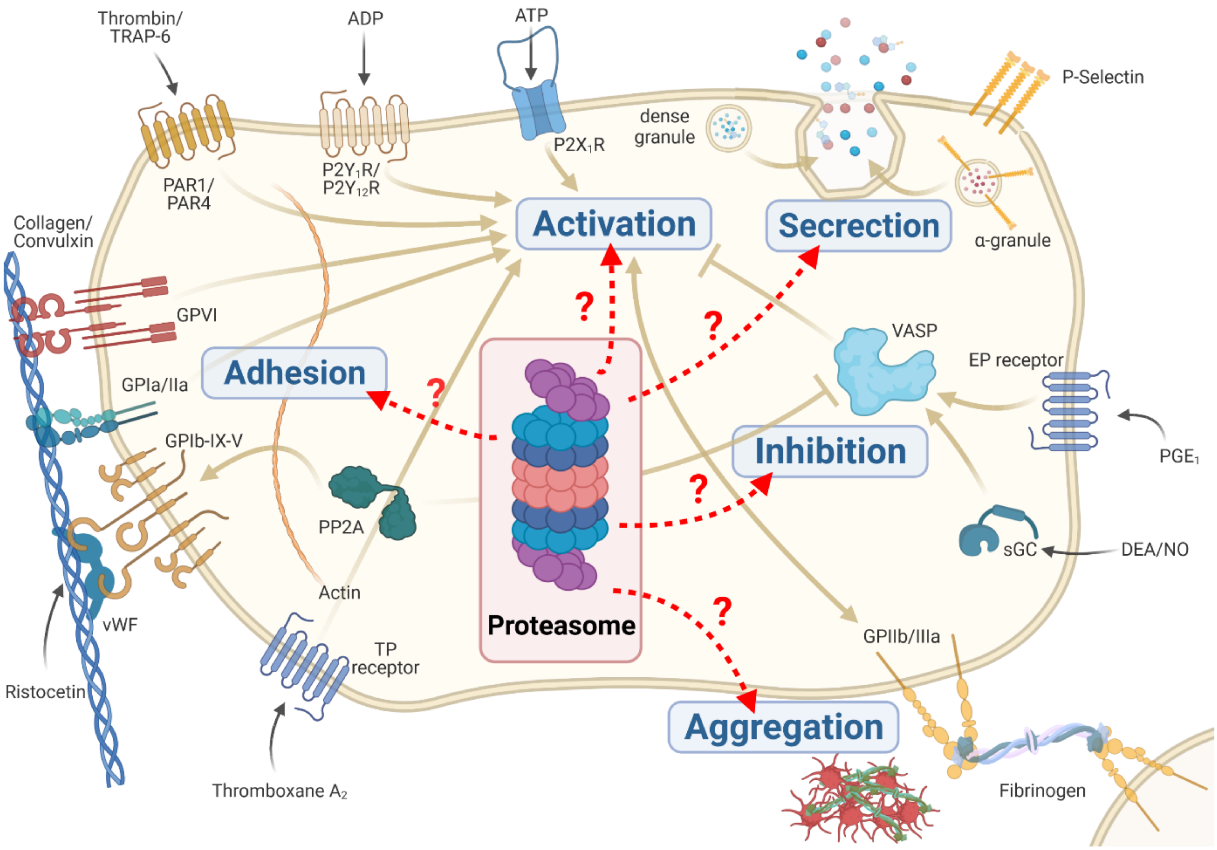

Figure 2.1: Overview of investigated functional platelet systems in dependence on proteasomal activity.

Different functional platelet systems addressing activation, adhesion, secretion, aggregation or inhibition were experimentally investigated in human platelets with the use of proteasome inhibitors. VASP – vasodilator-stimulated phosphoprotein, vWF – von Willebrand factor, PP2A – protein phosphatase 2A, PGE_1 – prostaglandin E_1, sGC – soluble guanylyl cyclase, TRAP-6 – Thrombin receptor-activating peptide 6, GP – glycoprotein. Created with BioRender.com.

3. Material and methods

3.1. Materials

3.1.1. Chemicals

Acetic acid	Merck KgaA (Darmstadt, Germany) 37381
Acetylsalicylic acid (ASS)	Sigma-Aldrich by Merck KgaA (Darmstadt, Germany) A5376
Acrylamide/Bis-acrylamide solution, 30 %, 37.5:1	ROTIPHORESE (Carl Roth GmbH + Co. KG, Karlsruhe, Germany) 3029.1
Adenosine diphosphate (ADP)	Haemochrom Diagnostica GmbH (Essen, Germany) HB-5502-FG
Ammonium persulfate (APS)	Sigma-Aldrich by Merck KgaA (Darmstadt, Germany) A3678
Blocking peptide for phospho-VASP (p-Ser^{239})	nanoTools Antikörpertechnik GmbH & Co. KG (Teningen, Germany) 2002-100/VASP-pSer239
Bortezomib	Selleck Chemicals LLC (Houston, TX, USA) S1013
Bovine serum albumin (BSA)	Sigma-Aldrich by Merck KgaA (Darmstadt, Germany) A2153
Bromophenol blue	Sigma-Aldrich by Merck KgaA (Darmstadt, Germany) B8026
Calcium chloride dihydrate ($CaCl_2$)	Merck KgaA (Darmstadt, Germany) 102382
Carfilzomib	Selleck Chemicals LLC (Houston, TX, USA) S2853
Collagen	Collagen Reagent Horm (Takeda, Osaka, Japan) 1130630
cOmplete, Mini, EDTA-free Protease Inhibitor Cocktail	Roche Diagnostics GmbH (Mannheim, Germany) 04693159001
Convulxin	Cayman Chemical (Ann Arbor, MI, USA) 19082

2-(N,N-Diethylamino)-diazenolate-2-oxide diethylammonium salt (DEA/NO)	Enzo Life Sciences GmbH (Loerrach, Germany) ALX-430-034
Dimethyl sulfoxide (DMSO)	Sigma-Aldrich by Merck KgaA (Darmstadt, Germany) D8418
Ethanol	Sigma-Aldrich by Merck KgaA (Darmstadt, Germany) 32205-M
Ethylenediaminetetraacetic acid (EDTA) disodium salt, 0.5 M	Sigma-Aldrich by Merck KgaA (Darmstadt, Germany) E7889
Fluo-4 AM	Invitrogen (Fisher Scientific GmbH, Schwerte, Germany) F14217
Formaldehyde solution (FA)	Sigma-Aldrich by Merck KgaA (Darmstadt, Germany) F8775
D-(+)-Glucose (glucose)	Sigma-Aldrich by Merck KgaA (Darmstadt, Germany) G7021
Glycine	Merck KgaA (Darmstadt, Germany) 104201
Ethylene glycol-bis(2-aminoethylether)-N,N,N′,N′-tetraacetic acid (EGTA)	Sigma-Aldrich by Merck KgaA (Darmstadt, Germany) E3889
Glycerol	Sigma-Aldrich by Merck KgaA (Darmstadt, Germany) G9012
Goat serum	Sigma-Aldrich by Merck KgaA (Darmstadt, Germany) S26-M
Hanks' Balanced Salt Solution (HBSS)	Gibco (Fisher Scientific GmbH, Schwerte, Germany) 14175-053
4-(2-hydroxyethyl)-1-piperazineethanesulfonic acid (HEPES)	Sigma-Aldrich by Merck KgaA (Darmstadt, Germany) H3784
Hydrochloric acid (HCl)	VWR International GmbH (Darmstadt, Germany) 20252.420
Magnesium chloride Hexahydrate ($MgCl_2$)	Merck KgaA (Darmstadt, Germany) 105833

α,β-MeATP	Bio-Techne GmbH (Wiesbaden-Nordenstadt, Germany) 3209
Methanol	Sigma-Aldrich by Merck KgaA (Darmstadt, Germany) 32213
β-Mercaptoethanol	Sigma-Aldrich by Merck KgaA (Darmstadt, Germany) M6250
Milk powder, skimmed	Blotting grade (Carl Roth GmbH + Co. KG, Karlsruhe, Germany) T145.2
Mounting medium	Invitrogen ProLong Diamond Antifade Mountant (Fisher Scientific GmbH, Schwerte, Germany) P36965
MRS2500	Bio-Techne GmbH (Wiesbaden-Nordenstadt, Germany) 2159
MRS2365	Bio-Techne GmbH (Wiesbaden-Nordenstadt, Germany) 2157
NF449	Bio-Techne GmbH (Wiesbaden-Nordenstadt, Germany) 1391
Phosphate-buffered saline (PBS), Ca^{2+}- and Mg^{2+}-free	Sigma-Aldrich by Merck KgaA (Darmstadt, Germany) D8537
Pluronic F-127	Sigma-Aldrich by Merck KgaA (Darmstadt, Germany) P2443
Ponceau S	Sigma-Aldrich by Merck KgaA (Darmstadt, Germany) P3504
Potassium Chloride (KCl)	Merck KgaA (Darmstadt, Germany) 104936
Probenecid	Sigma-Aldrich by Merck KgaA (Darmstadt, Germany) P8761
Prostaglandin E_1 (PGE_1)	Sigma-Aldrich by Merck KgaA (Darmstadt, Germany) P5515
Protein ladder mix, 10 to 180 kDa	PageRuler (Fisher Scientific GmbH, Schwerte, Germany) 26616

Ristocetin	Haemochrom Diagnostica GmbH (Essen, Germany) HB-5508-FG
Sheath fluid for flow cytometry	FACSFlow (Becton Dickinson, Franklin Lakes, NJ, USA) 342003
Sodium Chloride (NaCl)	Sigma-Aldrich by Merck KgaA (Darmstadt, Germany) 31434-M
Sodium dodecyl sulfate (SDS)	Sigma-Aldrich by Merck KgaA (Darmstadt, Germany) L3771
Sodium hydroxide solution (NaOH), 5 M	Merck KgaA (Darmstadt, Germany) 1.09913
Sterile water, 50 mL and 10 L	BERLIN-CHEMIE AG, (Berlin, Germany) Ampuwa (Fresenius Kabi Deutschland GmbH, Bad Homburg, Germany) 2599.99.99; 1080181
Tetramethylethylenediamine (TEMED)	Sigma-Aldrich by Merck KgaA (Darmstadt, Germany) T9281
Thrombin receptor-activating peptide 6 (TRAP-6)	Haemochrom Diagnostica GmbH (Essen, Germany) HB-5533-FG
Tris(hydroxymethyl)amino-methane (TRIS)	Merck KgaA (Darmstadt, Germany) 108382
Tri-Sodium citrate dihydrate (citrate)	Merck KgaA (Darmstadt, Germany) 106448
Triton X-100	Sigma-Aldrich by Merck KgaA (Darmstadt, Germany) T8532
TWEEN 20	Sigma-Aldrich by Merck KgaA (Darmstadt, Germany) P7949
Tyrode’s Salt Solution (Tyrode’s buffer)	Sigma-Aldrich by Merck KgaA (Darmstadt, Germany) T2397

3.1.2. Enzymes

Apyrase, from potatoes	Sigma-Aldrich by Merck KgaA (Darmstadt, Germany) A2230

3.1.3. Antibodies

Goat anti-Rabbit IgG StarBright Blue 700	Bio-Rad Technologies GmbH (Feldkirchen, Germany) 12004161
Goat polyclonal FITC anti-Rabbit IgG	Sigma-Aldrich by Merck KgaA (Darmstadt, Germany) F1262
Mouse FITC IgG1 isotype (for P-selectin)	OriGene Technologies, Inc. (Rockville, MD, USA) SM10F
Mouse FITC IgG1κ isotype (for fibrinogen)	BioCytex SARL (Marseille, France) 5108-F100T
Mouse FITC IgMκ isotype (for PAC-1)	Becton Dickinson (Franklin Lakes, NJ, USA) 551448
Mouse monoclonal FITC anti-P-selectin	OriGene Technologies, Inc. (Rockville, MD, USA) SM1150F
Mouse monoclonal FITC anti-human bound fibrinogen	BioCytex SARL (Marseille, France) 5009-F100T
Mouse monoclonal FITC anti-phospho-VASP (Ser^{239})	nanoTools Antikörpertechnik GmbH & Co. KG (Teningen, Germany) 0047-100FITC-VASP-16C2
Mouse monoclonal FITC PAC-1	Becton Dickinson (Franklin Lakes, NJ, USA) 340507
Mouse monoclonal PE anti-GPVI	BioCytex SARL (Marseille, France) 5131-PE100T
Mouse PE IgG2aλ isotype (for GPVI)	BioCytex SARL (Marseille, France) 5127-PE100T
Rabbit polyclonal anti-$P2X_1$ receptor	Alomone Labs (Jerusalem, Israel) #APR-022
Rabbit polyclonal anti-$P2Y_1$ receptor	Alomone Labs (Jerusalem, Israel) #APR-021
Rabbit polyclonal anti-$P2Y_{12}$ receptor	Alomone Labs (Jerusalem, Israel) #APR-020
Rabbit polyclonal anti-phospho-PP2A	Bio-Techne GmbH (Wiesbaden-Nordenstadt, Germany) AF3839

TRITC-conjugated phalloidin	Sigma-Aldrich by Merck KgaA (Darmstadt, Germany) P1951

3.1.4. Kits

20S Proteasome Activity Assay Kit	CHEMICON (Merck KgaA, Darmstadt, Germany) APT280
BCA Protein Assay Kit	Pierce (Fisher Scientific, Schwerte, Germany) 23225
PLT Gp/Receptors Kit	BioCytex SARL (Marseille, France) 7004
PLT VASP/P2Y12 Kit	BioCytex SARL (Marseille, France) 7014
Poly-Ubiquitinated Protein ELISA Kit	CycLex (MBL International Corporation, Woburn, MA, USA) Cy-7053

3.1.5. Disposable Materials

Blood collection tube	S-Monovette 10 mL 9NC (SARSTEDT AG & Co. KG, Nuembrecht, Germany) 02.1067.001
Chamber slides, 8-well	ibidi GmbH (Graefeling, Germany) 80841
Coverslips, 24 x 60 mm	ibidi GmbH (Graefeling, Germany) 10811
Cuvettes, plastic, for aggregometry	Haemochrom Diagnostica GmbH (Essen, Germany) 40.000.0098
Filter paper, for blotting	A. Hartenstein GmbH (Wuerzburg, Germany) GB33
Flow chamber, µ-slide 0.2 mm, uncoated	ibidi GmbH (Graefeling, Germany) 80161
Luer connectors for flow chamber	ibidi GmbH (Graefeling, Germany) 10825; 10802

Nitrocellulose membrane, 0.45 µm	Amersham Protran (A. Hartenstein GmbH, Wuerzburg, Germany) NCA4
Silicone tube, 0.8 mm	ibidi GmbH (Graefeling, Germany) 10841
Syringe, 10 mL	BD PlastiPak (Becton Dickinson, Franklin Lakes, NJ, USA) 300911
Syringe filter unit, 0.2 µm	Filtropur S 0.2 (SARSTEDT AG & Co. KG, Nuembrecht, Germany) 83.1826.001
Tubing set for automated blood collection system	Trima Accel LRS Platelet, Plasma Set (Terumo BCT, Lakewood, CO, USA)

3.1.6. Buffers and solutions

Buffers were prepared with sterile water (Ampuwa, Fresenius Kabi Deutschland GmbH, Bad Homburg, Germany), if not indicated otherwise and pH was adjusted using hydrochloric acid (HCl) or sodium hydroxide (NaOH).

Buffer	**Ingredients**
Blocking buffer for flow chamber analysis, pH 7.4	1 % (w/v) BSA, 0.1 % (w/v) glucose, 0.9 % (w/v) NaCl in HBSS
Blocking buffer for immunofluorescence	10 % (v/v) goat serum, 0.1 % (v/v) Triton X-100 in PBS
Blocking buffer for Western blot	5 % (w/v) BSA in TBS-T buffer
CGS buffer, pH 6.5	120 mM NaCl, 12.9 mM citrate, 30 mM glucose
Electrophoresis buffer	50 mM TRIS, 192 mM glycine, 0.1 % (w/v) SDS
FACS buffer	5 mM glucose, 0.5 % (w/v) BSA in PBS
Modified HBSS buffer, pH 7.4	10 mM HEPES, 2.5 mM probenecid, 1 mM EGTA, 0.1 % (w/v) BSA, 0.01 % (w/v) pluronic F-127, 2 µM Fluo-4 AM in HBSS

Modified Tyrode's buffer, pH 6.2	10 mM HEPES, 150 mM NaCl, 3 mM KCl, 1 mM $MgCl_2$, 5 mM glucose, 0.1 % (w/v) BSA
Ponceau S staining solution	0.1 % (w/v) Ponceau S, 5 % (v/v) acetic acid
3X SDS sample buffer	40 % (v/v) TRIS-HCl (pH 6.7), 15 % (v/v) glycerol, 0.03 % (w/v) bromophenol blue, 6 % (w/v) SDS, 10 % (v/v) β-mercaptoethanol
Transfer buffer	25 mM TRIS, 192 mM glycine, 20 % (v/v) methanol
TBS-T buffer	0.1 % (v/v) Tween 20 in TBS
TRIS buffered saline (TBS), pH 7.6	137 mM NaCl, 20 mM TRIS

3.1.7. Devices

Aggregometer	APACT 4004, 4-channel aggregometer (Labor BioMedical Technologies GmbH, Ahrensburg, Germany)
Automated blood collection system	Trima Accel (Terumo BCT Inc., Lakewood, CO, USA)
Balances	PLJ 3500-2NM; ABJ 120-4M (Kern & Sohn GmbH, Balingen, Germany)
Blood gas analyzer	cobas b 123 V4.14 (Roche Diagnostics GmbH Mannheim, Germany)
Blot systems	Trans-Blot Cell and Trans-Blot Turbo (Bio-Rad Technologies GmbH, Feldkirchen, Germany)
Centrifuges	Hettich Universal 320 R and Hettich Mikro 200 R (Hettich GmbH & Co. KG, Tuttlingen) neoLab 3-Speed Mini Zentrifuge D-6015 (neoLab Migge GmbH, Heidelberg)
Flow cytometer	FACSCalibur (Becton Dickinson, Franklin Lakes, NJ, USA)
Gel electrophoresis chamber	Mini-Protean Tetra Cell (Bio-Rad Technologies GmbH, Feldkirchen, Germany)

Gel imaging system	ChemiDoc MP (Bio-Rad Technologies GmbH, Feldkirchen, Germany)
Hematology analyzer	Sysmex KX-21N (Sysmex Deutschland GmbH, Norderstedt, Germany)
Incubator	BE 40 (Memmert GmbH & Co. KG, Schwabach, Germany)
Laminar flow cabinet	Thermo Scientific Heraeus HERAGUARD HPH 12/95 (Fisher Scientific GmbH, Schwerte, Germany)
Magnetic stirrer with heater	NeoMag D-6010 (neoLab Migge GmbH, Heidelberg)
Microplate fluorometer	Thermo Scientific Fluoroskan Ascent (Fisher Scientific GmbH, Schwerte, Germany)
Microplate reader	Thermo Scientific Multiskan FC (Fisher Scientific GmbH, Schwerte, Germany)
Microplate washer	Thermo Scientific Wellwash Versa V 1.02.5 (Fisher Scientific GmbH, Schwerte, Germany)
Microscope with incubator	Eclipse Ti2 (Nikon, Tokio, Japan) OKOLAB S.R.L. (Pozzuoli, NA, Italy)
Orbital plate shaker	VM 4 (Ingenieurbüro CAT, M. Zipperer GmbH, Ballrechten-Dottingen, Germany)
Overhead shaker	Intelli-Mixer RM-2M (neoLab Migge GmbH, Heidelberg)
pH Meter	HI2211 pH/ORP (Hanna Instrument Deutschland GmbH, Vöhringen, Germany)
Pipettes	Pipetman L (Gilson Inc., Middleton, WI, USA)
Pipetting aid	Sunlab SU1700 (Labdiscount GmbH, Mannheim, Germany)
Power supply	PowerPac Universal (Bio-Rad Technologies GmbH, Feldkirchen, Germany)
Recirculating cooler	Julabo FL300 (JULABO GmbH, Seelbach, Germany)
Rocking shaker	DRS-12 (neoLab Migge GmbH, Heidelberg)
Thermoblock heater	ThermoMixer C (Eppendorf AG, Hamburg, Germany)
Vortexer	Vortex Genie 2 G560E (Scientific Industries, Inc., Bohemia, NY, USA)

Water bath	SW23 (JULABO GmbH, Seelbach, Germany)

3.1.8. Software

Aggregometer	AS-IS Version 1.210
Flow Cytometer	CellQuest, Version 6.0
Microplate fluorometer	Ascent Software Version 2.6
Image processing program	ImageJ 1.53f51
Microplate reader	SkanIt 3.1
Microscope	NIS Elements AR 5.02.00
Scientific graphing program	GraphPad Prism, Version 9.00

3.2. Methods

3.2.1. Blood collection

The blood samples for the experiments were obtained as citrated venous whole blood (WB) from informed healthy voluntary donors without any medication intake. The peripheral blood was collected from a superficial brachial vein in polypropylene (PP) tubes, containing 3.2 % citrate buffer (106 mM trisodium citrate, SARSTEDT AG & Co. KG, Nuembrecht, Germany). Apheresis-derived platelet concentrates (APC) (2.5×10^{11} platelets in 250 mL of plasma) were collected using Trima Accel devices with version 11.3 software and the Trima Accel LRS Platelet, Plasma Set (Terumo BCT, Lakewood, CO, USA). The ratio of inlet blood volume to anticoagulant (ACD-A) was 10:1.

The studies with human platelets and the consent procedure were approved by our local ethics committee of the University of Wuerzburg (approval number 101/15). All blood donors who participated in the studies provided their written informed consent to participate in this study. All studies were performed according to our institutional guidelines and the Declaration of Helsinki.

3.2.2. Proteasome inhibition

For proteasome inhibition, WB was incubated with the proteasome inhibitor bortezomib for 24 hours (h) at room temperature (RT), if not indicated otherwise. For each experiment, four identical tubes of WB were obtained from one single donor as described in **3.2.1**. One tube was used immediately for investigation as untreated fresh blood (“day 0”). The other three tubes were left for 24 h at RT under continuous and gentle agitation on a rocking shaker after incubation with buffer as control (“day 1 – Ctrl”) or bortezomib with a final concentration of 5 nM (“day 1 – 5 nM bortezomib”) or 1 µM (“day 1 – 1 µM bortezomib”), respectively, under sterile conditions using laminar air flow technique to avoid bacterial contamination. Bortezomib was freshly diluted in phosphate-buffered saline (PBS) from 100 mM stock dissolved in dimethyl sulfoxide (DMSO, 100 %) and sterile filtered prior to every usage. In the first step, 100 mM bortezomib was diluted 1:1,000 with PBS, resulting in 100 µM bortezomib (0.1 % DMSO). The 100 µM bortezomib solution was used for incubation

of WB samples with a final dilution of 1:100, resulting in 0.001 % DMSO in WB tubes spiked with 1 µM bortezomib. For achieving 5 nM bortezomib, 100 µM bortezomib solution was further diluted 1:200 with PBS (0.0005 % DMSO), and then used 1:100 in WB samples, resulting in 5 nM bortezomib and 0.000005 % final DMSO concentration. The slight DMSO contamination did not affect blood cell count and basic blood characteristics, GP expression, aggregometry or VASP phosphorylation as recently shown [177, Supplementary Material]. According to previous studies [172], 5 nM bortezomib was used as concentration mediating partial inhibition, 1 µM bortezomib as high concentration mediating near-total inhibition of platelet proteasome activity. Whole blood was used for the incubation period with bortezomib due to the presence of all blood components (similar to conditions *in vivo* including possible interactions with other blood cell types) and due to superior preservation of platelet function for 24 h. For further platelet-specific experimentation, PRP was obtained as described in **3.2.3.1**.

Flow chamber analysis using life cell imaging system was conducted using PRP obtained from APC and incubation for 60 minutes (min) with 1 µM bortezomib (final concentration) at RT.

Proteasome inhibition using carfilzomib as alternative proteasome inhibitor was exerted for 60 min in PRP as described in **3.2.3.1**. Stock solution of carfilzomib, dissolved in 100 % DMSO, was further diluted in DMSO and used 1:1,000 in PRP samples, resulting in a final DMSO concentration of 0.1 % for each concentration of carfilzomib. Therefore, control samples were spiked with 0.1 % DMSO final concentration to avoid matrix-related effects by DMSO.

3.2.3. Platelet preparation

3.2.3.1. Preparation of platelet-rich-plasma and platelet-poor-plasma

To prepare PRP, WB was centrifuged (Hettich Universal 320 R) for 5 min at 280 *x g* at RT as previously described [172]. The centrifugation results in distinct blood layers, from which the top layer served as PRP. 75 % of this top layer was transferred to a fresh round bottom PP tube to minimize white blood cell contamination with concentrations below the detection limit of 0.1 × 10^3 /µL. Platelet concentration and

white blood cell contamination was determined with the hematology analyzer Sysmex KX-21N from Sysmex Deutschland GmbH (Norderstedt, Germany).

To yield platelet-poor-plasma (PPP), PRP was transferred to a 1.5 mL tube and was further centrifuged (Hettich Mikro 200 R) at 21,000 *x g* for 2 min at RT. The resulting supernatant was transferred to a fresh 1.5 mL tube and served as PPP, which was used as 100 % calibration for light transmission aggregometry as described in **3.2.4**.

3.2.3.2. Preparation of washed platelets

For the preparation of washed platelets (WP), 3 mM ethylene glycol-bis(2-aminoethylether)-N,N,N′,N′-tetraacetic acid (EGTA) was added to WB prior to preparation of PRP as described in **3.2.3.1** to prevent platelet activation [172]. Subsequently, obtained PRP was further centrifuged at 430 *x g* for 10 min at RT. The supernatant was discarded, the pellet was resuspended in 5 mL CGS buffer (120 mM NaCl, 30 mM glucose, 12.9 mM trisodium citrate, pH 6.5) as washing step and centrifuged again at 430 *x g* for 7 min at RT. The pellet was resuspended in Tyrode's Salt Solution (Tyrode's buffer). After determining the platelet concentration with the hematology analyzer, platelet count was adjusted to 3.0×10^8 platelets/mL with Tyrode's buffer for experimentation.

3.2.3.3. Preparation of platelets for $P2Y_1R$ activity measurement

For platelet $P2Y_1R$ activity measurement, PRP was obtained as described in **3.2.3.1** and subsequently spiked with 500 nM PGE_1 followed by centrifugation at 430 x *g* for 5 min at RT, with little modifications as described [178]. The pellet was washed in 5 mL modified Tyrode's buffer (10 mM HEPES, 150 mM NaCl, 3 mM KCl,1 mM $MgCl_2$, 5 mM glucose, 0.1 % (w/v) BSA, pH 6.2) containing 500 nM PGE_1 and centrifuged again at 430 *x g* for 5 min at RT. The supernatant was discarded and the pellet was resuspended in 1 mL modified Tyrode's buffer without PGE_1. After determination of the platelet concentration, platelet count was finally adjusted to 0.6×10^8 platelets/mL with modified Tyrode's buffer without PGE_1.

3.2.3.4. Preparation of platelets for $P2X_1R$ activity measurement

For platelet $P2X_1R$ activity measurement, PRP was obtained as described in **3.2.3.1** and subsequently supplemented with 1 mM acetylsalicylic acid (ASS) and 0.3 U/mL apyrase and centrifuged at 430 *x g* for 5 min at RT, with little modifications as described [178]. The pellet was washed in 5 mL modified Tyrode's buffer containing 1 mM ASS, 0.3 U/mL apyrase and 3 mM EGTA and centrifuged again at 430 *x g* for 5 min at RT. The pellet was resuspended in 1 mL modified Tyrode's buffer containing 0.3 U/mL apyrase. After determination of the platelet concentration, platelet count was finally adjusted to 0.6×10^8 platelets/mL with modified Tyrode's buffer containing 0.3 U/mL apyrase.

3.2.3.5. Preparation of platelet lysates for protein quantification, 20S proteasome activity assay and poly-ubiquitylated proteins ELISA

Platelets were obtained as WP as explained in **3.2.3.2**, aliquoted in fresh tubes (400 µL per tube) and were allowed to rest for 15 min at RT without shaking, followed by addition of 1 mM $CaCl_2$ as previously described [172]. Subsequently, platelets were stimulated according to experiments for 60 min at 37 °C. Samples were then centrifuged at 21,000 *x g* for 2 min at RT and the resulting pellets were lysed in 200 µL of cold ready-to-use cell extraction buffer from the CycLex Poly-Ubiquitinated Protein ELISA kit (MBL International Corporation, Woburn, MA, USA) for 30 min on ice, vortexing gently every 10 min. These crude lysates were used for the determination of the proteasome activity as described in **3.2.9** and for the determination of protein concentration in these samples with the bicinchoninic acid (BCA) assay as described in **3.2.8**.

Crude lysates were further centrifuged at 21,000 *x g* for 10 min at 4 °C and the resulting supernatant was transferred to fresh chilled tubes. Obtained clear lysates were used for the determination of poly-ubiquitylated proteins as described in **3.2.10** and for protein quantification as well.

3.2.4. Light transmission aggregometry

Aggregation studies were performed with 200 µL of corresponding PPP and PRP, obtained as described in **3.2.3.1,** in plastic cuvettes with stirrer under continuous stirring at 1,000 revolutions per minute (rpm) and 37 °C using Born aggregometry [109]. PRP was preincubated at 37 °C for 5 min. Before each measurement, the 4-channel platelet aggregometer APACT 4004 from Labor BioMedical Technologies GmbH (Ahrensburg, Germany) was calibrated with corresponding PPP as 100 % aggregation and PRP as 0 % aggregation. Finally, PRP was stimulated with distinct concentrations of ADP, collagen or TRAP-6 for irreversible platelet aggregation according to experimental design or with individual concentrations of ADP, collagen, convulxin, TRAP-6 or ristocetin for threshold aggregation and agglutination to induce a weak and submaximal response. Aggregation curves were measured for 5 min, recording aggregation every two seconds (s). For statistical evaluation, maximal aggregation values in percent were determined for each curve.

3.2.5. Flow cytometry

3.2.5.1. Expression of P-selectin, $P2Y_1R$, $P2Y_{12}R$, $P2X_1R$, GPVI, fibrinogen binding and PAC-1 antibody binding

Flow cytometric analysis of the expression of P-selectin, $P2Y_1R$, $P2Y_{12}R$, $P2X_1R$, GPVI, fibrinogen binding and PAC-1 antibody binding was performed using PRP as described in **3.2.3.1**. Platelets were stained with an appropriate amount of fluorescein isothiocyanate (FITC)-conjugated, phycoerythrin (PE)-conjugated or unconjugated primary antibody for 10 min at RT in the dark according to the following **Table 1**, accompanied by a suitable isotype control sample.

Antibody	Dilution in PRP
anti-P-selectin	1:10
anti-$P2Y_1R$	1:7.5
anti-$P2Y_{12}R$	1:7.5
anti-$P2X_1R$	1:7.5
anti-GPVI	1:15
anti-human bound fibrinogen	1:2
PAC-1	1:2

Table 1: **Used antibody dilutions for flow cytometry.**

Platelets were then stimulated with buffer as control or with 10 µM TRAP-6 for 2 min or for 150 min for GPVI measurement, respectively, according to experimental design. Afterwards, reaction was stopped by addition of 1 % final concentration of formaldehyde (FA) and fixed for 10 min at RT in the dark. Samples labeled with FITC-conjugated (anti-P-selectin, anti-human bound fibrinogen, PAC-1) or PE-conjugated (anti-GPVI) primary antibodies were directly diluted with 500 µL of FACS buffer. Samples incubated with unconjugated primary antibodies were centrifuged for 1 min at 14,000 *x g* at RT. The resulting pellet was resuspended in 100 µL FACS buffer, containing FITC-conjugated goat anti-rabbit secondary antibody (1:100 dilution) for 30 min at RT in the dark and finally diluted with 500 µL of FACS buffer. Samples were analyzed with the flow cytometer FACSCalibur from Becton Dickinson (Franklin Lakes, NJ, USA) using forward and side scatter distribution to identify platelet population. Mean fluorescence intensity (MFI) of 10,000 events was measured for statistical analysis.

Influence of inhibitory signaling on TRAP-6-stimulated fibrinogen binding was analyzed by preincubation of PRP samples (stained with anti-human bound fibrinogen antibody as described above) with buffer as control, with 1 µM DEA/NO or with 0.25 µM PGE_1, respectively, for 5 min at 37 °C, prior to stimulation with 10 µM TRAP-6, fixation and dilution, as described above.

3.2.5.2. Measurement of VASP phosphorylation

Phosphorylation of VASP was determined using PRP as described in **3.2.3.1**. Platelets were preincubated with buffer as control, 1 µM DEA/NO or 1 µM PGE_1 for 5 min at 37 °C and fixed with a final concentration of 2.5 % FA for 10 min at RT. Subsequently, the samples were centrifuged at 20,000 *x g* for 1 min at RT and obtained platelets were permeabilized with 0.2 % final concentration of Triton X-100 in FACS buffer for 10 min at RT prior to incubation with 10 µg/mL FITC-conjugated anti-pospho-VASP-Ser^{239} antibody (final concentration) in FACS buffer for 30 min at RT in the dark. Samples were finally diluted with 500 µL of FACS buffer and analyzed with the flow cytometer using forward and side scatter distribution to identify platelet population. MFI of 10,000 events was measured for statistical analysis.

3.2.5.3. Determination of $P2Y_{12}R$ activity

The PLT VASP/P2Y12 kit from BioCytex SARL (Marseille, France) was used in flow cytometry according to manufacturer's instructions to determine $P2Y_{12}R$ activity. In brief, WB samples were incubated with PGE_1 alone or with the combination of ADP and PGE_1 for 10 min at RT. Afterwards, samples were fixed for 5 min at RT, followed by permeabilization and staining with the primary antibody (anti-phospho-VASP-Ser^{239}) for 5 min at RT and additional 5 min at RT with the secondary FITC-conjugated antibody. Finally, samples were diluted and analyzed by flow cytometry. Platelet reactivity index (PRI) was used for statistical analysis calculated by the following equitation using corrected mean fluorescence intensities (MFIc):

$$PRI = \frac{MFIc_{\,PGE_1} - MFIc_{\,PGE_1+ADP}}{MFIc_{\,PGE_1}} \times 100\,\%$$

3.2.5.4. Count of platelet GPIIb and GPIb

For the quantitative measurement of GPIIb and GPIb on platelet surface, the PLT Gp/Receptors kit from BioCytex SARL (Marseille, France) was used in flow cytometry according to manufacturer's instructions. Shortly, WB samples were stimulated with

TRAP-6 or buffer as control for 5 min at RT, followed by incubation with the appropriate primary antibodies for GPIIb or GPIb for 10 min at RT. All samples and an additional tube with calibrated beads coated with increasing and defined quantities of mouse immunoglobulin G (IgG) were then stained with the secondary FITC-conjugated antibody for 10 min at RT. Finally, all samples were diluted and analyzed by flow cytometry for their MFI, measuring 20,000 events for stained platelets and at least 8,000 events for the beads in the selected gate. For quantitative evaluation, a standard curve with the MFI from the three calibrated beads and the corresponding count of mouse IgG antibodies is created. GPIIb and GPIb count is then calculated with the measured MFI based on the standard curve.

3.2.6. Fluorescence-based $P2Y_1R$ and $P2X_1R$ activity assay

Platelets were prepared as described in **3.2.3.3** for $P2Y_1R$ activity or in **3.2.3.4** for $P2X_1R$ activity, respectively. For the measurement of $P2Y_1R$ and $P2X_1R$ activity, a calcium flux-induced fluorescence assay was used with little modifications as described [178]. Platelets were loaded with Fluo-4 AM in a black-walled 96-well plate by mixing 100 µL of platelet suspension (0.6×10^8 platelets/mL) with an equal volume of Hanks' Balanced Salt Solution (HBSS), containing 10 mM HEPES, 0.1 % (w/v) BSA, 2.5 mM probenecid, 1 mM EGTA, 0.01 % (w/v) pluronic F-127 and 2 µM Fluo-4 AM at pH 7.4. For $P2X_1R$ activity measurements, 0.3 U/mL apyrase was additionally added and EGTA was substituted by 2.5 mM $CaCl_2$. The plate was first incubated at RT for 20 min in the dark, followed by 20 min incubation at 37 °C in the dark. To control receptor specificity, defined wells were spiked with 1 µM final concentration of (1*R**,2*S**)-4-[2-Iodo-6-(methylamino)-9*H*-purin-9-yl]-2-(phosphornooxy)bicyclo[3.1.0]-hexane-1-methanol dihydrogen phosphate ester tetraammonium salt (MRS2500) or 4,4',4'',4'''-[Carbonylbis(imino-5,1,3-benzenetriyl-*bis*(carbonylimino))] *tetrakis*-1,3-benzenedisulfonic acid octasodium salt (NF449) as $P2Y_1R$ or $P2X_1R$ antagonist, respectively, for the last 10 min of incubation at 37 °C. Afterwards, basal fluorescence was measured every second for 20 s with 488 nm excitation- and 538 nm emission-filter pair at the microplate fluorometer Fluoroskan Ascent from Fisher Scientific GmbH (Schwerte, Germany). Finally, platelets were stimulated with 1 µM final concentration of [(1*R*,2*R*,3*S*,4*R*,5*S*)-4-[6-Amino-2-(methylthio)-9*H*-purin-9-yl]-2,3-

dihydroxy-bicyclo[3.1.0]hex-1-yl]methyl] di-phosphoric acid mono ester trisodium salt (MRS2365) or α,β-Methyleneadenosine 5'-triphosphate trisodium salt (α,β-MeATP) as specific $P2Y_1R$ and $P2X_1R$ agonist or with buffer as control, respectively, and fluorescence was measured every second for 180 s. For statistical analysis, maximal calcium-flux-induced fluorescence in relative fluorescence units (RFU) was determined for each curve.

3.2.7. SDS-PAGE and Western blot analysis

Platelets were prepared as WP as described in **3.2.3.2**, spiked with 1 mM $CaCl_2$ and allowed to rest for 15 min at 37 °C. Samples were stopped and denatured by boiling with half sample volume of 3X SDS sample buffer (40 % (v/v) TRIS-HCl (pH 6.7), 15 % (v/v) glycerol, 0.03 % (w/v) bromophenol blue, 6 % (w/v) SDS, 10 % (v/v) β-mercaptoethanol) at 95 °C for 5 min. Samples were stored at - 20 °C and thawed at 65 °C for 5 min or used directly after preparation for protein separation in sodium dodecyl sulfate-polyacrylamide gel electrophoresis (SDS-PAGE) [179]. It was used a 5 % stacking gel and a 10 % resolving gel according to the following gel recipe in **Table** 2.

Components	10 % Resolving gel	5 % Stacking gel
Water	15.80 mL	10.28 mL
30 % Acrylamide/ Bisacrylamide (37.5 : 1)	10.00 mL	2.50 mL
3 M TRIS-HCl, pH 8.9	3.74 mL	-
0.5 M TRIS-HCl, pH 6.7	-	1.92 mL
10 % SDS	300 µL	150 µL
10 % APS	150 µL	150 µL
TEMED	15 µL	7.5 µL
Total	**30 mL**	**15 mL**

Table 2: Gel recipe for resolving and stacking gel for SDS-PAGE

After preparation of the polyacrylamide gel, 20 µL of each sample was loaded into the wells, accompanied by at least one well with 20 µL of protein marker (3 µL prestrained protein ladder in 17 µL 1X SDS sample buffer). Gel electrophoresis chamber was assembled, filled with electrophoresis buffer (50 mM TRIS, 192 mM glycine, 0.1 % (w/v) SDS) and applied to a voltage of 80 V for 30 min, followed by approximately 60 min at 150 V, until the running front arrived at the bottom border of the glass chamber.

Subsequently, Western blot system was used to transfer proteins from the polyacrylamide gel onto a nitrocellulose membrane for 1 h at 1,000 mA while cooling in tank-blot or 30 min at 500 mA in semi-dry blot system, using transfer buffer (25 mM TRIS, 192 mM glycine, 20 % (v/v) methanol) [180, 181]. Afterwards, the membrane was incubated for a few seconds in Ponceau S staining solution (0.1 % (w/v) Ponceau S, 5 % (v/v) acetic acid) to check protein transfer success and the membrane was scanned with the gel imaging system ChemiDoc MP from Bio-Rad Technologies GmbH (Feldkirchen, Germany).

To prevent unspecific antibody binding, the membrane was decolorized in water and blocked with blocking buffer, containing 5 % (w/v) BSA in TBS-T buffer (0.1 % (v/v) Tween 20, 137 mM NaCl, 20 mM TRIS) for 20 min. The membrane was incubated overnight at 4 °C while shaking with rabbit polyclonal anti-phospho-PP2A antibody diluted in 5 % (w/v) BSA in TBS-T buffer (1:100 dilution) as primary antibody. On the next day, the membrane was washed 3 times for 5 min with TBS-T buffer and was subsequently incubated for 1 h at RT while shaking with goat anti-rabbit StarBright Blue 700-conjugated secondary antibody, diluted in 5 % (w/v) BSA in TBS-T buffer (1:2,500 dilution). Finally, the membrane was washed 6 times for 10 min with TBS-T buffer and directly scanned using the gel imaging system.

For statistical analysis, actin bands from the Ponceau S-stained membrane and the specific phospho-protein bands were quantified with ImageJ (Wayne Rasband, NIH, USA) to determine relative expression patterns.

3.2.8. Protein concentration measurement

Protein concentration was determined with the BCA assay [182], using the Pierce BCA Protein Assay kit From Thermo Fisher (Schwerte, Germany) according to manufacturer's instructions with crude and clear lysates as described in **3.2.3.5**. Briefly, lysates were spiked with 50 mM NaOH and boiled for 5 min at 95 °C on the thermoblock heater. 10 µL of each sample was then transferred to a transparent microplate, which was thoroughly shaken after addition of 200 µL working reagent for 30 s. Subsequently, the plate was covered and incubated at 37 °C for 30 min. After cooling to RT, absorbance was finally measured at 550 nm wavelength at the microplate reader Multiskan FC from Thermo Fisher (Schwerte, Germany). Samples were measured as duplicates and protein concentration was calculated on basis of the recorded BSA standard curve.

3.2.9. Platelet 20S proteasome activity measurement

Basal and collagen-induced platelet proteasome activity was investigated with the CHEMICON 20S Proteasome Activity Assay kit from Merck KgaA (Darmstadt, Germany) according to manufacturer's instructions using crude platelet lysates as described in **3.2.3.5**. In short, 90 µL of diluted crude lysate (13 µL crude lysate in 77 µL 1X Assay buffer) was loaded in a black-walled 96-well plate with 10 µL proteasome substrate LLVY-AMC and incubated for 60 min at 37 °C. Active proteasome cleaves the fluorophore 7-Amino-4-methylcoumarin (AMC) from the substrate. Fluorescence of released AMC was then measured with the 380 nm excitation- and 460 nm emission-filter pair at the microplate fluorometer. All samples were measured in duplicates.

3.2.10. Measurement of poly-ubiquitylated protein levels

Poly-ubiquitylated protein levels were analyzed with the CycLex Poly-Ubiquitinated Protein ELISA kit from MBL International Corporation (Woburn, MA, USA) according to manufacturer's instructions using enzyme-linked immunosorbent assay (ELISA) technique with clear lysates as described in **3.2.3.5** [183]. In brief, clear lysates were

diluted 1:100 with the supplied dilution buffer and 100 µL of these diluted lysates were incubated on the provided microplate for 1 h at RT while shaking at 300 rpm on an orbital shaker. Afterwards, wells were washed 4 times with 350 µL 1X wash buffer with the microplate washer Wellwash Versa from Thermo Fisher (Schwerte, Germany). 100 µL of HRP-conjugated detection antibodies against poly-ubiquitin were added to the wells and incubated for 1 h at RT while shaking at 300 rpm. The plate was washed again 4 times with 350 µL 1X wash buffer, followed by addition of 100 µL substrate reagent to each well. Subsequently, the plate was incubated for 20 min at RT in the dark while shaking at 300 rpm. Finally, reaction was stopped by addition of 100 µL stop solution and the absorbance was measured in the microplate reader at dual wavelengths of 450 nm and 550 nm. All samples and standards were measured in duplicates. Data analysis was assessed with the microplate reader software SkanIt 3.1.

3.2.11. Immunofluorescence microscopy

The slides were coated with different materials (100 µg/mL fibrinogen, 0.25 µg/mL collagen or 0.5 mg/mL ristocetin) for 30 min at 37 °C and rinsed afterwards twice with PBS. Platelets from 24 h stored WB, with or without bortezomib, were prepared as PRP as described in **3.2.3.1** and subsequently diluted to a concentration of 0.1×10^8 platelets/mL with PBS. Diluted PRP was seeded onto the slides in the presence of 1 mM $CaCl_2$ for 20 min at RT without shaking. The slides were washed again once with PBS to remove unattached platelets and immediately fixed with 8 % FA for 15 min on ice. After a washing step with PBS, the platelets were permeabilized for 10 min with 0.2 % (v/v) Triton X-100 in PBS. The slides were blocked with blocking buffer (10 % (v/v) goat serum, 0.1 % (v/v) Triton X-100 in PBS) for 1 h and subsequently stained with tetramethylrhodamine thiocyanate (TRITC)-conjugated phalloidin from Sigma-Aldrich by Merck KgaA (Darmstadt, Germany), diluted in PBS containing 10 % (v/v) goat serum and 0.1 % (v/v) Triton X-100 overnight. Next day, the slides were rinsed five times with PBS and mounted with ProLong Diamond Antifade Mountant from Fisher Scientific GmbH (Schwerte, Germany). After 24 h of curing at RT, the slides were stored at 4 °C until immunofluorescence imaging was performed or directly analyzed. Method is based on the National Institute for Biological Standards

and Control (NIBSC) consensus protocol: Platelet Immunofluorescence Test Protocol published by von dem Borne *et al*. [184]. Mounted samples were imaged on an inverted Nikon Eclipse Ti2 microscope from Nikon GmbH (Duesseldorf, Germany) using a 60× oil immersion objective lens (CFI Plan Apo Lambda 60× Oil, MRD01605, Nikon), integrated 1.5× zoom and a DS-Qi2 monochrome microscope camera (14-bit digitalization). For statistical analysis of the platelet forms, more than 200 cells per setup were imaged, analyzed and manually assigned to the platelet adhesion steps “resting”, “dendritic” and “spread”.

3.2.12. Flow chamber live cell analysis

For live cell analysis, transparent flow chambers from ibidi GmbH (Graefeling, Germany) with a slit depth of 200 µm were used. First, the chambers were rinsed once with 1 mL HBSS, followed by coating with 100 µg/mL collagen at 4 °C overnight. Next day, coated chambers were rinsed once with 1 mL HBSS and subsequently blocked for 1 h with blocking buffer (1 % (w/v) BSA, 0.1 % (w/v) glucose, 0.9 % (w/v) NaCl in HBSS). Collagen-coated flow chambers were connected to a HBSS-filled syringe and loaded into the pulse-free syringe pump for 5 min and a shear rate of 150 1/s as final rinse step. Platelets were obtained as PRP from APC as described in **3.2.1**, adjusted to 2.5 × 10^8 platelets/mL with HBSS and spiked with 1 mM $CaCl_2$ final concentration. Platelets were transferred to a syringe and incubated for 10 min at 37 °C in the microscope incubating chamber. Afterwards, the syringe was connected to the prepared flow chamber and loaded to the pulse-free syringe pump, followed by perfusion with a shear rate of 150 1/s at 37 °C. During perfusion, phase-contrast images were recorded with the microscope Eclipse Ti2 using a 60× oil immersion objective lens (CFI Plan Apo Lambda 60× Oil, MRD01605, Nikon) and a DS-Qi2 monochrome microscope camera (14-bit digitalization) at six different spots longitudinal to the flow direction every two seconds for 10 min in real time. Results were qualitatively evaluated by visual consideration.

3.2.13. Statistical analysis

Statistical significance was calculated with the scientific graphing program GraphPad PRISM 9 (GraphPad Software, San Diego, CA, USA). The Shapiro-Wilk test was used for data distribution analysis. Differences of variances between groups were analyzed by one-way analysis of variance followed by post-hoc Tukey-Kramer-Test or by unpaired or paired, two-sided Student's *t*-test, as appropriate. For the analysis of platelet adhesion studies, the non-parametric Wilcoxon- and Kruskal-Wallis rank-based tests were used. $P < 0.05$ was considered as statistically significant.

4. Results

The involvement of the proteasome system in functional characteristics of human platelets is not entirely understood and is subject of current research. In parts, published data on the role and function of the proteasome system in human platelets display controversial results and conclusions. Therefore, in this thesis, specific effects of the potent and selective proteasome inhibitor bortezomib on human platelets were investigated to shed light on the involvement of the proteasome system in human platelet processes. The preincubation with bortezomib has been exerted in citrated WB for 24 h. First, to include long-term effects of proteasome inhibition, regarding the time-consuming process of protein turnover as one of the main functions of the proteasome, and second, to mimic the *in vivo* milieu of platelets most accurately. The doses of 5 nM and 1 µM bortezomib have been selected on the basis of actually occurring *in vivo* plasma concentrations after administration for clinical purposes and according to previous studies on dose-dependent inhibition of the human platelet proteasome system *in vitro* [154, 172]. The potent and selective proteasome inhibitor carfilzomib was used as a second inhibitor to rule out bortezomib-specific effects and to confirm that observed effects are related to proteasome inhibition.

4.1. Effect of proteasome inhibition on platelet activation

4.1.1. Irreversible platelet aggregation was not affected by bortezomib.

The very first consideration to evaluate the involvement of the proteasome system in activating mechanisms of human platelets was to determine the hemostatic function using light transmission aggregometry.

PRP was stimulated with 10 µM ADP, 10 µg/mL collagen or 10 µM TRAP-6 to induce stable and irreversible platelet aggregation, which was measured for 5 min with the APACT4004 aggregometer (Labor BioMedical Technologies GmbH, Ahrensburg, Germany) (**Figure 4.1**).

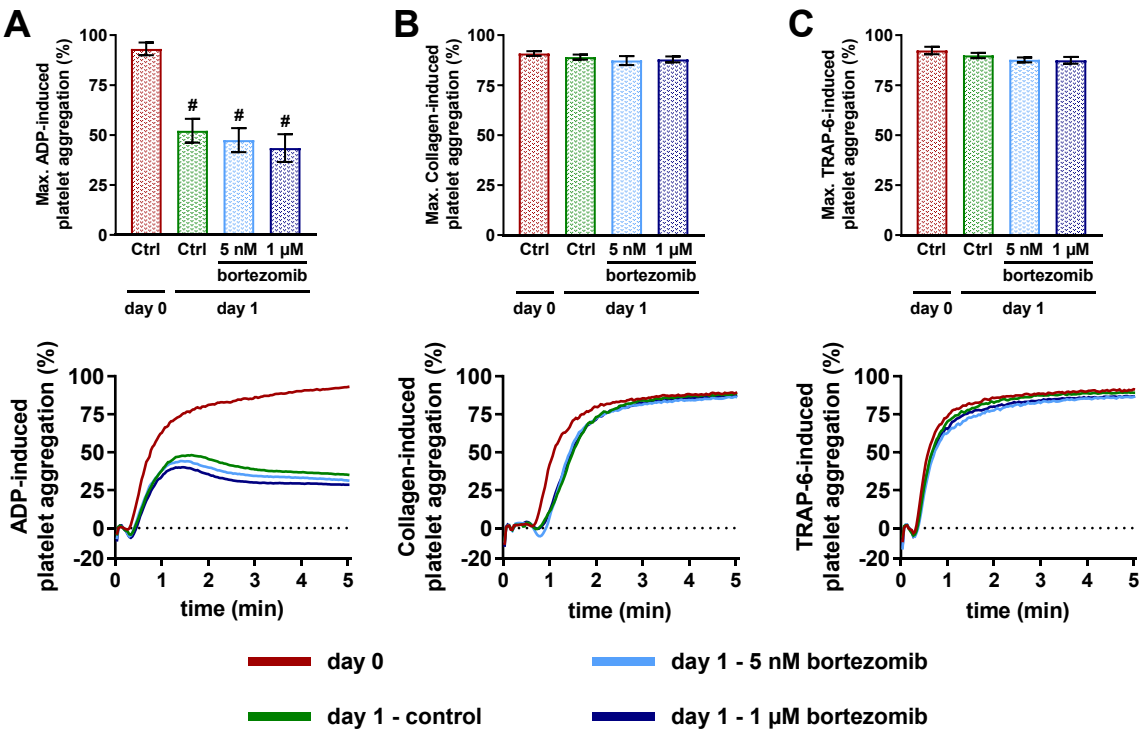

Figure 4.1: Irreversible platelet aggregation in PRP.

Data are presented as mean aggregation traces and as mean ± SEM of maximal aggregation. Light transmission aggregometry was induced with 10 µM ADP (**A**), 10 µg/mL collagen (**B**) or 10 µM TRAP-6 (**C**) in PRP prepared from fresh or 24 h stored citrated whole blood samples preincubated with or without bortezomib as indicated; $n = 6$; #: $p < 0.05$, compared to "day 0".

Using 10 µM ADP as agonist (**Figure 4.1A**), maximal aggregation reached 91.3 ± 2.1 % in PRP from fresh blood samples (day 0). Storage for 24 h led to a reduction of approximately 40 % to 52.2 ± 6.4 % in the control. Preincubation of WB with bortezomib for 24 h did not further affect platelet aggregation induced with 10 µM ADP.

Agonist-induced platelet aggregation with 10 µg/mL collagen (**Figure 4.1B**) and 10 µM TRAP-6 (**Figure 4.1C**) resulted in maximum aggregation values of 90.4 ± 1.2 % and 92.0 ± 1.6 %, respectively, in in PRP from fresh whole blood. In contrast to the induction with ADP, aggregation remained stable after 24 h of storage, irrespective whether bortezomib-preincubated or not.

Lower agonist concentrations of 5 µM ADP, 5 µg/mL collagen and 5 µM TRAP-6 showed comparable results.

4.1.2. Surface P-selectin expression and fibrinogen binding did not change under bortezomib.

The measurement of P-selectin and fibrinogen binding on the platelet surface, representing significant markers for the determination of platelet activation [185], was performed by flow cytometry using the FACSCalibur (Becton Dickinson, Franklin Lakes, NJ, USA) in PRP (**Figure 4.2**).

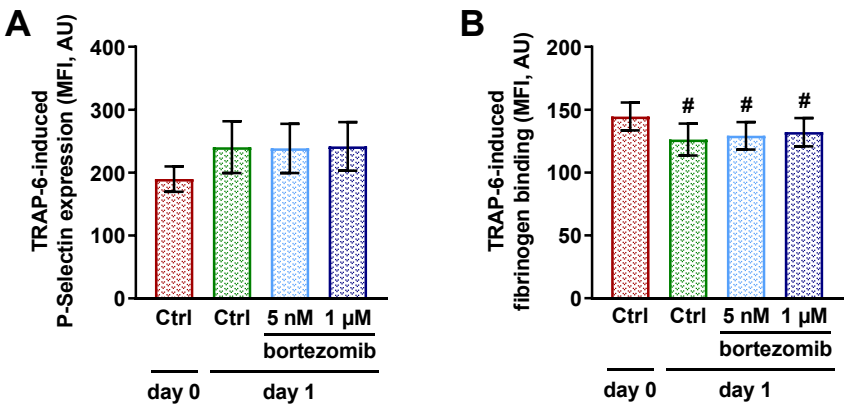

Figure 4.2: Surface expression of TRAP-6-induced P-selectin and fibrinogen binding in PRP.

10 µM TRAP-6-induced surface expression of P-selectin (**A**) and fibrinogen binding (**B**) in PRP prepared from fresh or 24 h stored citrated whole blood samples preincubated with or without bortezomib as indicated was determined by flow cytometry. Data are shown as mean of the MFI ± SEM; $n = 6$; #: $p < 0.05$, compared to "day 0".

TRAP-6-induced surface expression of P-selectin evoked 189.8 ± 20.1 MFI in PRP samples from fresh whole blood (**Figure 4.2A**), whereas expression showed a trend to higher levels with 240.4 ± 41.1 MFI in the control at day 1, comparable to bortezomib-incubated samples with 238.5 ± 39.2 MFI and 241.7 ± 38.7 MFI for 5 nM and 1 µM bortezomib, respectively. Basal values of P-selectin surface expression were moderately elevated after 24 h storage, from 16.5 ± 2.4 MFI to 27.8 ± 2.5 MFI. Samples treated with bortezomib remained unchanged, compared to control at day 1. Basal fibrinogen binding was slightly reduced after 24 h, from initially 26.0 ± 0.3 MFI to 18.6 ± 2.7 MFI, whereas values of bortezomib-treated samples were unchanged, compared to fresh samples. TRAP-6-stimulated fibrinogen binding values were slightly decreased from 144.6 ± 11.9 MFI to 126.2 ± 13.6 MFI after 24 h (**Figure 4.2B**). Blood samples preincubated with bortezomib did not differ from control at day 1 with 129.2 ± 11.7 MFI (5 nM bortezomib) and 132.1 ±12.0 MFI (1 µM bortezomib).

4.1.3. Platelet threshold aggregation and agglutination was enhanced under bortezomib.

In addition to irreversible aggregation, it was important to additionally analyze submaximal aggregation to detect potentially enhancing effects of bortezomib, which may be cached under strong induction of aggregation. Therefore, an individual concentration of ADP, collagen, convulxin, TRAP-6 or ristocetin was determined for each blood donor, required for submaximal threshold aggregation or agglutination in control samples at day 1 (**Figure 4.3**).

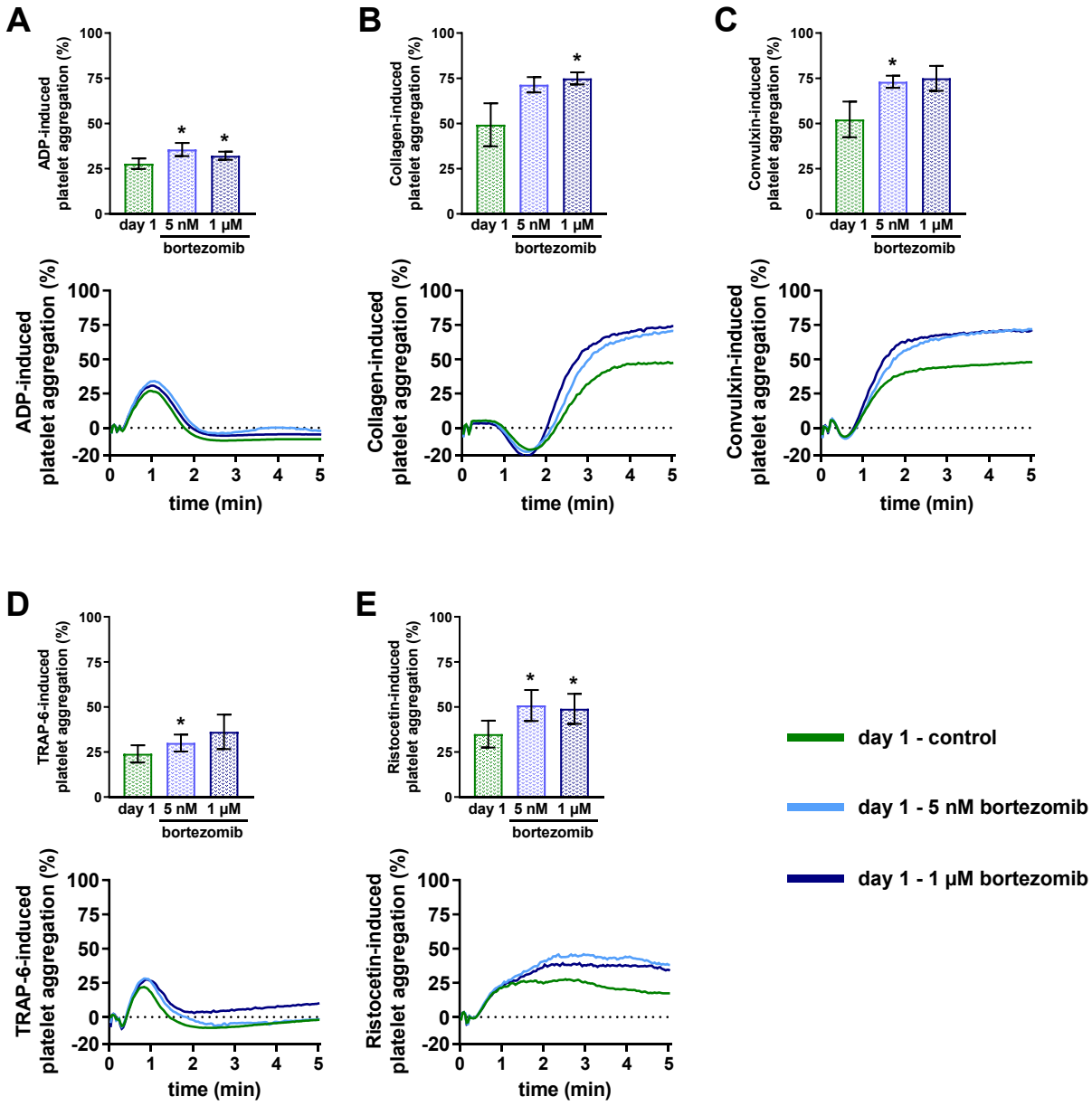

Figure 4.3: Threshold platelet aggregation or agglutination in PRP.

Mean aggregation traces and mean ± SEM of aggregation are shown for ADP (**A**), collagen (**B**), convulxin (**C**), TRAP-6 (**D**) and ristocetin (**E**) in PRP prepared from 24 h stored citrated whole blood samples preincubated with or without bortezomib as indicated. Data was assessed by light transmission aggregometry. Individual threshold concentrations (3 µM to 8 µM ADP, 1.5 µg/mL to 5 µg/mL collagen, 18.75 ng/mL to 28.75 ng/mL convulxin, 3 µM to 8 µM TRAP-6 or 562.5 µg/mL to 937.5 µg/mL ristocetin) mediating submaximal aggregation or agglutination were used; $n = 6$; *: $p \leq 0.05$, compared to "day 1".

Individual threshold concentrations of agonists were 3 µM to 8 µM ADP, 1.5 µg/mL to 5 µg/mL collagen, 18.75 to 28.75 ng/mL convulxin, 3 µM to 8 µM TRAP-6 or 562.5 µg/mL to 937.5 µg/mL ristocetin, inducing a weak and submaximal aggregation. ADP-induced aggregation reached 27.8 ± 3.3 % in PRP of 24 h stored whole blood without bortezomib (**Figure 4.3A**), whereas preincubation with 5 nM and 1 µM bortezomib caused a significant increase to 35.8 ± 4.0 % and 33.6 ± 3.0 %, respectively. Values for collagen-induced aggregation were 49.3 ± 13.0 % in 24 h stored platelets without bortezomib and increased to 71.4 ± 4.6 % under 5 nM bortezomib and significantly to 74.9 ± 3.7 % under 1 µM bortezomib (**Figure 4.3B**). For convulxin, aggregation rose from 52.2 ± 10.7 % in control samples to 73.1 ± 3.6 % and 74.9 ± 7.4 % in bortezomib-treated samples (**Figure 4.3C**). TRAP-6 induced a platelet aggregation of 24.0 ± 5.9 % in platelets stored for 24 h without bortezomib and was significantly elevated to 30.0 ± 5.8 % under preincubation with 5 nM bortezomib and to 36.21 ± 11.7 % with 1 µM bortezomib (**Figure 4.3D**). Ristocetin induced an agglutination of 34.9 ± 8.0 % without bortezomib, and significantly enhanced values with 50.8 ± 9.2 % and 49.0 ± 8.9 % under 5 nM and 1 µM bortezomib, respectively (**Figure 4.3E**).

4.1.4. Surface expression and activity of purinergic receptors remained stable under inhibition with bortezomib.

Further investigations focused on regulation of receptor levels, potentially involved in enhanced platelet aggregation and agglutination. Hereby, an important system mediating ADP-dependent effects is represented by the purinergic receptors comprising $P2Y_1R$, $P2Y_{12}R$ (ADP receptors) and $P2X_1R$ (ATP receptor). The surface expression of these receptors was determined by flow cytometry (**Figure 4.4**).

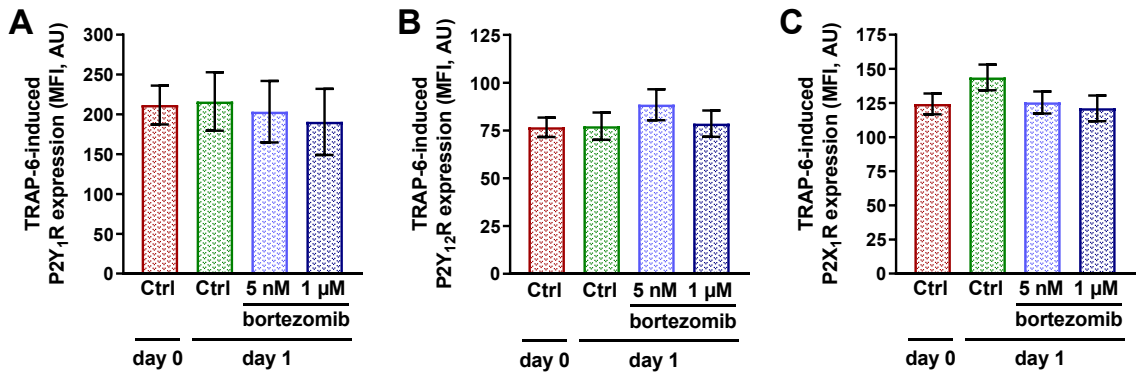

Figure 4.4: Surface expression of purinergic receptors in PRP.

Data are presented as mean MFI ± SEM for 10 µM TRAP-6-stimulated surface receptor expression for the $P2Y_1R$ (**A**), the $P2Y_{12}R$ (**B**) and the $P2X_1R$ (**C**) in PRP prepared from fresh or 24 h stored whole blood preincubated with or without bortezomib as indicated, determined by flow cytometry; *n* = 6.

The basal expression of all three receptors was stable under storage and under bortezomib-preincubation. Stimulation of platelets with 10 µM TRAP-6 led to an approximately 3-fold increase for the $P2Y_1R$ from 61.5 ± 0.7 MFI to 188.3 ± 27.1 MFI (**Figure 4.4A**), 2.5-fold for the $P2Y_{12}R$ from 31.0 ± 0.5 MFI to 76.7 ± 5.5 MFI (**Figure 4.4B**) and 2-fold for the $P2X_1R$ from 61.6 ± 1.1 MFI to 124.3 ± 124.3 ± 8.4 MFI (**Figure 4.4C**). The same effects were observable after 24 h of storage, irrespective of proteasome inhibition with 5 nM or 1 µM bortezomib.

Beyond surface expression patterns, the functional activity of purinergic receptors is a crucial characteristic contributing to ADP-mediated responsiveness in platelets. Activities of the $P2Y_1R$ and $P2X_1R$ were determined by calcium-induced fluorescence assay using Fluo-4 AM, a fluorescent calcium indicator. $P2Y_{12}R$ activity was assessed by the PRI using the PLT VASP/P2Y12 Kit from BioCytex SARL (Marseille, France) for flow cytometry (**Figure 4.5**).

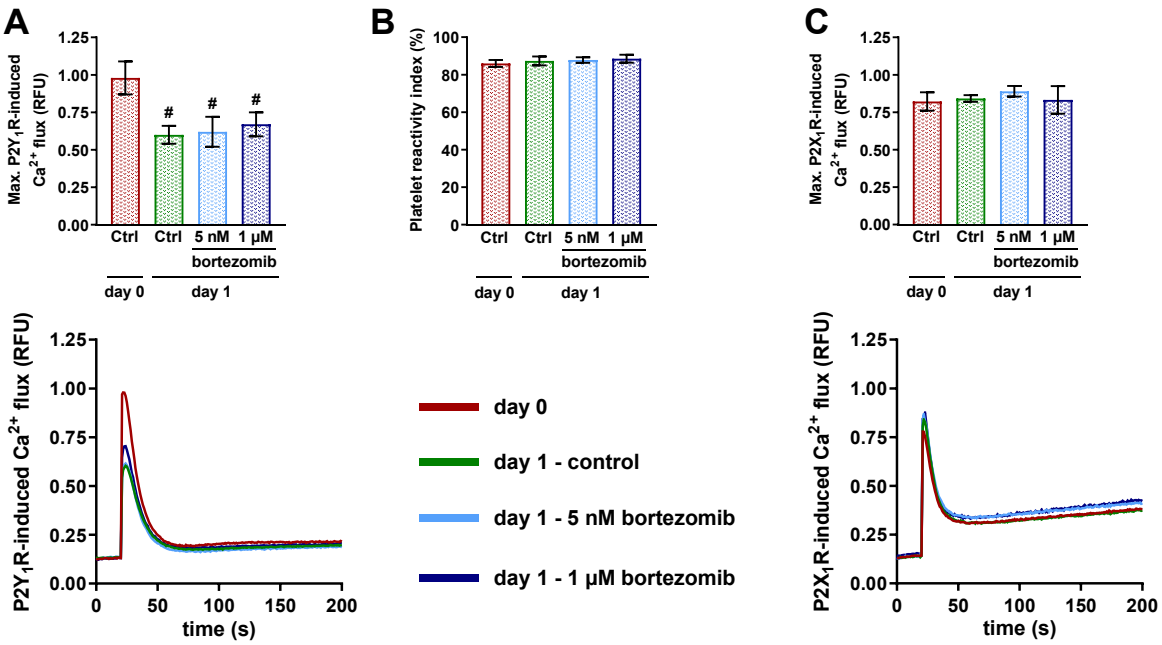

Figure 4.5: Purinergic receptor activity in platelets.

For determination of $P2Y_1R$ activity (**A**) or $P2X_1R$ activity (**C**), calcium-induced fluorescence curves were generated with Fluo-4 AM-loaded, freshly washed platelets (0.6×10^8 platelets/mL, diluted with modified Tyrode's buffer) from fresh or stored citrated whole blood samples preincubated with or without bortezomib as indicated, after stimulation with the $P2Y_1R$ agonist MRS2365 or the $P2X_1R$ agonist α,β-MeATP. Mean fluorescence traces, expressed in RFU and corresponding mean values of maximal induced fluorescence ± SEM are shown; $n = 6$; #: $p < 0.05$, compared to "day 0". For the $P2Y_{12}R$ activity (**B**), PRI values were determined by flow cytometry directly from citrated whole blood samples with or without bortezomib, as indicated. Results are presented as mean % ± SEM; $n = 6$.

Blood storage resulted in the reduction of $P2Y_1R$ activity from 0.98 ± 0.11 RFU to 0.60 ± 0.06 RFU without bortezomib and similarly to 0.62 ± 0.10 RFU and 0.67 ± 0.08 RFU with 5 nM and 1 µM bortezomib, respectively (**Figure 4.5A**). The PRI, representing $P2Y_{12}R$ activity with 86.0 ± 2.1 % in fresh platelets was also unaffected by storage or proteasome blockade (**Figure 4.5B**). $P2X_1R$-dependent fluorescence levels were not different in fresh, stored or bortezomib-incubated platelets (**Figure 4.5C**).

4.1.5. Expression of GPIIb, GPIb and GPVI were unaffected by bortezomib.

Further important receptor systems, comprising different GPs mediating responses to fibrinogen (GPIIb/IIIa), to vWF (GPIb-IX-V) and to collagen (GPVI) were also investigated. The long-term effect of proteasome inhibition on molecular expression

patterns upon platelet activation was determined by flow cytometric detection of GPIIb molecules (PLT Gp/Receptors Kit, BioCytex SARL, Marseille, France) and PAC-1 antibody binding for the fibrinogen receptor (**Figure 4.6**) or detection of GPIb and GPVI molecules for the vWF and collagen receptor, respectively (**Figure 4.7**).

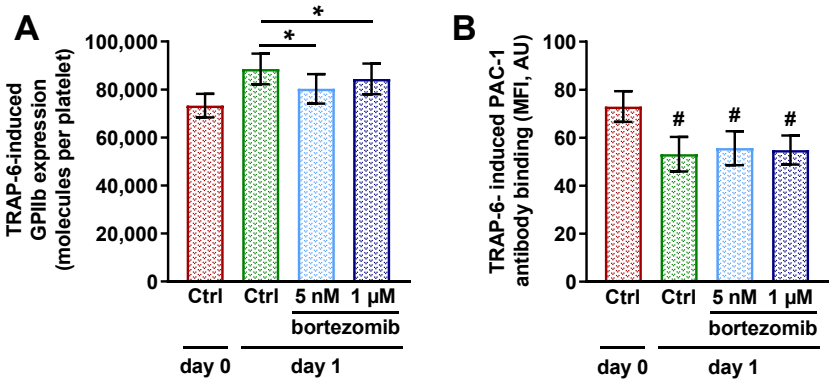

Figure 4.6: TRAP-6-induced GPIIb surface expression and PAC-1 antibody binding.

(**A**) TRAP-6-induced GPIIb expression as molecules per platelet ± SEM, measured by flow cytometry in fresh or 24 h stored citrated whole blood samples preincubated with or without bortezomib as indicated is shown; n = 6; *: $p < 0.05$, comparison as indicated. (**B**) Flow cytometric determination of 10 µM TRAP-6-stimulated PAC-1 antibody binding in PRP from fresh or 24 h stored citrated whole blood preincubated with or without bortezomib as indicated is presented as mean MFI ± SEM; n = 6; #: $p < 0.05$, compared to "day 0".

Fresh unstimulated platelets contained 48.0 ± 2.2 × 10^3 GPIIb molecules on their surface, identical with stored and bortezomib-incubated platelets. Upon activation with TRAP-6, the count of GPIIb molecules experienced a significant increase to 73.3 ± 5.4 × 10^3 molecules in fresh samples and to 88.5 ± 7.0 × 10^3 molecules after 24 h (**Figure 4.6A**). The shift in proteasome-inhibited samples was reduced with 80.3 ± 6.7 × 10^3 molecules (5 nM bortezomib) and 84.4 ± 7.0 × 10^3 molecules (1 µM bortezomib) in a significant manner. The analysis of the activated fibrinogen receptor expression, as TRAP-6-induced PAC-1 antibody binding, showed approximately 25 % decreased values after 24 h in control and bortezomib-incubated platelets (**Figure 4.6B**). While fresh platelets evoked 73.0 ± 6.8 MFI, PAC-1 antibody binding-induced fluorescence decreased significantly to 53.1 ± 7.7 MFI after 24 h of storage and to 55.7 ± 7.6 MFI or 54.9 ± 6.5 MFI in samples preincubated with 5 nM or 1 µM bortezomib, respectively. Basal values of PAC-1 antibody binding dropped similarly after 24 h storage, without further change upon proteasome blockade.

Expression of GPIb, as part of the vWF receptor complex GPIb-IX-V, and expression of the collagen receptor GPVI were determined using flow cytometry (**Figure 4.7**).

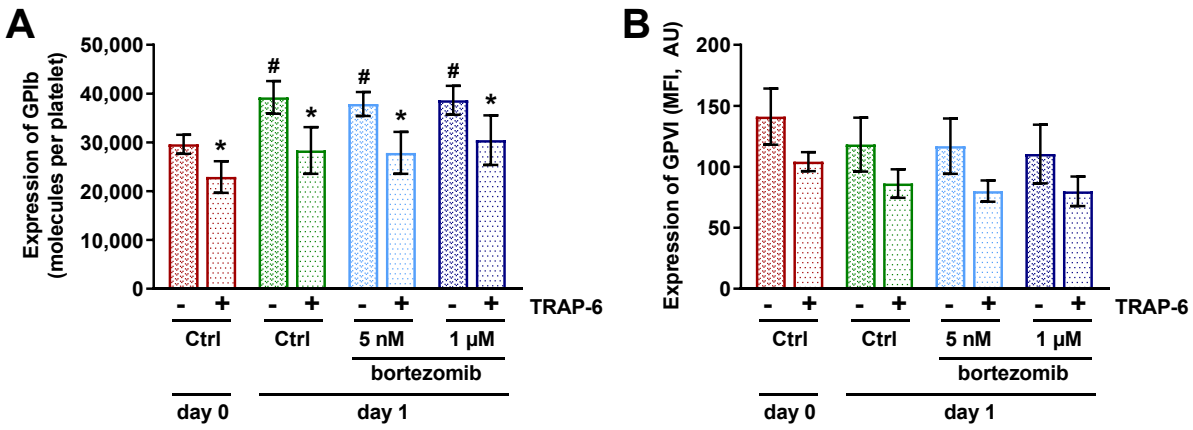

Figure 4.7: Surface expression of GPIb and GPVI.

(**A**) Basal and TRAP-6-stimulated GPIb expression in molecules per platelet ± SEM was measured by flow cytometry in fresh or 24 h stored citrated whole blood preincubated with or without bortezomib as indicated; $n = 6$; #: $p < 0.05$, compared to basal control at day 0; *: $p < 0.05$, TRAP-6-stimulation compared to corresponding basal expression. (**B**) GPVI expression was determined by flow cytometry in PRP from fresh or stored citrated whole blood preincubated with or without bortezomib as indicated. Results are presented as mean MFI ± SEM; $n = 3$.

Platelets from fresh whole blood expressed 29.6 ± 2.1 × 10^3 GPIb molecules on their surface. Stimulation with TRAP-6 reduced GPIb expression to 22.9 ± 3.5 × 10^3 molecules (**Figure 4.7A**). In stored platelets, the amount of surface GPIb molecules rose to 39.3 ± 3.7 × 10^3 per platelet. After TRAP-6-stimulation, the values decreased to 28.3 ± 5.2 × 10^3 molecules. Bortezomib incubation was not able to relevantly modify expression levels of GPIb.

Similar to GPIb, expression patterns of TRAP-6-induced GPVI levels were merely affected by storage for 24 h with values slightly decreasing from 104.2 ± 7.8 MFI to 86.3 ± 11.7 MFI in the control on day 1 (**Figure 4.7B**). Preincubation with bortezomib did not further influence TRAP-6-stimulated GPVI expression.

Basal GPVI expression evoked 141.1 ± 23.1 MFI in platelets from fresh whole blood samples and showed reduced values of 118.2 ± 22.1 MFI after 24 h of storage. Proteasome blockade did not affect expression levels beyond that.

4.1.6. Phosphorylation of PP2A was reduced by bortezomib.

PP2A is a key phosphatase for phosphorylated VASP and considered to be a regulator of GPIb. Thus, PP2A plays a potential role in platelet adhesion and platelet inhibition and serves, in addition, as phosphatase for other important platelet proteins. Phosphorylation of PP2A, indicating its activity, was investigated using Western blot analysis (**Figure 4.8**).

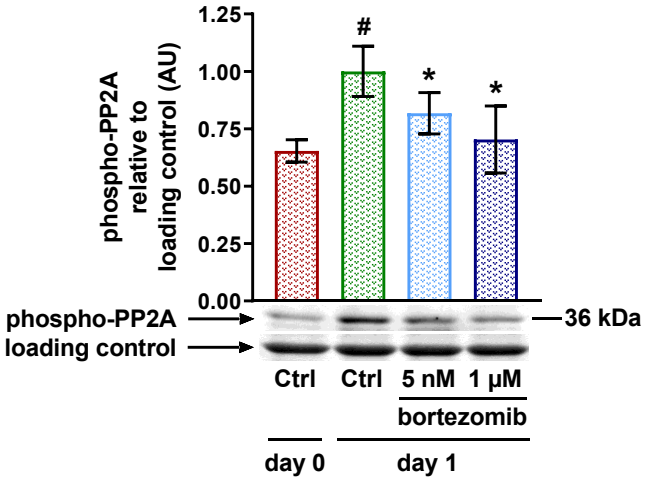

Figure 4.8: Phosphorylation of PP2A in WP.

Washed platelets (3 × 10^8 platelets/mL, diluted with Tyrode's buffer) from fresh or 24 h stored citrated whole blood preincubated with or without bortezomib as indicated were lysed and analyzed by Western blot using an anti-phospho-PP2A-Tyr^{307} antibody. The histograms show the levels of phospho-PP2A relative to loading control (Ponceau S-stained actin), normalized to control at day 1 with representative blots of phospho-PP2A bands and loading control bands. Results are presented as mean arbitrary units (AU) ± SEM; *n* = 3; #: $p < 0.05$, compared to "day 0"; *: $p < 0.05$, compared to control at day 1.

The phosphorylation levels of PP2A at Tyr^{307} showed a significant increase after 24 h storage without bortezomib, from 0.65 ± 0.05 AU to 1.00 ± 0.11 AU (**Figure 4.8**), whereas PP2A phosphorylation was significantly decreased to 0.82 ± 0.09 AU and 0.70 ± 0.15 AU after incubation with 5 nM or 1 µM bortezomib, respectively.

4.2. Interaction of proteasome blockade with platelet inhibition

4.2.1. VASP phosphorylation was attenuated under proteasome inhibition.

VASP is a protein, which interacts with actin in its phosphorylated form and keeps platelets in the resting state through inhibition of conformational changes of the GPIIb/IIIa receptor and inhibition of shape change [115]. Two major phosphorylation sites of VASP are Ser^{239} and Ser^{157}, inducible with elevating cGMP or cAMP levels using the NO donor DEA/NO or PGE_1 as experimental inductors, respectively. Therefore, induced VASP phosphorylation levels, determined by flow cytometry, were used to study effects of bortezomib on inhibitory pathways (**Figure 4.9**).

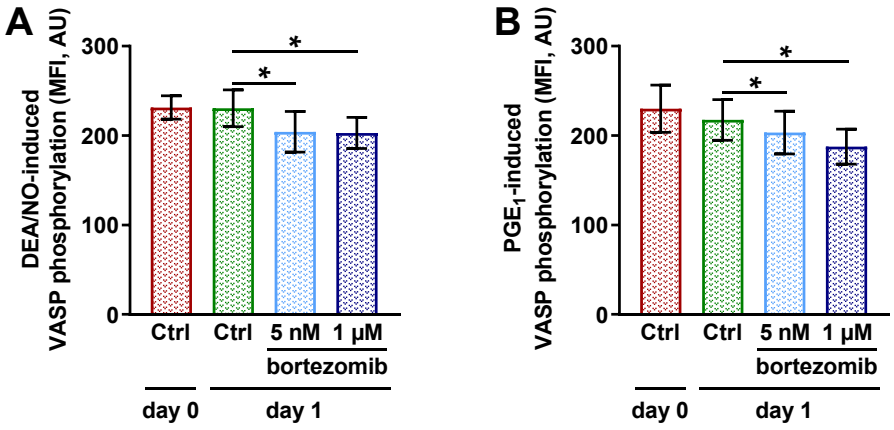

Figure 4.9: DEA/NO- and PGE_1-induced VASP phosphorylation in PRP.

VASP phosphorylation in platelets was measured by flow cytometry after preparation of PRP from fresh or 24 h stored citrated whole blood preincubated with or without bortezomib as indicated. Samples were stimulated with 1 µM DEA/NO (**A**) or 1 µM PGE_1 (**B**) for 5 min. Data are presented as mean MFI ± SEM; $n = 6$; *: $p < 0.05$, comparison as indicated.

Both, DEA/NO- and PGE_1-induced phosphorylation levels were not different in platelets obtained from fresh whole blood or 24 h stored whole blood. However, compared to untreated platelets, 5 nM bortezomib provoked a significant decrease of phosphorylation from 230.6 ± 22.9 MFI to 204.2 ± 25.5 MFI for DEA/NO-stimulation, similar to 1 µM bortezomib (**Figure 4.9A**). For PGE_1-stimulation, proteasome blockade weakened the VASP phosphorylation from 217.5 ± 25.4 MFI to 203.4 ± 26.7 MFI under 5 nM bortezomib and to 187.6 ± 21.7 MFI under 1 µM bortezomib (**Figure 4.9B**), which was both in a significant manner.

4.2.2. Inhibition of induced fibrinogen binding was less pronounced under bortezomib.

In addition, the effect of bortezomib on inhibitory systems was determined by flow cytometric measurement of DEA/NO- or PGE_1-mediated suppression of TRAP-6-induced fibrinogen binding (**Figure 4.10**).

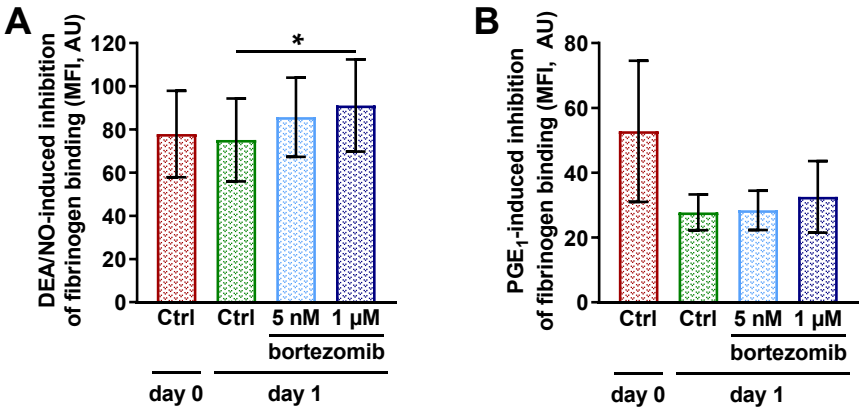

Figure 4.10: DEA/NO- and PGE_1-induced inhibition of fibrinogen binding in PRP.

1 µM DEA/NO-mediated (**A**) and 0.25 µM PGE_1-mediated (**B**) inhibition of 10 µM TRAP-6-stimulated fibrinogen binding was determined by flow cytometry in PRP from fresh or 24 h stored citrated whole blood preincubated with or without bortezomib as indicated. Data are presented as mean MFI ± SEM; $n = 6$; *: $p < 0.05$, comparison as indicated.

Under 1 µM DEA/NO, TRAP-6-induced fibrinogen binding reached 77.9 ± 20.0 MFI in fresh platelets and 75.1 ± 19.2 MFI after 24 h of storage (**Figure 4.10A**). In bortezomib-treated samples, the values were 15 % - 20 % higher with 85.7 ± 18.3 MFI and 91.1 ± 21.3 MFI for 5 nM and 1 µM bortezomib, respectively. PGE_1-stimulation reduced TRAP-6-induced fibrinogen binding levels to 52.8 ± 21.8 MFI in fresh samples and near-totally to 27.8 ± 5.5 MFI in stored samples (**Figure 4.10B**). Fibrinogen binding showed slightly higher levels under bortezomib, but still markedly suppressed with 28.4 ± 6.1 MFI for 5 nM bortezomib and with 32.5 ± 11.0 MFI for 1 µM bortezomib.

4.3. Proteasome-dependent adhesive platelet function under static and flow conditions

4.3.1. Platelet adhesion on coated surfaces was facilitated under bortezomib.

Platelet adhesion is an essential characteristic of platelets contributing to the initiation of thrombus formation to stop hemorrhage. The effects of proteasome blockade on platelet adhesive properties on coated slides under static conditions were determined by fluorescence microscopy (**Figure 4.11**).

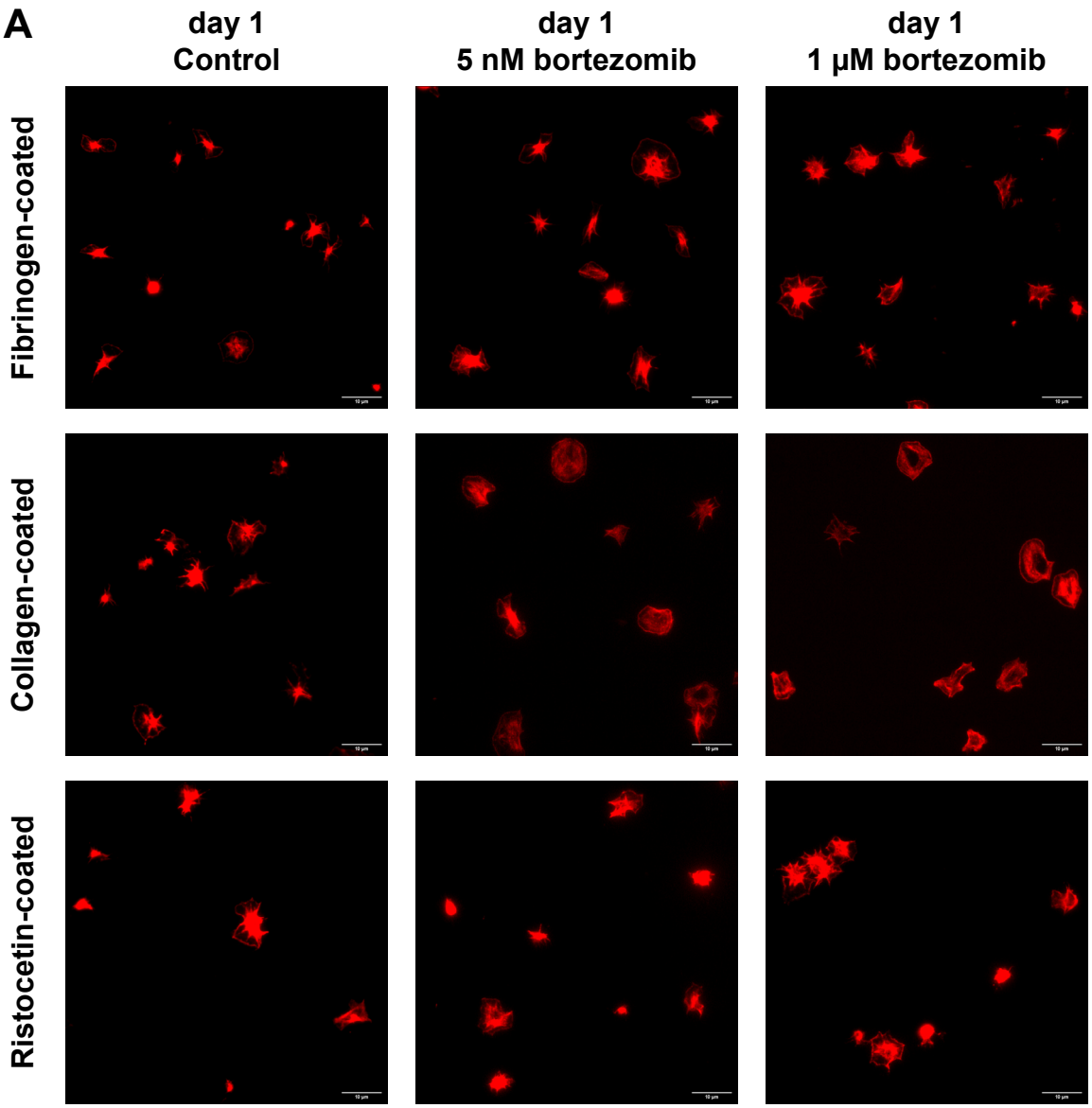

B

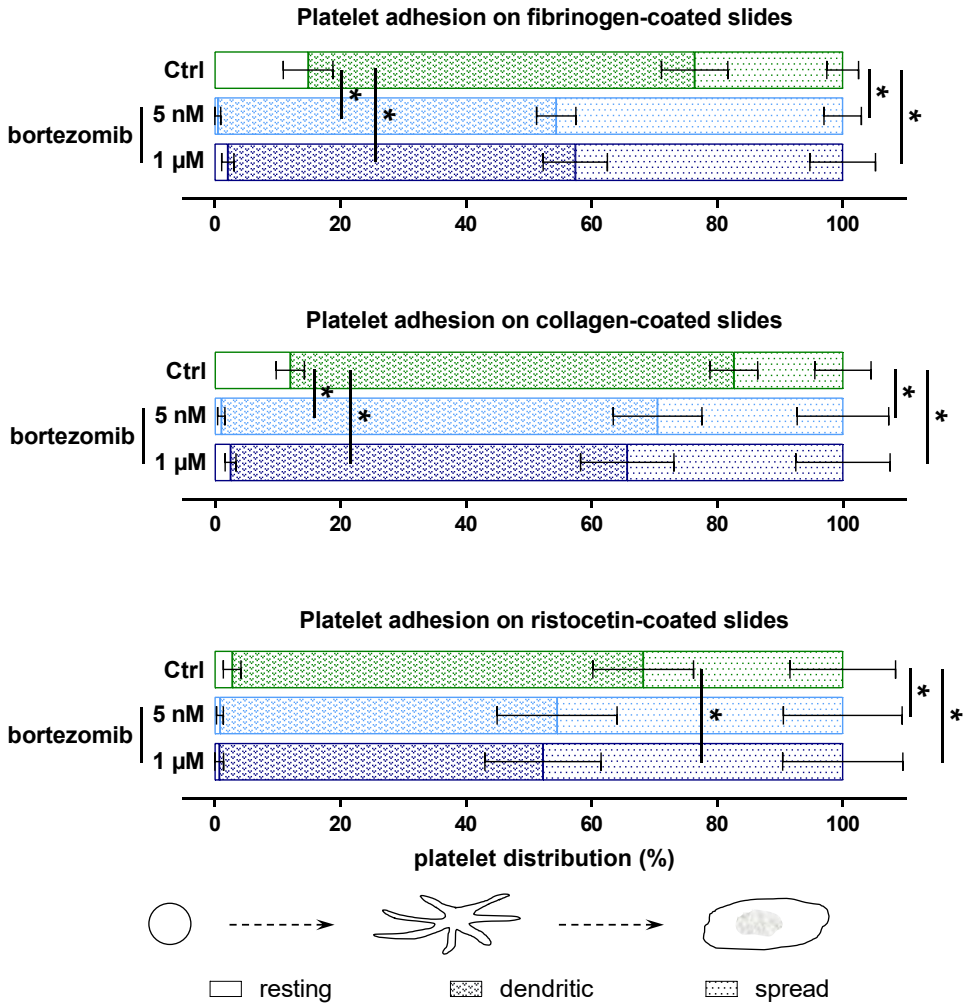

Figure 4.11: Platelet adhesion on coated surfaces under static conditions.

The adhesive characteristics of stained platelets on coated surfaces are shown. PRP from 24 h stored citrated whole blood preincubated with or without bortezomib as indicated diluted with PBS to 0.1 × 10^8 platelets/mL was seeded onto slides coated with fibrinogen (100 µg/mL), collagen (0.25 µg/mL) or ristocetin (0.5 mg/mL). After fixation, platelets were stained for actin with TRITC-conjugated phalloidin overnight followed by mounting and subsequent analysis on an inverted Nikon Eclipse Ti2 microscope using 60× oil immersion objective and 1.5× zoom lens (14-bit digitalization). For statistical analysis, at least 200 cells were imaged and analyzed in each single experiment using the on-board software tools. The images show representative slide cutouts with adherent stained platelets from samples as indicated (**A**). In addition, the quantitative distribution is given (**B**), results are presented as mean % ± SEM, quantified by their characteristic platelet adhesion forms ("resting", "dendritic" "spread"); $n = 3$; *: $p < 0.05$, comparison as indicated.

The analysis of platelet form distribution on fibrinogen-coated slides showed that 14.9 ± 4.2 % of platelets kept their resting shape after incubation for 20 min (**Figure 4.11B**, upper panel), only 23.6 ± 2.7 % of them were in the spread form. In contrast, bortezomib-treated platelets almost completely developed a dendritic form (53.9 ± 3.3 % under 5 nM bortezomib and 55.4 ± 5.4 % under 1 µM bortezomib) or a

spread form (45.6 ± 3.2 % under 5 nM bortezomib and 42.6 ± 5.6 % under 1 µM bortezomib), leaving only 0.5 % - 2 % of platelets in the resting form. A very similar distribution was observed on collagen-coated slides (**Figure 4.11B,** middle panel). On ristocetin-coated slides, 2.8 ± 1.5 % of detected platelets were in their resting shape, while 65.5 ± 8.5 % were in a dendritic and 31.8 ± 8.9 % in a spread form. Treatment with 5 nM or 1 µM bortezomib led to a significant shift towards dendritic shaped platelets (53.7 ± 10.1 % and 51.6 ± 9.8 %, respectively) and spread platelets with 45.5 ± 10.0 % under 5 nM and 47.7 ± 10.1 % under 1 µM bortezomib (**Figure 4.11B**, lower panel). Representative slide cutouts with adherent stained platelets for each coating and treatment are shown in **Figure 4.11A**.

4.3.2. Platelets showed higher aggregate-covered area under flow conditions under bortezomib.

Furthermore, platelet adhesion characteristics were investigated under flow conditions using a life cell imaging system with collagen-coated flow chamber (**Figure 4.12**).

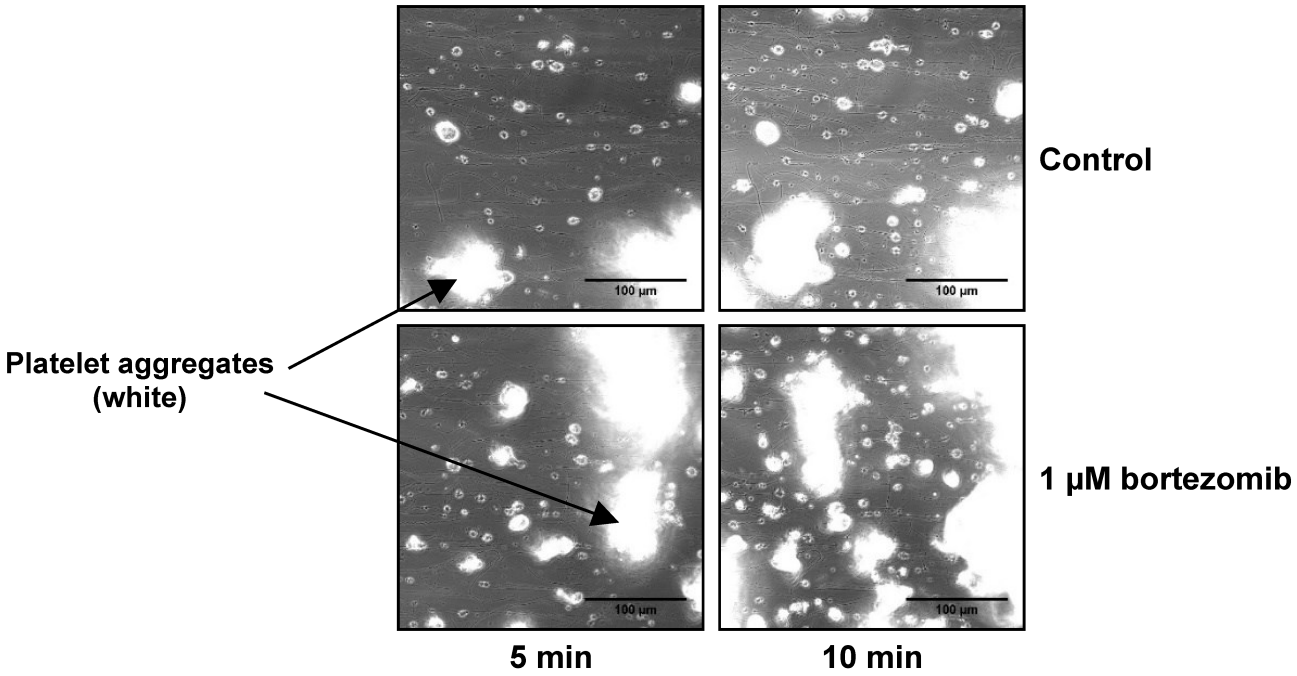

Figure 4.12: Platelet adhesion under flow conditions in collagen-coated chamber.

Representative microscopic images of one corresponding spot at 5 min (left) and 10 min (right) from control and 60 min bortezomib-treated platelets (2.5 × 10^8 platelets/mL from APC diluted with HBSS) on the collagen-coated flow chamber are shown. Images were recorded on an inverted Nikon Eclipse Ti2 microscope using 60× oil immersion objective (14-bit digitalization); *n* = 3; 200 µm chamber slit depth; shear rate: 150 1/s.

Platelets from bortezomib-preincubated samples showed a higher number of aggregates and larger aggregates, compared to platelets from control samples after 5 min of constant platelet flow (**Figure 4.12,** left). This effect was progressive and could also be observed after 10 min in a higher extent (**Figure 4.12,** right), where the total aggregate-covered area was higher after treatment with bortezomib, compared to control samples.

4.4. Effect of proteasome inhibition with carfilzomib on human platelets

Key experiments were repeated using the proteasome inhibitor carfilzomib to confirm specificity of the obtained results shown for the inhibitor bortezomib and to rule out compound-related effects. Carfilzomib itself is a specific proteasome inhibitor also used in the treatment of patients suffering from multiple myeloma and approved by the FDA in 2012 [186]. In contrast to bortezomib, carfilzomib binds irreversibly to the β5-subunit of the proteasome. The mechanism of action for irreversible binding is mediated through an epoxide as active group. Since carfilzomib was used for the first time for functional experimentation in platelets, the first step was to evaluate the potential of carfilzomib for proteasome inhibition in platelets.

4.4.1. Carfilzomib inhibited platelet 20S proteasome activity in a dose-dependent manner.

A dose-response analysis was performed using the 20S Proteasome Activity Assay kit (Merck KgaA, Darmstadt, Germany) accompanied by the measurement of poly-ubiquitylated proteins using the CycLex Poly-Ubiquitinated Protein ELISA kit (MBL International Corporation, Woburn, MA, USA) (**Figure 4.13**). Since DMSO is required for the dissolution of carfilzomib, all samples, including control samples, contain the highest DMSO concentration (0.1 % final DMSO concentration) as used in carfilzomib-treated samples to rule out DMSO-induced effects on platelet function.

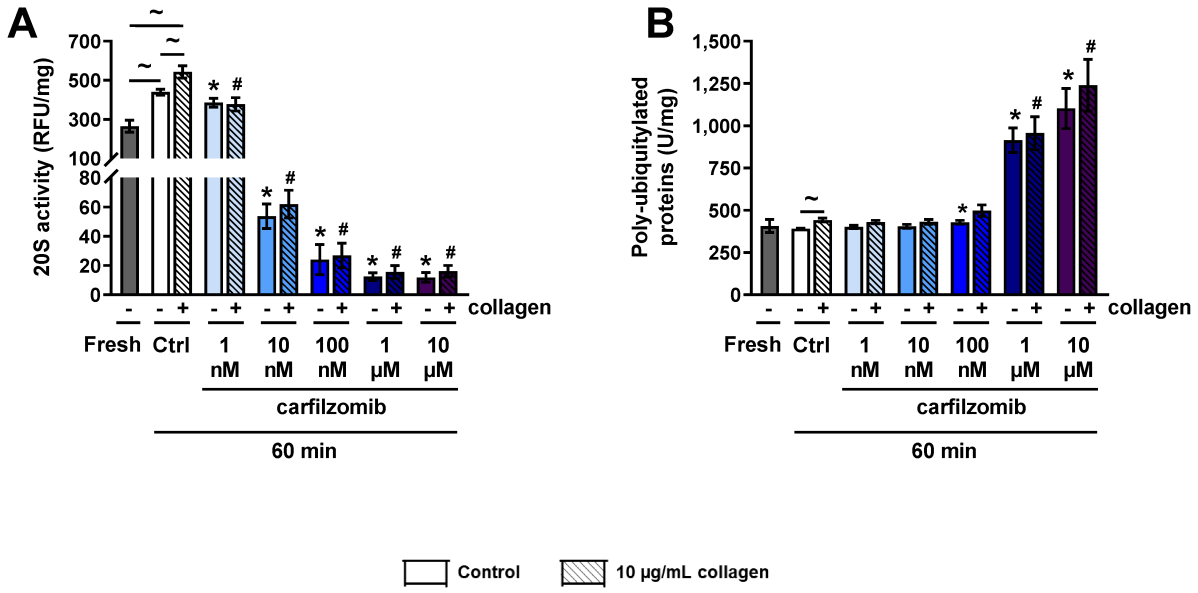

Figure 4.13: Basal and collagen-induced 20S activity and poly-ubiquitylated proteins under carfilzomib.

The graphs show basal and 10 µg/mL collagen-induced proteasome activity (**A**) and poly-ubiquitylated proteins (**B**) after incubation of freshly washed platelets (3×10^8 platelets/mL, diluted with Tyrode's buffer) prepared from PRP with indicated concentrations of carfilzomib or 0.1 % DMSO as control for 60 min. Results are presented as mean ± SEM (RFU per mg protein for 20S activity or relative units per mg protein for poly-ubiquitylated proteins); $n = 8$; *: $p < 0.05$, compared to untreated DMSO control at 60 min; #: $p < 0.05$, compared to 10 µg/mL collagen-stimulated DMSO control at 60 min; ~: $p < 0.05$, comparison as indicated.

The basal chymotrypsin-like activity of the 20S platelet proteasome, measured by converted fluorescent substrate, evoked 264.3 ± 33.8 RFU/mg in platelets from fresh samples. This value was increased to 439.5 ± 16.3 RFU/mg after 60 min incubation at 37 °C without stimulation or inhibition (**Figure 4.13A**). Stimulation with 10 µg/mL collagen for 60 min resulted in enhanced 20S activity of 542.8 ± 33.5 RFU/mg. Preincubation with carfilzomib for 60 min in PRP at RT resulted in a dose-dependent decrease of 20S activity with 385.5 ± 26.2 RFU/mg and 377.0 ± 36.2 RFU/mg for basal and collagen-induced proteasome activity under 1 nM carfilzomib. Incubation with 10 nM carfilzomib weakened 20S activity significantly to 53.7 ± 9.0 RFU/mg and 61.9 ± 10.1 RFU/mg in basal and collagen-induced samples, respectively. Inhibition with 100 nM carfilzomib further suppressed 20S activity to 23.9 ± 11.0 RFU/mg without collagen and to 26.8 ± 9.0 RFU/mg in collagen-stimulated samples. Almost full inhibition of basal and collagen-induced 20S activity was reached under preincubation

with 1 µM or 10 µM carfilzomib (1 µM: 12.3 ± 2.9 RFU/mg; 15.4 ± 4.7 RFU/mg; 10 µM: 11.9 ± 3.5 RFU/mg; 16.1 ± 4.2 RFU/mg).

Proteasome inhibition resulted in a significant accumulation of poly-ubiquitylated proteins using 1 µM or 10 µM carfilzomib from 391.4 ± 3.5 U/mg in the DMSO control after 60 min incubation at 37 °C to 915.2 ± 77.5 U/mg and 1102.2 ± 126.7 U/mg, respectively (**Figure 4.13B**). The amount of poly-ubiquitylated proteins was hardly affected by lower carfilzomib concentrations. Stimulation with 10 µg/mL collagen increased the amount of poly-ubiquitylated proteins in the 60 min control to 442.3 ± 10.5 RFU/mg. This effect could not be observed in carfilzomib-treated samples.

On the basis of these results, further investigations using carfilzomib as proteasome inhibitor were conducted with 10 nM, 100 nM and 1 µM carfilzomib, mediating submaximal to maximal proteasome inhibition and observable accumulation of poly-ubiquitylated proteins in platelets.

4.4.2. Carfilzomib enhanced platelet threshold aggregation.

In analogue to the investigation of threshold aggregation performed with bortezomib, platelet aggregation under carfilzomib was measured using ADP and collagen in concentrations inducing submaximal aggregation in the DMSO control samples (**Figure 4.14**).

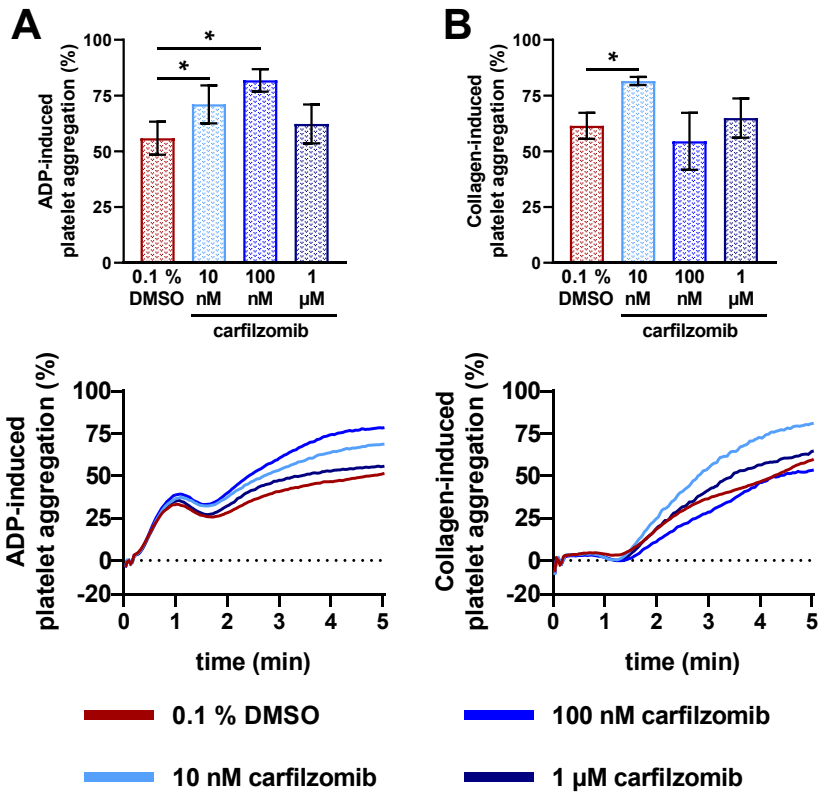

Figure 4.14: Threshold platelet aggregation using collagen and ADP under carfilzomib in PRP.

Mean aggregation traces and mean ± SEM of aggregation are shown for induction with ADP (**A**) and collagen (**B**) in PRP preincubated with or without carfilzomib for 60 min as indicated prepared from citrated whole blood samples and measured by light transmission aggregometry. Individual threshold concentrations (0.5 µM to 1.25 µM ADP or 0.2 µg/mL to 0.5 µg/mL collagen), mediating submaximal aggregation were used; $n = 6$; *: $p \leq 0.05$, comparison as indicated.

Individual threshold concentrations of ADP (0.5 µM to 1.25 µM) induced aggregation values of 55.9 ± 7.8 % in PRP spiked with 0.1 % DMSO as control (**Figure 4.14A**). Preincubation with 10 nM carfilzomib for 60 min resulted in an enhanced threshold aggregation of 71.1 ± 9.0 %. 100 nM carfilzomib was able to further increase aggregation significantly to 81.8 ± 5.3 %. Preincubation with 1 µM carfilzomib increased ADP-induced threshold aggregation only slightly in comparison with the DMSO control. Threshold aggregation values induced with individual concentrations of collagen (0.2 µg/mL to 0.5 µg/mL) were 61.5 ± 6.3 % in control samples (**Figure 4.14B**), whereas preincubation with 10 nM carfilzomib enhanced aggregation to 81.5 ± 2.0 %. This effect was not observable for higher carfilzomib concentrations.

4.4.3. DEA/NO- and PGE_1-induced VASP phosphorylation is attenuated by carfilzomib.

Furthermore, the influence of carfilzomib on platelet inhibitory signaling was investigated by measuring DEA/NO- and PGE_1-induced VASP phosphorylation using flow cytometry (**Figure 4.15**) in analogue to the results shown for bortezomib in **4.2.1**.

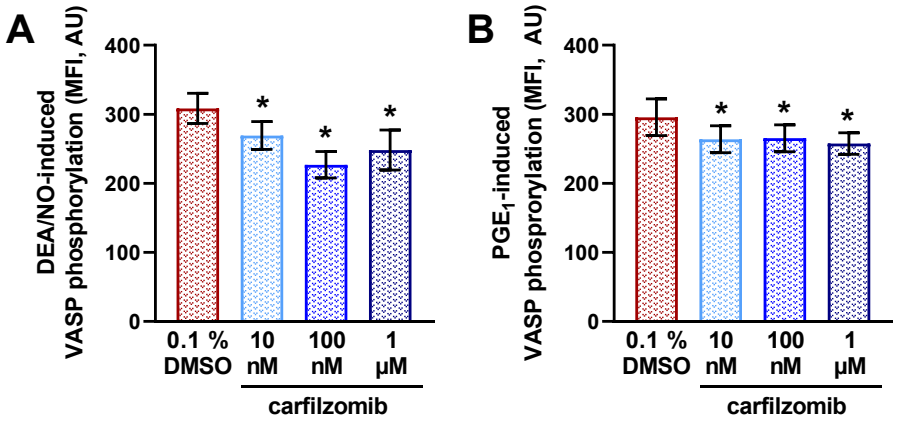

Figure 4.15: DEA/NO- and PGE1-induced VASP phosphorylation under carfilzomib in PRP.

VASP phosphorylation in platelets was measured by flow cytometry after preparation of PRP with or without preincubation with carfilzomib for 60 min as indicated, stimulated with 1 µM DEA/NO (**A**) or 1 µM PGE_1 (**B**) for 5 min. Data are presented as mean MFI ± SEM; $n = 6$; *: $p < 0.05$, compared to "0.1 % DMSO".

Induction with DEA/NO evoked VASP phosphorylation levels of 308.4 ± 24.2 MFI in the DMSO control. The values were significantly reduced to 269.2 ± 22.1 MFI, 226.9 ± 21.3 MFI and 248.3 ± 31.7 MFI for 10 nM, 100 nM and 1 µM carfilzomib, respectively (**Figure 4.15A**). In PGE_1-stimulated platelets, proteasome blockade weakened the VASP phosphorylation significantly from 295.6 ± 29.2 MFI in the DMSO control to 263.8 ± 21.5 MFI under 10 nM carfilzomib, similar to the incubation with 100 nM and 1 µM carfilzomib for 60 min, respectively (**Figure 4.15B**).

5. Discussion

The significance of the proteasome system in eukaryotic cells for elimination of misfolded proteins, cell cycle progression and cell growth, signal transduction, immune response and regulation of apoptosis, on the basis of its function as multicatalytic protein degrading enzyme, was intensively investigated in many studies [187-192].

Since the group of Yukawa *et al.* was able to find that proteasomes are also present in anucleated human platelets [166], the examination of its relevance in platelets has been forced.

In the meantime, the functional role of the proteasome system in platelets has been addressed in several studies with some controversial findings [168, 171, 175, 193-195]. As a limitation, heterogenic study designs with various inhibitors in different concentrations, variable preparation methods of platelets, incubation times, supplemental agents, etc. could have led to inconsistent findings.

Therefore, this thesis was conducted to systematically elucidate particular effects of long-term proteasome inhibition for 24 h with the potent and selective inhibitor bortezomib in whole blood to resolve existing controversies. The long-term incubation period was used with the aim to incorporate potentially time-consuming processes of the proteasome, responsible for protein turnover [196]. Whole blood was selected to simulate *in vivo* blood composition, where bortezomib is acting on all blood components during its therapeutical administration, potentially associated with intercellular effects. Furthermore, carfilzomib, as the second FDA-approved proteasome inhibitor, was used for key experiments to rule out bortezomib-related effects and to prove the generalizability of the results affiliated to proteasome inhibition.

5.1. Potent platelet activation is not influenced by proteasome inhibition.

As previously shown for 60 min preincubation with bortezomib in washed platelets [173], irreversible platelet aggregation induced with ADP, collagen or TRAP-6 is not affected by proteasome inhibition for 24 h in whole blood, irrespective of the bortezomib concentration. This finding strongly suggests that there is no direct involvement of the proteasome system in potent agonist-induced platelet aggregation,

neither in rapid, nor in time-delayed processes. The general reduction in ADP-induced platelet aggregation, independent of proteasome blockade, can be attributed to the storage-related functional deterioration of the $P2Y_1R$ with diminished induced calcium-flux as demonstrated in **4.1.4** for platelets derived from 24 h stored whole blood [197]. This in line with recent studies addressing washed human platelets and apheresis-derived platelet concentrates, respectively [198, 199].

Concomitantly to platelet aggregation, potent TRAP-6-induced expression of P-selectin and of fibrinogen binding, as markers for platelet activation, remain unchanged by preincubation with bortezomib. The general increase of induced P-selectin levels and the reduction of induced fibrinogen binding are obviously caused by storage and are observable for samples with or without bortezomib. Ghansah *et al.* recently demonstrated a significant increase in P-selectin expression after preincubation of gel-filtered human platelets with bortezomib [194], indicating that bortezomib bears the potential to support platelet activation. Gel-filtered platelets were used to minimize the influence of human plasma proteins, since bortezomib tends to bind to these proteins by approximately 83 % at therapeutic concentrations [155]. Thus, a probably higher platelet responsiveness under bortezomib for 24 h may have been cached by the presence of plasma proteins. However, for shorter proteasome inhibition periods of 60 min in washed platelets, it was demonstrated that kinases involved in platelet activating signaling like p38 mitogen-activated protein kinase, extracellular signal-regulated kinase 1/2 or proteinkinase B remain unaffected [200], according to the current findings for aggregation, P-selectin expression or fibrinogen binding with potent agonist concentrations like 10 µM TRAP-6.

5.2. Threshold aggregation and agglutination is supported by proteasome inhibition.

Irreversible aggregation studies were complemented with the use of individual threshold concentrations of platelet agonists for each experiment. Under these conditions, aggregation and agglutination responses were enhanced in bortezomib-treated platelets, indicating that proteasome inhibition with bortezomib leads to a procoagulant state of platelets under weak platelet activation rather than under strong platelet activation with higher agonist concentrations (*e.g.* 10 µM ADP).

Noteworthy, aggregation responses were remarkably increased for the standard platelet agonists collagen and convulxin, and similarly for the glycopeptide antibiotic ristocetin inducing agglutination by binding of vWF [201]. These agonists share the characteristic that their effects are mediated via the GPIb receptor [201-204], representing one of the main adhesion receptors in platelets.

Flow cytometric analysis excluded direct interference of proteasome inhibition with GPIb expression. The basal and TRAP-6-induced GPIb levels are comparably elevated in bortezomib-treated samples and control samples after storage for 24 h. Nevertheless, additional experiments showed that proteasome inhibition is functionally involved in mechanisms of platelet adhesion. Bortezomib-treated platelets show different morphological characteristics, shifting from resting to dendritic and spread forms on fibrinogen-, collagen-, or ristocetin-coated surfaces, whereas untreated platelets mainly stay in the resting form. Static adhesion studies were also complemented by live cell analysis of platelet adhesion under flow conditions. Here, PRP from APC was preincubated for 60 min with 1 µM bortezomib for experimentation with the use of a collagen-coated chamber. Pronounced aggregate-covered area and faster adhesion were observed, confirming the findings of static adhesion studies. In this conclusion, the proteasome system may inflect GPIb-mediated functional responses, as it is described for GPVI-induced platelet activation [205].

The phosphorylation levels at Ser^{166} and Ser^{609} of the GPIb receptor may also play a role, which were found to be important for its binding affinity to vWF or the intracellular signaling molecule 14-3-3ζ, respectively [206, 207], in this way controlling the adhesive properties of the platelet GPIb-IX-V complex [208]. For these phosphorylation sites, PP2A could be considered as an essential phosphatase, since PP2A gets translocated to the cytoskeleton upon platelet activation and is involved in surface regulation [209, 210]. In cell culture, it was shown that proteasome inhibition using MG-132 or lactacystin leads to translocation of PP2A from the cytosol to the membrane [211]. In addition, PP2A dephosphorylates VASP, a central protein of platelet inhibitory pathways [116, 212]. Indeed, PP2A phosphorylation is reduced by preincubation of whole blood for 24 h with bortezomib as illustrated in **4.1.6**, implicating increased activation of PP2A and possibly resulting in the modification of GPIb towards a higher binding affinity and facilitated platelet adhesion.

The proteasome is not merely responsible for protein degradation, but it represents an intriguing multiprotein-complex, interfering with numerous proteins. PP2A is involved in the dephosphorylation of the proteasome and may be attached to it [213]. Inhibition of the proteasome may lead to weakened anchorage of the PP2A molecule, becoming available for signaling processes. For example, a similar mechanism is described for the NFκB-IκB-PKAc complex and PKA in platelets [214].

Alongside with agonists interacting with the GPIb receptor, threshold aggregation responses were also increased using ADP and TRAP-6 as agonists. Therefore, modulation of GPIb may only be one of the potential triggers for facilitated platelet aggregation or agglutination. In platelets, aggregation represents the endpoint of an activation cascade mediated by various pathways and, among others, leading to conformational changes of the GPIIb/IIIa receptor (fibrinogen receptor) and crosslinking of platelets via fibrinogen [215]. Compared to fresh platelets, the number of GPIIb molecules on the surface of stored TRAP-6-stimulated platelets is enhanced, presumably representing a storage-related lesion with disintegration of the platelet membrane. Analysis of PAC-1 antibody binding, recognizing the activated form of the platelet fibrinogen receptor, reveals a strong decrease in relation to the whole fibrinogen receptor pool (as GPIIb) on the surface of stored platelets. This phenomenon is another explanation for the reduction of induced fibrinogen binding after 24 h of storage, as shown in **4.1.2**. The increase in GPIIb expression after 24 h is significantly prevented by the preincubation of whole blood with bortezomib, but as PAC-1 antibody binding is similar among all stored platelet conditions, there is no functional consequence of this observation.

5.3. Proteasome inhibition alleviates inhibitory pathways.

As illustrated in section **4.2.1** of the results part, the responsiveness of inhibitory pathways to stimulation with DEA/NO or PGE_1 was attenuated after preincubation with bortezomib for 24 h in whole blood, indicated by partially reduced VASP phosphorylation of 10 to 15 %. We could recently show that tampered inhibition is similarly observable already after 60 min of bortezomib preincubation [173]. Therefore, there is no further progression of this effect and obviously develops within 1 h, which implicates a direct functional interaction of the proteasome system rather than an

indirect effect, caused by the suppression of protein degradation. As the inhibition of proteasome activity by bortezomib increases dynamically in the range from 1 nM (low inhibition) to 10 nM (already strong inhibition) [172], possible differences between 5 nM and 1 µM bortezomib may have been cached. Furthermore, the reduction of VASP phosphorylation might be higher using lower concentrations of DEA/NO or PGE_1, respectively.

Alleviated VASP phosphorylation is related to diminished counterregulation to platelet activating stimuli. After phosphorylation at Ser^{157} or Ser^{239}, VASP retains the fibrinogen receptor GPIIb/IIIa in the resting conformation [216, 217] and prevents platelets from cytoskeletal rearrangements required for shape change and aggregation [218]. In that way, the bortezomib-mediated reduction of inhibitory effects may support GP recruitment during platelet activation. According to the findings for facilitated platelet adhesion under proteasome inhibition, it was reported that platelet adhesion *in vivo* was enhanced in VASP-deficient mice [217], confirming a potential link between reduced VASP phosphorylation in bortezomib-treated samples and elevated platelet adhesion on coated surfaces.

Furthermore, attenuated VASP phosphorylation under preincubation with bortezomib is obviously elicited by enhanced PP2A activity and results in emphasized platelet aggregation and agglutination using threshold concentrations of platelet agonists, largely independent from the activating signaling pathway and based on reduced inhibitory counterregulation. The aforementioned NFκB-IκB-PKAc complex may be another relevant system affected by proteasome inhibition. Omitted proteasomal activity could lead to enhanced anchorage of PKA in the complex becoming unavailable for signal transduction, which could be an explanation for reduced VASP phosphorylation, since PKA acts as the main kinase for phosphorylation of the VASP protein [112, 214].

Concomitantly with the reduction of induced VASP phosphorylation, the degree of diminished fibrinogen binding mediated by DEA/NO is attenuated under proteasome inhibition. In this regard, the effect on PGE_1-mediated inhibition is only weak, probably due to the commonly higher susceptibility of stored platelets to inhibitors [219].

5.4. The purinergic receptor system is unaffected by bortezomib.

ADP-dependent responsiveness, mediated via the purinergic receptors $P2Y_1R$, $P2Y_{12}R$ and $P2X_1R$, represents an essential characteristic of platelet integrity [197, 220, 221].

The agonist-induced surface expression of all three investigated purinergic receptors, namely $P2Y_1R$ and $P2Y_{12}R$ as ADP receptors and $P2X_1R$ as receptor for ATP, is stable under storage of whole blood for 24 h and is not tampered by proteasome blockade. Since activation of purinergic receptors potentiates GPIIb/IIIa activation and Ca^{2+} influx, resulting in platelet shape change and aggregation, respectively [222-225], it was important to analyze the functionality of the receptors in addition to the surface expression.

The activity of the purinergic receptor $P2Y_{12}R$, measured with the platelet VASP assay kit for flow cytometry and expressed as PRI as well as the activity of $P2X_1R$, determined by induced calcium flux, remain intact after 24 h of storage, irrespective whether proteasome is inhibited or not. Apart from that, the $P2Y_1R$ is equally reduced under all three storage conditions after 24 h. Aberrant $P2Y_1R$ may be subjected to storage-related lesions. In summary, an active proteasome system appears to be dispensable for direct ADP-mediated or purinergic receptor-related mechanisms in platelet function.

5.5. Carfilzomib is able to suppress platelet proteasome activity.

Additional experiments have been implemented with the proteasome inhibitor carfilzomib to rule out bortezomib-specific effects. Carfilzomib is also used for the treatment of multiple myeloma [226]. In contrast to bortezomib, it binds irreversibly and with higher selectivity to the β5-subunit of the proteasome with its epoxyketone as active site [186, 227]. Hence, carfilzomib bears a different inhibition profile for the proteasome, compared to bortezomib. Carfilzomib has not been used for proteasome inhibition in platelets yet, thus the potential to block the 20S activity had to be determined. In PRP, preincubation with 10 nM carfilzomib for 60 min was able to reduce chymotrypsin-like activity > 80 % and higher concentrations totally blocked proteasome activity. In accordance with bortezomib studies [172], the amount of

accumulated poly-ubiquitylated proteins is strongly elevated by preincubation of human platelets with concentrations above 100 nM carfilzomib, confirming adequate inhibition of proteasomal activity [162].

5.6. Like bortezomib, carfilzomib mediates an alleviation of platelet inhibition.

The bortezomib-mediated alleviation of induced VASP phosphorylation as central part in the inhibitory system of platelets is a major finding in this work. Therefore, this system was also investigated under proteasome blockade with carfilzomib. DEA/NO- and PGE_1-induced VASP phosphorylation levels in PRP, preincubated for 60 min with carfilzomib, are also reduced. The extent of attenuated VASP phosphorylation is quite similar to the results obtained for bortezomib with 10 nM carfilzomib, indicating a consistent reduction. Inhibition with the potent concentration of 1 µM carfilzomib shows already heterogenic results, as the reduction of VASP phosphorylation is less pronounced. In conclusion, these findings strongly suggest a similar mechanism of action with carfilzomib as determined for bortezomib, providing further evidence that the proteasome system is actually involved in inhibitory platelet signaling.

Furthermore, functional consequences of preincubation with carfilzomib as proteasome inhibitor were elucidated in threshold platelet aggregation using ADP and collagen as agonists. Here, enhanced ADP-induced platelet threshold aggregation can be observed for 10 nM and 100 nM carfilzomib, whereas 1 µM carfilzomib rather leads to a small increase, apparently pointing to unspecific responses under higher carfilzomib concentrations in the µM-range. Comparable effects are detectable for collagen as agonist, although doses of 100 nM carfilzomib already evoke heterogenic aggregation results. In general, these findings for carfilzomib confirm the results obtained with bortezomib, at least for short-term incubation of 60 min, indicating that observed bortezomib- and carfilzomib-induced effects on platelet function are caused by proteasome inhibition rather than by substance-specific effects. The main findings of this thesis are graphically summarized in the following **Figure 5.1**.

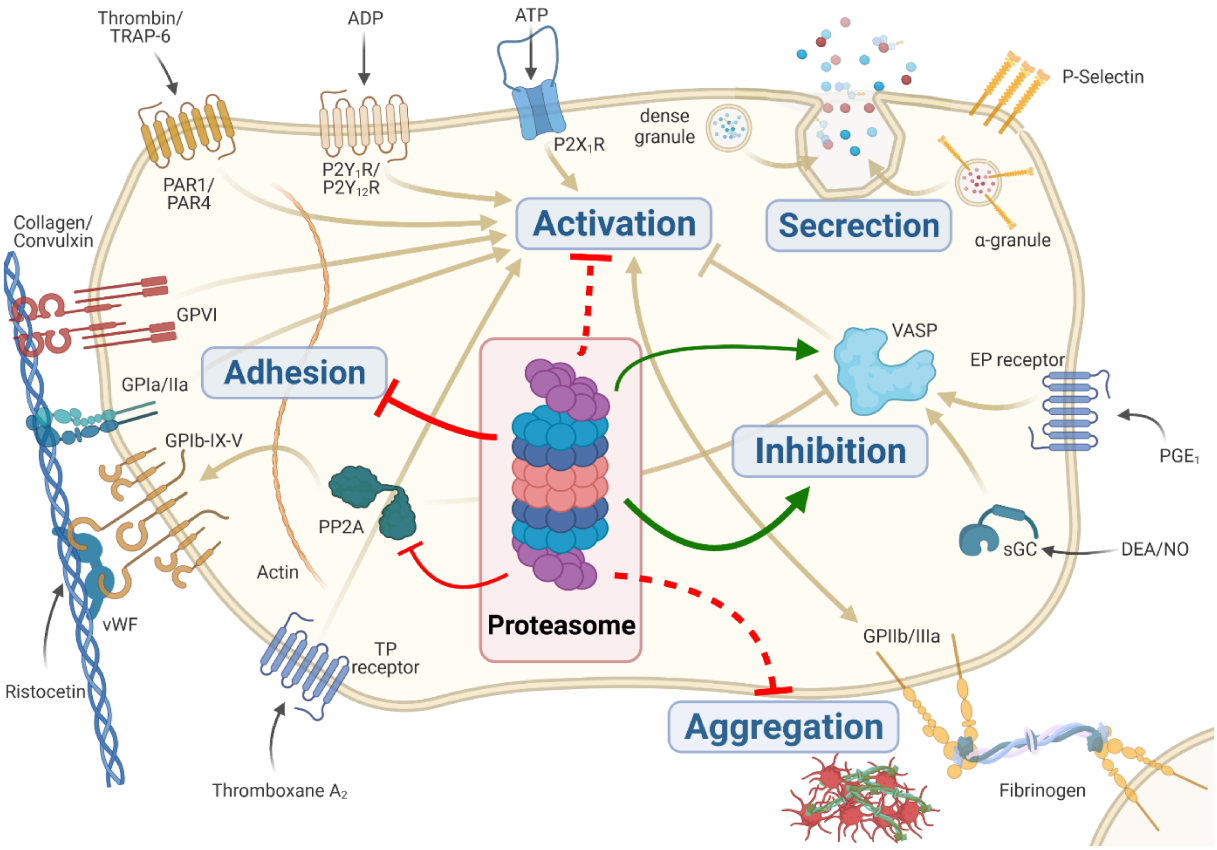

Figure 5.1: Overview of the main findings of this thesis.

Different functional platelet systems in human platelets with the use of proteasome inhibitors were investigated. Proteasome blockade has affected platelet inhibition, accompanied by enhanced platelet aggregation and agglutination. Furthermore, PP2A activity was affected as well as platelet adhesion characteristics. Green arrows indicate activation, red arrows indicate inhibition, dashed arrows indicate indirect influence; VASP – vasodilator-stimulated phosphoprotein, vWF – von Willebrand factor, PP2A – protein phosphatase 2A, PGE_1 – prostaglandin E_1, sGC – soluble guanylyl cyclase, TRAP-6 – Thrombin receptor-activating peptide 6, GP – glycoprotein. Created with BioRender.com.

5.7. Limitations of the study

As a limiting factor in this thesis, it should be mentioned that the presence of different cell types, due to the usage of citrated whole blood as subject or used agents, may have contributed to dampened or milieu-dependent effects of proteasome inhibition on platelets. Especially white blood cells, containing a nucleus and proteasomes, may have led to diminished impact of the proteasome inhibitor bortezomib on platelets in whole blood, depending on the level of white blood cells in the samples. Furthermore, red blood cells may also promote disturbing effects. For example, released hemoglobin from these cells under storage for 24 h has the potential to act as NO scavenger [228], possibly leading to altered responses to the NO donor DEA/NO. However, the

observed reduction of DEA/NO- and PGE_1-induced VASP phosphorylation in bortezomib-treated samples, although moderate, were consistently detectable and confirmed by attenuated inhibition in activating signaling, aggregation and agglutination.

Storage lesions and functional deterioration or preactivation during processes of platelet preparation are a general problem of platelet research. Nevertheless, responses in light transmission aggregometry in stored platelets showed reliable results as expected for normal platelet function [229], except for ADP as agonist, as discussed above. Washed platelets would lose their ADP-related integrity even within 2 h [198]. Therefore, whole blood represents an acceptable physiological milieu for platelets and preserves platelet integrity well for in *in vitro* investigations [230].

It has to be considered that functional effects of alleviated inhibitory signaling may be cached by strong platelet activation (*e.g.* with 10 µM TRAP-6, causing full and irreversible platelet aggregation *in vitro,* as shown in **4.1.1**). In flow cytometry, the detection of slight changes on TRAP-6-induced PAC-1 antibody binding or fibrinogen binding is difficult since this method has a different sensitivity and the titration of threshold agonist concentrations is barely achievable. Therefore, it was important to complement the aggregation studies with the use of individual threshold concentrations of platelet agonists. Under these conditions, the aggregation responses were enhanced in proteasome-inhibited platelets, indicating that the partial impairment of inhibitory signaling plays a functional role in weak platelet stimulation rather than in potent platelet activation with higher agonist concentrations (*e.g.* 10 µM ADP). In regard to investigations of the inhibitory signaling pathways, storage-related lesions of cyclic nucleotide-regulated inhibition may contribute to the stronger PGE_1-mediated reduction of induced fibrinogen binding after 24 h. As a possible explanation, the increasing cGMP levels in stored platelets [219, 231] might potentially interact with the cAMP-dependent pathways resulting in decreased phosphodiesterase 3 activity and emphasized PGE_1-mediated inhibitory effects [232].

5.8. Clinical and pharmacological implications

Since proteasome inhibitors like bortezomib are used for the clinical treatment of patients suffering multiple myeloma, it is important to explore potential risks of

inhibitor-related adverse effects mediated by affected platelet integrity. There is only a limited number of *in vivo* studies investigating direct effects of proteasome inhibitors on platelet function, as discussed in [177]. Zangari *et al.* found a decrease of aggregation responses 1 h after bortezomib administration in ten patients treated due to multiple myeloma [233]. However, the high variation of aggregation values and the role of co-medication make the interpretation of the results difficult. In another clinical study with patients suffering from multiple myeloma, prolonged effects of bortezomib on platelet aggregation were measured during two consecutive treatment cycles [234]. A slight reduction of aggregation responses was observed for different platelet agonists only during the second cycle of bortezomib administration. The platelet count decreased during the observational periods of 11 days, which potentially raises interferences with light transmission aggregometry in addition to ongoing platelet regeneration, making conclusions challenging. In general, induced thrombocytopenia due to treatment with bortezomib is well known [235], conflicting the analysis of platelet function *in vivo* or *ex vivo*. Although evidence is limited, clinical data of treatment with bortezomib or carfilzomib have shown that they may contribute to the risk of thrombotic events [236, 237]. The measured effects of this *in vitro* study are of weak character, but consistent and they support *ex vivo* results found by Rupa-Matysek *et al.* [234]. In conclusion, it should be reassuring for patients with bortezomib medication that direct changes of platelet function observed *in vitro* and *ex vivo* are only moderate.

Another application-oriented aspect of proteasome inhibitors could be the use as supplemental agent in platelet concentrates to modify the hemostatic capacity of stored platelets. Platelet quality decreases during storage after preparation of platelet concentrates due to storage lesions [238]. It has been demonstrated that reduced responsiveness to TRAP-6 as agonist in stored platelets is caused by elevated phosphorylation levels of VASP [231], which is triggered by the accumulation of cGMP due to reduced amount and activity of the cyclic guanosine monophosphate-specific phosphodiesterase type 5A. This decrease could be the consequence of ongoing proteasomal activity with degradation of this enzyme. In this context, Colberg *et al.* could show that the proteasome expression and activity remains stable over 7 days of storage [239].

The addition of non-toxic proteasome inhibitors to platelet concentrates could be an option to improve or to maintain platelet integrity during storage. Proteasome inhibition

may contribute to prevent phosphodiesterase type 5A degradation and to increase the hemostatic capacity of platelets by alleviating the inhibitory pathways. For such experimental approaches, naturally occurring proteasome inhibitors like resveratrol would be available to block proteasome activity [240].

5.9. Outlook

In addition to the investigated receptor and signaling pathway systems, it would be of interest to focus on further important platelet systems, *e.g.* on thrombin-mediated responsiveness. Collagen and convulxin are ligands for the GPVI receptor, which is required for stable platelet adhesion [241-243]. Convulxin is considered to bind to the native human GPIb [203], providing an association and bridging of platelet GPVI with GPIb [204]. First preliminary results indicate that there is no influence of proteasome blockade on expression levels of GPVI, but the interaction of the proteasome and GPVI may play a functional role for platelet adhesion, which should be thoroughly investigated.

For experimentation, several novel proteasome inhibitors are available, *e.g.* carfilzomib, an approved epoxyketone for the treatment of multiple myeloma, or ixazomib, which is an orally available proteasome inhibitor. Marizomib, a β-lactone was tested in clinical trials for the treatment of glioblastoma since it is able to cross the blood-brain-barrier [244, 245]. Their use for clinical and experimental investigations could provide more evidence in respect to pharmacological and hemostatic effects of proteasome inhibition for platelets [237]. Furthermore, additional studies are required investigating the involvement of ubiquitin-dependent processes in the line with proteasome function or downstream effectors like the transcription factor NF-κB, which was also found to be present in the anucleated human platelets [119, 246]. Proteomic analysis could reveal novel information on key proteins interacting with the proteasome system, pointing to essential downstream signaling pathways involved in proteasome-mediated platelet regulation, *e.g.* important for the linkage between proteasome inhibition and PP2A activity or alleviated inhibitory signaling, as discovered in this thesis.

6. References

[1] Schultze, M. Ein heizbarer Objecttisch und seine Verwendung bei Untersuchungen des Blutes. *Archiv f. mikrosk. Anatomie.* **1865**, *1* (1), 1-42.

[2] Bizzozero, J. Ueber einen neuen Formbestandtheil des Blutes und dessen Rolle bei der Thrombose und der Blutgerinnung. *Archiv f. pathol. Anat.* **1882**, *90* (2), 261-332.

[3] Daly, M. E. Determinants of platelet count in humans. *Haematologica.* **2011**, *96* (1), 10-13.

[4] Harker, L. A., Roskos, L. K., Marzec, U. M., Carter, R. A., Cherry, J. K.*, et al.* Effects of megakaryocyte growth and development factor on platelet production, platelet life span, and platelet function in healthy human volunteers. *Blood.* **2000**, *95* (8), 2514-2522.

[5] Kaushansky, K. Determinants of platelet number and regulation of thrombopoiesis. *Hematology Am Soc Hematol Educ Program.* **2009**, 147-152.

[6] Rumjantseva, V., Hoffmeister, K. M. Novel and unexpected clearance mechanisms for cold platelets. *Transfus Apher Sci.* **2010**, *42* (1), 63-70.

[7] Grozovsky, R., Hoffmeister, K. M., Falet, H. Novel clearance mechanisms of platelets. *Curr Opin Hematol.* **2010**, *17* (6), 585-589.

[8] Mason, K. D., Carpinelli, M. R., Fletcher, J. I., Collinge, J. E., Hilton, A. A.*, et al.* Programmed anuclear cell death delimits platelet life span. *Cell.* **2007**, *128* (6), 1173-1186.

[9] Savage, B., Saldivar, E., Ruggeri, Z. M. Initiation of platelet adhesion by arrest onto fibrinogen or translocation on von Willebrand factor. *Cell.* **1996**, *84* (2), 289-297.

[10] Eisinger, F., Patzelt, J., Langer, H. F. The Platelet Response to Tissue Injury. *Front Med (Lausanne).* **2018**, *5*, 317.

[11] Lecut, C., Schoolmeester, A., Kuijpers, M. J., Broers, J. L., van Zandvoort, M. A.*, et al.* Principal role of glycoprotein VI in alpha2beta1 and alphaIIbbeta3 activation during collagen-induced thrombus formation. *Arterioscler Thromb Vasc Biol.* **2004**, *24* (9), 1727-1733.

[12] Gudbrandsdottir, S., Hasselbalch, H. C., Nielsen, C. H. Activated platelets enhance IL-10 secretion and reduce TNF-alpha secretion by monocytes. *J Immunol.* **2013**, *191* (8), 4059-4067.

[13] Wagner, D. D., Burger, P. C. Platelets in inflammation and thrombosis. *Arterioscler Thromb Vasc Biol.* **2003**, *23* (12), 2131-2137.

[14] Rondina, M. T., Garraud, O. Emerging evidence for platelets as immune and inflammatory effector cells. *Front Immunol.* **2014**, *5*, 653.

[15] Ali, R. A., Wuescher, L. M., Worth, R. G. Platelets: essential components of the immune system. *Curr Trends Immunol.* **2015**, *16*, 65-78.

[16] Thomas, S. G. The Structure of Resting and Activated Platelets. In: Michelson A. D., Ed: Platelets. 4th ed. *Elsevier, Cambridge, MA*. **2019**, 47-77.

[17] Wright, J. H. The Origin and Nature of the Blood Plates. *The Boston Medical and Surgical Journal.* **1906**, *154* (23), 643-645.

[18] Lefrancais, E., Ortiz-Munoz, G., Caudrillier, A., Mallavia, B., Liu, F.*, et al.* The lung is a site of platelet biogenesis and a reservoir for haematopoietic progenitors. *Nature.* **2017**, *544* (7648), 105-109.

[19] Young, J. C., Bruno, E., Luens, K. M., Wu, S., Backer, M.*, et al.* Thrombopoietin stimulates megakaryocytopoiesis, myelopoiesis, and expansion of CD34+ progenitor cells from single CD34+Thy-1+Lin- primitive progenitor cells. *Blood.* **1996**, *88* (5), 1619-1631.

[20] Solar, G. P., Kerr, W. G., Zeigler, F. C., Hess, D., Donahue, C.*, et al.* Role of c-mpl in early hematopoiesis. *Blood.* **1998**, *92* (1), 4-10.

[21] Bluteau, D., Lordier, L., Di Stefano, A., Chang, Y., Raslova, H.*, et al.* Regulation of megakaryocyte maturation and platelet formation. *J Thromb Haemost.* **2009**, *7 Suppl 1*, 227-234.

[22] Szalai, G., LaRue, A. C., Watson, D. K. Molecular mechanisms of megakaryopoiesis. *Cell Mol Life Sci.* **2006**, *63* (21), 2460-2476.

[23] Geddis, A. E. Megakaryopoiesis. *Semin Hematol.* **2010**, *47* (3), 212-219.

[24] Deutsch, V. R., Tomer, A. Megakaryocyte development and platelet production. *Br J Haematol.* **2006**, *134* (5), 453-466.

[25] Richardson, J. L., Shivdasani, R. A., Boers, C., Hartwig, J. H., Italiano, J. E., Jr. Mechanisms of organelle transport and capture along proplatelets during platelet production. *Blood.* **2005**, *106* (13), 4066-4075.

[26] Patel, S. R., Hartwig, J. H., Italiano, J. E., Jr. The biogenesis of platelets from megakaryocyte proplatelets. *J Clin Invest.* **2005**, *115* (12), 3348-3354.

[27] Tomer, A., Harker, L. A., Burstein, S. A. Purification of human megakaryocytes by fluorescence-activated cell sorting. *Blood.* **1987**, *70* (6), 1735-1742.

[28] Junt, T., Schulze, H., Chen, Z., Massberg, S., Goerge, T.*, et al.* Dynamic visualization of thrombopoiesis within bone marrow. *Science.* **2007**, *317* (5845), 1767-1770.

[29] Long, M. W. Megakaryocyte differentiation events. *Semin Hematol.* **1998**, *35* (3), 192-199.

[30] Tomer, A. Human marrow megakaryocyte differentiation: multiparameter correlative analysis identifies von Willebrand factor as a sensitive and distinctive marker for early (2N and 4N) megakaryocytes. *Blood.* **2004**, *104* (9), 2722-2727.

[31] Garraud, O., Cognasse, F. Are Platelets Cells? And if Yes, are They Immune Cells? *Front Immunol.* **2015**, *6*, 70.

[32] Geddis, A. E., Kaushansky, K. The root of platelet production. *Science.* **2007**, *317* (5845), 1689-1691.

[33] Lhermusier, T., Chap, H., Payrastre, B. Platelet membrane phospholipid asymmetry: from the characterization of a scramblase activity to the identification of an essential protein mutated in Scott syndrome. *J Thromb Haemost.* **2011**, *9* (10), 1883-1891.

[34] Saboor, M., Ayub, Q., Ilyas, S., Moinuddin Platelet receptors; an instrumental of platelet physiology. *Pak J Med Sci.* **2013**, *29* (3), 891-896.

[35] Rivera, J., Lozano, M. L., Navarro-Nunez, L., Vicente, V. Platelet receptors and signaling in the dynamics of thrombus formation. *Haematologica.* **2009**, *94* (5), 700-711.

[36] Platelet Inhibitory Receptors. In '*Platelets (Fourth Edition)*', Academic Press: **2019**, 279-293.

[37] Horstrup, K., Jablonka, B., Honig-Liedl, P., Just, M., Kochsiek, K.*, et al.* Phosphorylation of focal adhesion vasodilator-stimulated phosphoprotein at Ser157 in intact human platelets correlates with fibrinogen receptor inhibition. *Eur J Biochem.* **1994**, *225* (1), 21-27.

[38] Smolenski, A., Bachmann, C., Reinhard, K., Honig-Liedl, P., Jarchau, T.*, et al.* Analysis and regulation of vasodilator-stimulated phosphoprotein serine 239 phosphorylation in vitro and in intact cells using a phosphospecific monoclonal antibody. *J Biol Chem.* **1998**, *273* (32), 20029-20035.

[39] Hauser, W., Knobeloch, K. P., Eigenthaler, M., Gambaryan, S., Krenn, V.*, et al.* Megakaryocyte hyperplasia and enhanced agonist-induced platelet activation in vasodilator-stimulated phosphoprotein knockout mice. *Proc Natl Acad Sci U S A.* **1999**, *96* (14), 8120-8125.

[40] Evans, R. J., Lewis, C., Virginio, C., Lundstrom, K., Buell, G.*, et al.* Ionic permeability of, and divalent cation effects on, two ATP-gated cation channels (P2X receptors) expressed in mammalian cells. *J Physiol.* **1996**, *497 (Pt 2)*, 413-422.

[41] Moore, K. L., Patel, K. D., Bruehl, R. E., Li, F., Johnson, D. A.*, et al.* P-selectin glycoprotein ligand-1 mediates rolling of human neutrophils on P-selectin. *J Cell Biol.* **1995**, *128* (4), 661-671.

[42] Cognasse, F., Hamzeh, H., Chavarin, P., Acquart, S., Genin, C.*, et al.* Evidence of Toll-like receptor molecules on human platelets. *Immunol Cell Biol.* **2005**, *83* (2), 196-198.

[43] Shiraki, R., Inoue, N., Kawasaki, S., Takei, A., Kadotani, M.*, et al.* Expression of Toll-like receptors on human platelets. *Thromb Res.* **2004**, *113* (6), 379-385.

[44] Mukherjee, S., Karmakar, S., Babu, S. P. TLR2 and TLR4 mediated host immune responses in major infectious diseases: a review. *Braz J Infect Dis.* **2016**, *20* (2), 193-204.

[45] Semple, J. W., Italiano, J. E., Jr., Freedman, J. Platelets and the immune continuum. *Nat Rev Immunol.* **2011**, *11* (4), 264-274.

[46] Niklaus, M., Klingler, P., Weber, K., Koessler, A., Boeck, M.*, et al.* The involvement of toll-like receptors 2 and 4 in human platelet signalling pathways. *Cell Signal.* **2020**, *76*, 109817.

[47] Cerecedo, D. Platelet cytoskeleton and its hemostatic role. *Blood Coagul Fibrinolysis.* **2013**, *24* (8), 798-808.

[48] Thon, J. N., Italiano, J. E. Platelets: production, morphology and ultrastructure. *Handb Exp Pharmacol.* **2012**, (210), 3-22.

[49] Sharda, A., Flaumenhaft, R. The life cycle of platelet granules. *F1000Res.* **2018**, *7*, 236.

[50] Holt, J. C., Niewiarowski, S. Biochemistry of alpha granule proteins. *Semin Hematol.* **1985**, *22* (2), 151-163.

[51] Handagama, P., Scarborough, R. M., Shuman, M. A., Bainton, D. F. Endocytosis of fibrinogen into megakaryocyte and platelet alpha-granules is mediated by alpha IIb beta 3 (glycoprotein IIb-IIIa). *Blood.* **1993**, *82* (1), 135-138.

[52] Ciferri, S., Emiliani, C., Guglielmini, G., Orlacchio, A., Nenci, G. G.*, et al.* Platelets release their lysosomal content in vivo in humans upon activation. *Thromb Haemost.* **2000**, *83* (1), 157-164.

[53] Rozario, T., DeSimone, D. W. The extracellular matrix in development and morphogenesis: a dynamic view. *Dev Biol.* **2010**, *341* (1), 126-140.

[54] Manon-Jensen, T., Kjeld, N. G., Karsdal, M. A. Collagen-mediated hemostasis. *J Thromb Haemost.* **2016**, *14* (3), 438-448.

[55] Farndale, R. W., Sixma, J. J., Barnes, M. J., de Groot, P. G. The role of collagen in thrombosis and hemostasis. *J Thromb Haemost.* **2004**, *2* (4), 561-573.

[56] Coller, B. S., Beer, J. H., Scudder, L. E., Steinberg, M. H. Collagen-platelet interactions: evidence for a direct interaction of collagen with platelet GPIa/IIa and an indirect interaction with platelet GPIIb/IIIa mediated by adhesive proteins. *Blood.* **1989**, *74* (1), 182-192.

[57] Jung, S. M., Moroi, M. Platelet glycoprotein VI. *Adv Exp Med Biol.* **2008**, *640*, 53-63.

[58] De Meyer, S. F., Vanhoorelbeke K Fau - Ulrichts, H., Ulrichts H Fau - Staelens, S., Staelens S Fau - Feys, H. B., Feys Hb Fau - Salles, I.*, et al.* Development of monoclonal antibodies that inhibit platelet adhesion or aggregation as potential anti-thrombotic drugs. **2006**, *5* (3), 197-207.

[59] Lopez, J. A., Andrews, R. K., Afshar-Kharghan, V., Berndt, M. C. Bernard-Soulier syndrome. *Blood.* **1998**, *91* (12), 4397-4418.

[60] Qi, Q. M., Dunne, E., Oglesby, I., Schoen, I., Ricco, A. J.*, et al.* In Vitro Measurement and Modeling of Platelet Adhesion on VWF-Coated Surfaces in Channel Flow. *Biophys J.* **2019**, *116* (6), 1136-1151.

[61] Mody, N. A., Lomakin, O., Doggett, T. A., Diacovo, T. G., King, M. R. Mechanics of transient platelet adhesion to von Willebrand factor under flow. *Biophys J.* **2005**, *88* (2), 1432-1443.

[62] Varughese, K. I., Celikel, R., Ruggeri, Z. M. Structure and function of the von Willebrand factor A1 domain. *Curr Protein Pept Sci.* **2002**, *3* (3), 301-312.

[63] Arce, N. A., Cao, W., Brown, A. K., Legan, E. R., Wilson, M. S.*, et al.* Activation of von Willebrand factor via mechanical unfolding of its discontinuous autoinhibitory module. *Nat Commun.* **2021**, *12* (1), 2360.

[64] Di Stasio, E., Romitelli, F., Lancellotti, S., Arcovito, A., Giardina, B.*, et al.* Kinetic study of von Willebrand factor self-aggregation induced by ristocetin. *Biophysical Chemistry.* **2009**, *144* (3), 101-107.

[65] Okumura, T., Hasitz, M., Jamieson, G. A. Platelet glycocalicin. Interaction with thrombin and role as thrombin receptor of the platelet surface. *J Biol Chem.* **1978**, *253* (10), 3435-3443.

[66] Romo, G. M., Dong, J. F., Schade, A. J., Gardiner, E. E., Kansas, G. S.*, et al.* The glycoprotein Ib-IX-V complex is a platelet counterreceptor for P-selectin. *J Exp Med.* **1999**, *190* (6), 803-814.

[67] Ozaki, Y., Asazuma, N., Suzuki-Inoue, K., Berndt, M. C. Platelet GPIb-IX-V-dependent signaling. *J Thromb Haemost.* **2005**, *3* (8), 1745-1751.

[68] Slater, A., Di, Y., Clark, J. C., Jooss, N. J., Martin, E. M.*, et al.* Structural characterization of a novel GPVI-nanobody complex reveals a biologically active domain-swapped GPVI dimer. *Blood.* **2021**, *137* (24), 3443-3453.

[69] Stalker, T. J., Newman, D. K., Ma, P., Wannemacher, K. M., Brass, L. F. Platelet signaling. *Handb Exp Pharmacol.* **2012**, (210), 59-85.

[70] Ezumi, Y., Shindoh, K., Tsuji, M., Takayama, H. Physical and functional association of the Src family kinases Fyn and Lyn with the collagen receptor glycoprotein VI-Fc receptor gamma chain complex on human platelets. *J Exp Med.* **1998**, *188* (2), 267-276.

[71] Watson, S. P., Asazuma, N., Atkinson, B., Berlanga, O., Best, D.*, et al.* The role of ITAM- and ITIM-coupled receptors in platelet activation by collagen. *Thromb Haemost.* **2001**, *86* (1), 276-288.

[72] Daniel, J. L., Dangelmaier, C., Smith, J. B. Evidence for a role for tyrosine phosphorylation of phospholipase C gamma 2 in collagen-induced platelet cytosolic calcium mobilization. *Biochem J.* **1994**, *302 (Pt 2)*, 617-622.

[73] Kim, S., Mangin, P., Dangelmaier, C., Lillian, R., Jackson, S. P.*, et al.* Role of phosphoinositide 3-kinase beta in glycoprotein VI-mediated Akt activation in platelets. *J Biol Chem.* **2009**, *284* (49), 33763-33772.

[74] Miura, Y., Takahashi, T., Jung, S. M., Moroi, M. Analysis of the interaction of platelet collagen receptor glycoprotein VI (GPVI) with collagen. A dimeric form of GPVI, but not the monomeric form, shows affinity to fibrous collagen. *J Biol Chem.* **2002**, *277* (48), 46197-46204.

[75] Jung, S. M., Moroi, M. Signal-transducing mechanisms involved in activation of the platelet collagen receptor integrin alpha(2)beta(1). *J Biol Chem.* **2000**, *275* (11), 8016-8026.

[76] Inoue, O., Suzuki-Inoue, K., Dean, W. L., Frampton, J., Watson, S. P. Integrin alpha2beta1 mediates outside-in regulation of platelet spreading on collagen through activation of Src kinases and PLCgamma2. *J Cell Biol.* **2003**, *160* (5), 769-780.

[77] Gibbins, J. M. Platelet adhesion signalling and the regulation of thrombus formation. *J Cell Sci.* **2004**, *117* (Pt 16), 3415-3425.

[78] Chen, J., Lopez, J. A. Interactions of platelets with subendothelium and endothelium. *Microcirculation.* **2005**, *12* (3), 235-246.

[79] Auger, J. M., Kuijpers, M. J., Senis, Y. A., Watson, S. P., Heemskerk, J. W. Adhesion of human and mouse platelets to collagen under shear: a unifying model. *FASEB J.* **2005**, *19* (7), 825-827.

[80] Göbel, K., Eichler, S., Wiendl, H., Chavakis, T., Kleinschnitz, C.*, et al.* The Coagulation Factors Fibrinogen, Thrombin, and Factor XII in Inflammatory Disorders—A Systematic Review. *Frontiers in Immunology.* **2018**, *9* (1731).

[81] Coughlin, S. R. How the protease thrombin talks to cells. *Proc Natl Acad Sci U S A.* **1999**, *96* (20), 11023-11027.

[82] Woulfe, D. S. Platelet G protein-coupled receptors in hemostasis and thrombosis. *J Thromb Haemost.* **2005**, *3* (10), 2193-2200.

[83] Heo, Y., Jeon, H., Namkung, W. PAR4-Mediated PI3K/Akt and RhoA/ROCK Signaling Pathways Are Essential for Thrombin-Induced Morphological Changes in MEG-01 Cells. *International Journal of Molecular Sciences.* **2022**, *23* (2), 776.

[84] Covic, L., Gresser, A. L., Kuliopulos, A. Biphasic kinetics of activation and signaling for PAR1 and PAR4 thrombin receptors in platelets. *Biochemistry.* **2000**, *39* (18), 5458-5467.

[85] Andersen, H., Greenberg, D. L., Fujikawa, K., Xu, W., Chung, D. W.*, et al.* Protease-activated receptor 1 is the primary mediator of thrombin-stimulated platelet procoagulant activity. *Proc Natl Acad Sci U S A.* **1999**, *96* (20), 11189-11193.

[86] Ramachandran, R., Noorbakhsh, F., Defea, K., Hollenberg, M. D. Targeting proteinase-activated receptors: therapeutic potential and challenges. *Nat Rev Drug Discov.* **2012**, *11* (1), 69-86.

[87] Barr, A. J., Brass, L. F., Manning, D. R. Reconstitution of receptors and GTP-binding regulatory proteins (G proteins) in Sf9 cells. A direct evaluation of selectivity in receptor.G protein coupling. *J Biol Chem.* **1997**, *272* (4), 2223-2229.

[88] Broos, K., Feys, H. B., De Meyer, S. F., Vanhoorelbeke, K., Deckmyn, H. Platelets at work in primary hemostasis. *Blood Rev.* **2011**, *25* (4), 155-167.

[89] Oury, C., Toth-Zsamboki, E., Vermylen, J., Hoylaerts, M. F. The platelet ATP and ADP receptors. *Curr Pharm Des.* **2006**, *12* (7), 859-875.

[90] Ohlmann, P., Laugwitz, K. L., Nurnberg, B., Spicher, K., Schultz, G.*, et al.* The human platelet ADP receptor activates Gi2 proteins. *Biochem J.* **1995**, *312 (Pt 3)*, 775-779.

[91] Cosemans, J. M., Munnix, I. C., Wetzker, R., Heller, R., Jackson, S. P.*, et al.* Continuous signaling via PI3K isoforms beta and gamma is required for platelet ADP receptor function in dynamic thrombus stabilization. *Blood.* **2006**, *108* (9), 3045-3052.

[92] Kim, S., Jin, J., Kunapuli, S. P. Akt activation in platelets depends on Gi signaling pathways. *J Biol Chem.* **2004**, *279* (6), 4186-4195.

[93] Geiger, J., Brich, J., Honig-Liedl, P., Eigenthaler, M., Schanzenbacher, P.*, et al.* Specific impairment of human platelet P2Y(AC) ADP receptor-mediated signaling by the antiplatelet drug clopidogrel. *Arterioscler Thromb Vasc Biol.* **1999**, *19* (8), 2007-2011.

[94] Damman, P., Woudstra, P., Kuijt, W. J., de Winter, R. J., James, S. K. P2Y12 platelet inhibition in clinical practice. *J Thromb Thrombolysis.* **2012**, *33* (2), 143-153.

[95] Jin, J., Daniel, J. L., Kunapuli, S. P. Molecular basis for ADP-induced platelet activation. II. The P2Y1 receptor mediates ADP-induced intracellular calcium mobilization and shape change in platelets. *J Biol Chem.* **1998**, *273* (4), 2030-2034.

[96] Ohlmann, P., de Castro, S., Brown, G. G., Jr., Gachet, C., Jacobson, K. A.*, et al.* Quantification of recombinant and platelet P2Y(1) receptors utilizing a [(125)I]-labeled high-affinity antagonist 2-iodo-N(6)-methyl-(N)-methanocarba-2'-deoxyadenosine-3',5'-bisphosphate ([(125)I]MRS2500). *Pharmacol Res.* **2010**, *62* (4), 344-351.

[97] Jin, J., Kunapuli, S. P. Coactivation of two different G protein-coupled receptors is essential for ADP-induced platelet aggregation. *Proc Natl Acad Sci U S A.* **1998**, *95* (14), 8070-8074.

[98] Jin, J., Quinton, T. M., Zhang, J., Rittenhouse, S. E., Kunapuli, S. P. Adenosine diphosphate (ADP)-induced thromboxane A(2) generation in human platelets requires coordinated signaling through integrin alpha(IIb)beta(3) and ADP receptors. *Blood.* **2002**, *99* (1), 193-198.

[99] Cattaneo, M., Marchese, P., Jacobson, K., Ruggeri, Z. New insights into the role of P2X1 in platelet function. *Haematologica.* **2002**, *87* (10), 13-14.

[100] Ferri, N., Corsini, A., Bellosta, S. Pharmacology of the new P2Y12 receptor inhibitors: insights on pharmacokinetic and pharmacodynamic properties. *Drugs.* **2013**, *73* (15), 1681-1709.

[101] Wagner, C. L., Mascelli, M. A., Neblock, D. S., Weisman, H. F., Coller, B. S.*, et al.* Analysis of GPIIb/IIIa receptor number by quantification of 7E3 binding to human platelets. *Blood.* **1996**, *88* (3), 907-914.

[102] Wencel-Drake, J. D., Plow, E. F., Kunicki, T. J., Woods, V. L., Keller, D. M.*, et al.* Localization of internal pools of membrane glycoproteins involved in platelet adhesive responses. *Am J Pathol.* **1986**, *124* (2), 324-334.

[103] Bergmeier, W., Hynes, R. O. Extracellular matrix proteins in hemostasis and thrombosis. *Cold Spring Harb Perspect Biol.* **2012**, *4* (2).

[104] Kamata, T., Handa, M., Ito, S., Sato, Y., Ohtani, T.*, et al.* Structural requirements for activation in alphaIIb beta3 integrin. *J Biol Chem.* **2010**, *285* (49), 38428-38437.

[105] Huang, J., Li, X., Shi, X., Zhu, M., Wang, J.*, et al.* Platelet integrin alphaIIbbeta3: signal transduction, regulation, and its therapeutic targeting. *J Hematol Oncol.* **2019**, *12* (1), 26.

[106] Nieswandt, B., Watson, S. P. Platelet-collagen interaction: is GPVI the central receptor? *Blood.* **2003**, *102* (2), 449-461.

[107] Shattil, S. J., Cunningham, M., Hoxie, J. A. Detection of activated platelets in whole blood using activation-dependent monoclonal antibodies and flow cytometry. *Blood.* **1987**, *70* (1), 307-315.

[108] van den Kerkhof, D. L., van der Meijden, P. E. J., Hackeng, T. M., Dijkgraaf, I. Exogenous Integrin alphaIIbbeta3 Inhibitors Revisited: Past, Present and Future Applications. *Int J Mol Sci.* **2021**, *22* (7).

[109] Born, G. V., Cross, M. J. The Aggregation of Blood Platelets. *J Physiol.* **1963**, *168*, 178-195.

[110] Wang, G. R., Zhu, Y., Halushka, P. V., Lincoln, T. M., Mendelsohn, M. E. Mechanism of platelet inhibition by nitric oxide: in vivo phosphorylation of thromboxane receptor by cyclic GMP-dependent protein kinase. *Proc Natl Acad Sci U S A.* **1998**, *95* (9), 4888-4893.

[111] Marjanovic, J. A., Stojanovic, A., Brovkovych, V. M., Skidgel, R. A., Du, X. Signaling-mediated functional activation of inducible nitric-oxide synthase and its role in stimulating platelet activation. *J Biol Chem.* **2008**, *283* (43), 28827-28834.

[112] Butt, E., Abel, K., Krieger, M., Palm, D., Hoppe, V.*, et al.* cAMP- and cGMP-dependent protein kinase phosphorylation sites of the focal adhesion vasodilator-stimulated phosphoprotein (VASP) in vitro and in intact human platelets. *J Biol Chem.* **1994**, *269* (20), 14509-14517.

[113] Weiss, H. J., Turitto, V. T. Prostacyclin (prostaglandin I2, PGI2) inhibits platelet adhesion and thrombus formation on subendothelium. *Blood.* **1979**, *53* (2), 244-250.

[114] Reinhard, M., Halbrugge, M., Scheer, U., Wiegand, C., Jockusch, B. M.*, et al.* The 46/50 kDa phosphoprotein VASP purified from human platelets is a novel protein associated with actin filaments and focal contacts. *EMBO J.* **1992**, *11* (6), 2063-2070.

[115] Harbeck, B., Huttelmaier, S., Schluter, K., Jockusch, B. M., Illenberger, S. Phosphorylation of the vasodilator-stimulated phosphoprotein regulates its interaction with actin. *J Biol Chem.* **2000**, *275* (40), 30817-30825.

[116] Abel, K., Mieskes, G., Walter, U. Dephosphorylation of the focal adhesion protein VASP in vitro and in intact human platelets. *FEBS Lett.* **1995**, *370* (3), 184-188.

[117] Dangel, O., Mergia, E., Karlisch, K., Groneberg, D., Koesling, D.*, et al.* Nitric oxide-sensitive guanylyl cyclase is the only nitric oxide receptor mediating platelet inhibition. *J Thromb Haemost.* **2010**, *8* (6), 1343-1352.

[118] Waldmann, R., Nieberding, M., Walter, U. Vasodilator-stimulated protein phosphorylation in platelets is mediated by cAMP- and cGMP-dependent protein kinases. *Eur J Biochem.* **1987**, *167* (3), 441-448.

[119] Lannan, K. L., Sahler, J., Kim, N., Spinelli, S. L., Maggirwar, S. B.*, et al.* Breaking the mold: transcription factors in the anucleate platelet and platelet-derived microparticles. *Front Immunol.* **2015**, *6*, 48.

[120] Warshaw, A. L., Laster, L., Shulman, N. R. Protein synthesis by human platelets. *J Biol Chem.* **1967**, *242* (9), 2094-2097.

[121] Rowley, J. W., Schwertz, H., Weyrich, A. S. Platelet mRNA: the meaning behind the message. *Curr Opin Hematol.* **2012**, *19* (5), 385-391.

[122] Denis, M. M., Tolley, N. D., Bunting, M., Schwertz, H., Jiang, H.*, et al.* Escaping the nuclear confines: signal-dependent pre-mRNA splicing in anucleate platelets. *Cell.* **2005**, *122* (3), 379-391.

[123] Weyrich, A. S., Dixon, D. A., Pabla, R., Elstad, M. R., McIntyre, T. M.*, et al.* Signal-dependent translation of a regulatory protein, Bcl-3, in activated human platelets. *Proc Natl Acad Sci U S A.* **1998**, *95* (10), 5556-5561.

[124] Croce, K., Flaumenhaft, R., Rivers, M., Furie, B., Furie, B. C.*, et al.* Inhibition of calpain blocks platelet secretion, aggregation, and spreading. *J Biol Chem.* **1999**, *274* (51), 36321-36327.

[125] Kraemer, B. F., Weyrich, A. S., Lindemann, S. Protein degradation systems in platelets. *Thromb Haemost.* **2013**, *110* (5), 920-924.

[126] Acharji, S., Lakshmanadoss, U., Rudzinski, W., Stapleton, D. D., Kaluski, E. Use of antiplatelet agents in patients with atherosclerotic disease. *Postgrad Med.* **2013**, *125* (5), 19-30.

[127] Schror, K. Aspirin and platelets: the antiplatelet action of aspirin and its role in thrombosis treatment and prophylaxis. *Semin Thromb Hemost.* **1997**, *23* (4), 349-356.

[128] Tsigkou, V., Siasos, G., Rovos, K., Tripyla, N., Tousoulis, D. Peripheral artery disease and antiplatelet treatment. *Curr Opin Pharmacol.* **2018**, *39*, 43-52.

[129] Harbrecht, U. Old and new anticoagulants. *Hamostaseologie.* **2011**, *31* (1), 21-27.

[130] Nurden, A. T. Glanzmann thrombasthenia. *Orphanet J Rare Dis.* **2006**, *1*, 10.

[131] Krishnegowda, M., Rajashekaraiah, V. Platelet disorders: an overview. *Blood Coagul Fibrinolysis.* **2015**, *26* (5), 479-491.

[132] The Board of the German Medical Association on the Recommendation of the Scientific Advisory Board (Bundesärztekammer): Platelet Concentrates. In '*Cross-Sectional Guidelines for Therapy with Blood Components and Plasma Derivatives*', *Transfusion Medicine and Hemotherapy*. **2009**, Vol. 36 (6), 372-382.

[133] Palmer, A., Rivett, A. J., Thomson, S., Hendil, K. B., Butcher, G. W.*, et al.* Subpopulations of proteasomes in rat liver nuclei, microsomes and cytosol. *Biochem J.* **1996**, *316 (Pt 2)*, 401-407.

[134] Coux, O., Tanaka, K., Goldberg, A. L. Structure and functions of the 20S and 26S proteasomes. *Annu Rev Biochem.* **1996**, *65*, 801-847.

[135] Finley, D., Chau, V. Ubiquitination. *Annu Rev Cell Biol.* **1991**, *7*, 25-69.

[136] Hershko, A., Ciechanover, A. The ubiquitin system. *Annu Rev Biochem.* **1998**, *67*, 425-479.

[137] Pickart, C. M. Mechanisms underlying ubiquitination. *Annu Rev Biochem.* **2001**, *70*, 503-533.

[138] Thrower, J. S., Hoffman, L., Rechsteiner, M., Pickart, C. M. Recognition of the polyubiquitin proteolytic signal. *EMBO J.* **2000**, *19* (1), 94-102.

[139] Bonifacino, J. S., Weissman, A. M. Ubiquitin and the control of protein fate in the secretory and endocytic pathways. *Annu Rev Cell Dev Biol.* **1998**, *14*, 19-57.

[140] Tanaka, K. The proteasome: overview of structure and functions. *Proc Jpn Acad Ser B Phys Biol Sci.* **2009**, *85* (1), 12-36.

[141] Zwickl, P., Kleinz, J., Baumeister, W. Critical elements in proteasome assembly. *Nat Struct Biol.* **1994**, *1* (11), 765-770.

[142] Groll, M., Heinemeyer, W., Jager, S., Ullrich, T., Bochtler, M.*, et al.* The catalytic sites of 20S proteasomes and their role in subunit maturation: a mutational and crystallographic study. *Proc Natl Acad Sci U S A.* **1999**, *96* (20), 10976-10983.

[143] Kisselev, A. F., Garcia-Calvo, M., Overkleeft, H. S., Peterson, E., Pennington, M. W.*, et al.* The caspase-like sites of proteasomes, their substrate specificity, new inhibitors and substrates, and allosteric interactions with the trypsin-like sites. *J Biol Chem.* **2003**, *278* (38), 35869-35877.

[144] Cundiff, M. D., Hurley, C. M., Wong, J. D., Boscia, J. A. t., Bashyal, A.*, et al.* Ubiquitin receptors are required for substrate-mediated activation of the proteasome's unfolding ability. *Sci Rep.* **2019**, *9* (1), 14506.

[145] Verma, R., Aravind, L., Oania, R., McDonald, W. H., Yates, J. R., 3rd, *et al.* Role of Rpn11 metalloprotease in deubiquitination and degradation by the 26S proteasome. *Science.* **2002**, *298* (5593), 611-615.

[146] Reits, E., Griekspoor, A., Neijssen, J., Groothuis, T., Jalink, K., *et al.* Peptide diffusion, protection, and degradation in nuclear and cytoplasmic compartments before antigen presentation by MHC class I. *Immunity.* **2003**, *18* (1), 97-108.

[147] Dubiel, W., Pratt, G., Ferrell, K., Rechsteiner, M. Purification of an 11 S regulator of the multicatalytic protease. *J Biol Chem.* **1992**, *267* (31), 22369-22377.

[148] Kasahara, M. Role of immunoproteasomes and thymoproteasomes in health and disease. *Pathol Int.* **2021**, *71* (6), 371-382.

[149] Dou, Q. P., Li, B. Proteasome inhibitors as potential novel anticancer agents. *Drug Resist Updat.* **1999**, *2* (4), 215-223.

[150] Chen, D., Frezza, M., Schmitt, S., Kanwar, J., Dou, Q. P. Bortezomib as the first proteasome inhibitor anticancer drug: current status and future perspectives. *Curr Cancer Drug Targets.* **2011**, *11* (3), 239-253.

[151] Kisselev, A. F., Goldberg, A. L. Proteasome inhibitors: from research tools to drug candidates. *Chem Biol.* **2001**, *8* (8), 739-758.

[152] Shen, M., Chan, T. H., Dou, Q. P. Targeting tumor ubiquitin-proteasome pathway with polyphenols for chemosensitization. *Anticancer Agents Med Chem.* **2012**, *12* (8), 891-901.

[153] Jung, T., Catalgol, B., Grune, T. The proteasomal system. *Mol Aspects Med.* **2009**, *30* (4), 191-296.

[154] Tan, C. R. C., Abdul-Majeed, S., Cael, B., Barta, S. K. Clinical Pharmacokinetics and Pharmacodynamics of Bortezomib. *Clin Pharmacokinet.* **2019**, *58* (2), 157-168.

[155] Bross, P. F., Kane, R., Farrell, A. T., Abraham, S., Benson, K., *et al.* Approval summary for bortezomib for injection in the treatment of multiple myeloma. *Clin Cancer Res.* **2004**, *10* (12 Pt 1), 3954-3964.

[156] Soave, C. L., Guerin, T., Liu, J., Dou, Q. P. Targeting the ubiquitin-proteasome system for cancer treatment: discovering novel inhibitors from nature and drug repurposing. *Cancer Metastasis Rev.* **2017**, *36* (4), 717-736.

[157] Chauhan, D., Hideshima, T., Mitsiades, C., Richardson, P., Anderson, K. C. Proteasome inhibitor therapy in multiple myeloma. *Mol Cancer Ther.* **2005**, *4* (4), 686-692.

[158] Gandolfi, S., Laubach, J. P., Hideshima, T., Chauhan, D., Anderson, K. C., *et al.* The proteasome and proteasome inhibitors in multiple myeloma. *Cancer Metastasis Rev.* **2017**, *36* (4), 561-584.

[159] Miceli, T., Colson, K., Gavino, M., Lilleby, K., Board, I. M. F. N. L. Myelosuppression associated with novel therapies in patients with multiple myeloma:

consensus statement of the IMF Nurse Leadership Board. *Clin J Oncol Nurs.* **2008**, *12* (3 Suppl), 13-20.

[160] Moreau, P., Richardson, P. G., Cavo, M., Orlowski, R. Z., San Miguel, J. F.*, et al.* Proteasome inhibitors in multiple myeloma: 10 years later. *Blood.* **2012**, *120* (5), 947-959.

[161] Breitkreutz, I., Raab, M., Goldschmidt, H. [First-line treatment of multiple myeloma]. *Internist (Berl).* **2019**, *60* (1), 23-33.

[162] Adams, J. The proteasome: structure, function, and role in the cell. *Cancer Treat Rev.* **2003**, *29 Suppl 1*, 3-9.

[163] Lub, S., Maes, K., Menu, E., De Bruyne, E., Vanderkerken, K.*, et al.* Novel strategies to target the ubiquitin proteasome system in multiple myeloma. *Oncotarget.* **2016**, *7* (6), 6521-6537.

[164] Scott, K., Hayden, P. J., Will, A., Wheatley, K., Coyne, I. Bortezomib for the treatment of multiple myeloma. *Cochrane Database Syst Rev.* **2016**, *4*, CD010816.

[165] Nunes, A. T., Annunziata, C. M. Proteasome inhibitors: structure and function. *Semin Oncol.* **2017**, *44* (6), 377-380.

[166] Yukawa, M., Sakon, M., Kambayashi, J., Shiba, E., Kawasaki, T.*, et al.* Proteasome and its novel endogeneous activator in human platelets. *Biochem Biophys Res Commun.* **1991**, *178* (1), 256-262.

[167] Klockenbusch, C., Walsh, G. M., Brown, L. M., Hoffman, M. D., Ignatchenko, V.*, et al.* Global proteome analysis identifies active immunoproteasome subunits in human platelets. *Mol Cell Proteomics.* **2014**, *13* (12), 3308-3319.

[168] Gupta, N., Li, W., Willard, B., Silverstein, R. L., McIntyre, T. M. Proteasome proteolysis supports stimulated platelet function and thrombosis. *Arterioscler Thromb Vasc Biol.* **2014**, *34* (1), 160-168.

[169] Burkhart, J. M., Vaudel, M., Gambaryan, S., Radau, S., Walter, U.*, et al.* The first comprehensive and quantitative analysis of human platelet protein composition allows the comparative analysis of structural and functional pathways. *Blood.* **2012**, *120* (15), e73-82.

[170] Ostrowska, H., Ostrowska, J. K., Worowski, K., Radziwon, P. Human platelet 20S proteasome: inhibition of its chymotrypsin-like activity and identification of the proteasome activator PA28. A preliminary report. *Platelets.* **2003**, *14* (3), 151-157.

[171] Grundler, K., Rotter, R., Tilley, S., Pircher, J., Czermak, T.*, et al.* The proteasome regulates collagen-induced platelet aggregation via nuclear-factor-kappa-B (NFkB) activation. *Thromb Res.* **2016**, *148*, 15-22.

[172] Koessler, J., Etzel, J., Weber, K., Boeck, M., Kobsar, A. Evaluation of dose-dependent effects of the proteasome inhibitor bortezomib in human platelets. *Eur J Pharmacol.* **2016**, *791*, 99-104.

[173] Koessler, J., Schuepferling, A., Klingler, P., Koessler, A., Weber, K., *et al.* The role of proteasome activity for activating and inhibitory signalling in human platelets. *Cell Signal.* **2019**, 109351.

[174] Salem, K., McCormick, M. L., Wendlandt, E., Zhan, F., Goel, A. Copper-zinc superoxide dismutase-mediated redox regulation of bortezomib resistance in multiple myeloma. *Redox Biol.* **2015**, *4*, 23-33.

[175] Nayak, M. K., Kulkarni, P. P., Dash, D. Regulatory role of proteasome in determination of platelet life span. *J Biol Chem.* **2013**, *288* (10), 6826-6834.

[176] Janssen-Cilag International NV: Prescribing information of Velcade. Beerse, Belgium, January 2014.

[177] Klingler, P., Niklaus, M., Koessler, J., Weber, K., Koessler, A., *et al.* Influence of long-term proteasome inhibition on platelet responsiveness mediated by bortezomib. *Vascular Pharmacology.* **2021**, *138*, 106830.

[178] Liu, E. C., Abell, L. M. Development and validation of a platelet calcium flux assay using a fluorescent imaging plate reader. *Anal Biochem.* **2006**, *357* (2), 216-224.

[179] Laemmli, U. K. Cleavage of structural proteins during the assembly of the head of bacteriophage T4. *Nature.* **1970**, *227* (5259), 680-685.

[180] Renart, J., Reiser, J., Stark, G. R. Transfer of proteins from gels to diazobenzyloxymethyl-paper and detection with antisera: a method for studying antibody specificity and antigen structure. *Proc Natl Acad Sci U S A.* **1979**, *76* (7), 3116-3120.

[181] Kyhse-Andersen, J. Electroblotting of multiple gels: a simple apparatus without buffer tank for rapid transfer of proteins from polyacrylamide to nitrocellulose. *J Biochem Biophys Methods.* **1984**, *10* (3-4), 203-209.

[182] Smith, P. K., Krohn, R. I., Hermanson, G. T., Mallia, A. K., Gartner, F. H., *et al.* Measurement of protein using bicinchoninic acid. *Anal Biochem.* **1985**, *150* (1), 76-85.

[183] Engvall, E., Perlmann, P. Enzyme-linked immunosorbent assay (ELISA). Quantitative assay of immunoglobulin G. *Immunochemistry.* **1971**, *8* (9), 871-874.

[184] von dem Borne, A. E., Verheugt, F. W., Oosterhof, F., von Riesz, E., de la Riviere, A. B., *et al.* A simple immunofluorescence test for the detection of platelet antibodies. *Br J Haematol.* **1978**, *39* (2), 195-207.

[185] Ruf, A., Patscheke, H. Flow cytometric detection of activated platelets: comparison of determining shape change, fibrinogen binding, and P-selectin expression. *Semin Thromb Hemost.* **1995**, *21* (2), 146-151.

[186] Mushtaq, A., Kapoor, V., Latif, A., Iftikhar, A., Zahid, U., *et al.* Efficacy and toxicity profile of carfilzomib based regimens for treatment of multiple myeloma: A systematic review. *Crit Rev Oncol Hematol.* **2018**, *125*, 1-11.

[187] Palombella, V. J., Rando, O. J., Goldberg, A. L., Maniatis, T. The ubiquitin-proteasome pathway is required for processing the NF-kappa B1 precursor protein and the activation of NF-kappa B. *Cell.* **1994**, *78* (5), 773-785.

[188] Ichihara, A., Tanaka, K. Roles of proteasomes in cell growth. *Mol Biol Rep.* **1995**, *21* (1), 49-52.

[189] Pagano, M., Tam, S. W., Theodoras, A. M., Beer-Romero, P., Del Sal, G.*, et al.* Role of the ubiquitin-proteasome pathway in regulating abundance of the cyclin-dependent kinase inhibitor p27. *Science.* **1995**, *269* (5224), 682-685.

[190] Dimmeler, S., Breitschopf, K., Haendeler, J., Zeiher, A. M. Dephosphorylation targets Bcl-2 for ubiquitin-dependent degradation: a link between the apoptosome and the proteasome pathway. *J Exp Med.* **1999**, *189* (11), 1815-1822.

[191] Rock, K. L., Goldberg, A. L. Degradation of cell proteins and the generation of MHC class I-presented peptides. *Annu Rev Immunol.* **1999**, *17*, 739-779.

[192] Aberle, H., Bauer, A., Stappert, J., Kispert, A., Kemler, R. beta-catenin is a target for the ubiquitin-proteasome pathway. *EMBO J.* **1997**, *16* (13), 3797-3804.

[193] Avcu, F., Ural, A. U., Cetin, T., Nevruz, O. Effects of bortezomib on platelet aggregation and ATP release in human platelets, in vitro. *Thromb Res.* **2008**, *121* (4), 567-571.

[194] Ghansah, H., Debreceni, I. B., Fejes, Z., Nagy, B., Jr., Kappelmayer, J. The Proteasome Inhibitor Bortezomib Induces Apoptosis and Activation in Gel-Filtered Human Platelets. *Int J Mol Sci.* **2021**, *22* (16).

[195] Nayak, M. K., Kumar, K., Dash, D. Regulation of proteasome activity in activated human platelets. *Cell Calcium.* **2011**, *49* (4), 226-232.

[196] Hochstrasser, M. Ubiquitin and intracellular protein degradation. *Curr Opin Cell Biol.* **1992**, *4* (6), 1024-1031.

[197] Keuren, J. F., Cauwenberghs, S., Heeremans, J., de Kort, W., Heemskerk, J. W.*, et al.* Platelet ADP response deteriorates in synthetic storage media. *Transfusion.* **2006**, *46* (2), 204-212.

[198] Koessler, J., Hermann, S., Weber, K., Koessler, A., Kuhn, S.*, et al.* Role of Purinergic Receptor Expression and Function for Reduced Responsiveness to Adenosine Diphosphate in Washed Human Platelets. *PLoS One.* **2016**, *11* (1), e0147370.

[199] Koessler, J., Weber, K., Koessler, A., Yilmaz, P., Boeck, M.*, et al.* Expression and function of purinergic receptors in platelets from apheresis-derived platelet concentrates. *Blood Transfus.* **2016**, *14* (6), 545-551.

[200] Koessler, J., Schuepferling, A., Klingler, P., Koessler, A., Weber, K.*, et al.* The role of proteasome activity for activating and inhibitory signalling in human platelets. *Cell Signal.* **2019**, *62*, 109351.

[201] Hoylaerts, M. F., Nuyts, K., Peerlinck, K., Deckmyn, H., Vermylen, J. Promotion of binding of von Willebrand factor to platelet glycoprotein Ib by dimers of ristocetin. *Biochem J.* **1995**, *306 (Pt 2)*, 453-463.

[202] Reininger, A. J. Function of von Willebrand factor in haemostasis and thrombosis. *Haemophilia.* **2008**, *14 Suppl 5*, 11-26.

[203] Kanaji, S., Kanaji, T., Furihata, K., Kato, K., Ware, J. L.*, et al.* Convulxin binds to native, human glycoprotein Ib alpha. *J Biol Chem.* **2003**, *278* (41), 39452-39460.

[204] Gardiner, E. E., Arthur, J. F., Kahn, M. L., Berndt, M. C., Andrews, R. K. Regulation of platelet membrane levels of glycoprotein VI by a platelet-derived metalloproteinase. *Blood.* **2004**, *104* (12), 3611-3617.

[205] Unsworth, A. J., Bombik, I., Pinto-Fernandez, A., McGouran, J. F., Konietzny, R.*, et al.* Human Platelet Protein Ubiquitylation and Changes following GPVI Activation. *Thromb Haemost.* **2019**, *119* (1), 104-116.

[206] Bodnar, R. J., Xi, X., Li, Z., Berndt, M. C., Du, X. Regulation of glycoprotein Ib-IX-von Willebrand factor interaction by cAMP-dependent protein kinase-mediated phosphorylation at Ser 166 of glycoprotein Ib(beta). *J Biol Chem.* **2002**, *277* (49), 47080-47087.

[207] Bodnar, R. J., Gu, M., Li, Z., Englund, G. D., Du, X. The cytoplasmic domain of the platelet glycoprotein Ibalpha is phosphorylated at serine 609. *J Biol Chem.* **1999**, *274* (47), 33474-33479.

[208] Perrault, C., Mangin, P., Santer, M., Baas, M. J., Moog, S.*, et al.* Role of the intracellular domains of GPIb in controlling the adhesive properties of the platelet GPIb/V/IX complex. *Blood.* **2003**, *101* (9), 3477-3484.

[209] Simon, Z., Kiss, A., Erdodi, F., Setiadi, H., Beke Debreceni, I.*, et al.* Protein phosphatase inhibitor calyculin-A modulates activation markers in TRAP-stimulated human platelets. *Platelets.* **2010**, *21* (7), 555-562.

[210] Toyoda, H., Nakai, K., Omay, S. B., Shima, H., Nagao, M.*, et al.* Differential association of protein Ser/Thr phosphatase types 1 and 2A with the cytoskeleton upon platelet activation. *Thromb Haemost.* **1996**, *76* (6), 1053-1062.

[211] Wei, Q., Xia, Y. Proteasome inhibition down-regulates endothelial nitric-oxide synthase phosphorylation and function. *J Biol Chem.* **2006**, *281* (31), 21652-21659.

[212] Kumm, E. J., Pagel, O., Gambaryan, S., Walter, U., Zahedi, R. P.*, et al.* The Cell Cycle Checkpoint System MAST(L)-ENSA/ARPP19-PP2A is Targeted by cAMP/PKA and cGMP/PKG in Anucleate Human Platelets. *Cells.* **2020**, *9* (2).

[213] Kors, S., Geijtenbeek, K., Reits, E., Schipper-Krom, S. Regulation of Proteasome Activity by (Post-)transcriptional Mechanisms. *Front Mol Biosci.* **2019**, *6*, 48.

[214] Gambaryan, S., Kobsar, A., Rukoyatkina, N., Herterich, S., Geiger, J.*, et al.* Thrombin and collagen induce a feedback inhibitory signaling pathway in platelets

involving dissociation of the catalytic subunit of protein kinase A from an NFkappaB-IkappaB complex. *J Biol Chem.* **2010**, *285* (24), 18352-18363.

[215] Shattil, S. J., Hoxie, J. A., Cunningham, M., Brass, L. F. Changes in the platelet membrane glycoprotein IIb.IIIa complex during platelet activation. *J Biol Chem.* **1985**, *260* (20), 11107-11114.

[216] Aszodi, A., Pfeifer, A., Ahmad, M., Glauner, M., Zhou, X. H.*, et al.* The vasodilator-stimulated phosphoprotein (VASP) is involved in cGMP- and cAMP-mediated inhibition of agonist-induced platelet aggregation, but is dispensable for smooth muscle function. *EMBO J.* **1999**, *18* (1), 37-48.

[217] Massberg, S., Gruner, S., Konrad, I., Garcia Arguinzonis, M. I., Eigenthaler, M.*, et al.* Enhanced in vivo platelet adhesion in vasodilator-stimulated phosphoprotein (VASP)-deficient mice. *Blood.* **2004**, *103* (1), 136-142.

[218] Reinhard, M., Jarchau, T., Walter, U. Actin-based motility: stop and go with Ena/VASP proteins. *Trends Biochem Sci.* **2001**, *26* (4), 243-249.

[219] Kobsar, A., Klinker, E., Kuhn, S., Koessler, A., Yilmaz, P.*, et al.* Increasing susceptibility of nitric oxide-mediated inhibitory platelet signaling during storage of apheresis-derived platelet concentrates. *Transfusion.* **2014**, *54* (7), 1782-1789.

[220] Gachet, C. P2 receptors, platelet function and pharmacological implications. *Thromb Haemost.* **2008**, *99* (3), 466-472.

[221] Koessler, J., Trulley, V. N., Bosch, A., Weber, K., Koessler, A.*, et al.* The role of agonist-induced activation and inhibition for the regulation of purinergic receptor expression in human platelets. *Thromb Res.* **2018**, *168*, 40-46.

[222] Erhardt, J. A., Pillarisetti, K., Toomey, J. R. Potentiation of platelet activation through the stimulation of P2X1 receptors. *J Thromb Haemost.* **2003**, *1* (12), 2626-2635.

[223] Rolf, M. G., Mahaut-Smith, M. P. Effects of enhanced P2X1 receptor Ca2+ influx on functional responses in human platelets. *Thromb Haemost.* **2002**, *88* (3), 495-502.

[224] Dorsam, R. T., Kim, S., Jin, J., Kunapuli, S. P. Coordinated signaling through both G12/13 and G(i) pathways is sufficient to activate GPIIb/IIIa in human platelets. *J Biol Chem.* **2002**, *277* (49), 47588-47595.

[225] Nieswandt, B., Schulte, V., Zywietz, A., Gratacap, M. P., Offermanns, S. Costimulation of Gi- and G12/G13-mediated signaling pathways induces integrin alpha IIbbeta 3 activation in platelets. *J Biol Chem.* **2002**, *277* (42), 39493-39498.

[226] Dimopoulos, M. A., Moreau, P., Palumbo, A., Joshua, D., Pour, L.*, et al.* Carfilzomib and dexamethasone versus bortezomib and dexamethasone for patients with relapsed or refractory multiple myeloma (ENDEAVOR): a randomised, phase 3, open-label, multicentre study. *The Lancet Oncology.* **2016**, *17* (1), 27-38.

[227] Demo, S. D., Kirk, C. J., Aujay, M. A., Buchholz, T. J., Dajee, M.*, et al.* Antitumor activity of PR-171, a novel irreversible inhibitor of the proteasome. *Cancer Res.* **2007**, *67* (13), 6383-6391.

[228] Rother, R. P., Bell, L., Hillmen, P., Gladwin, M. T. The clinical sequelae of intravascular hemolysis and extracellular plasma hemoglobin: a novel mechanism of human disease. *JAMA.* **2005**, *293* (13), 1653-1662.

[229] Douglas, J. C., Avari, T., Carrington, R. L., Platelet Function Testing by Aggregometry; Approved Guideline, 1st ed. 2008, p 56.

[230] van der Meer, P. F., Klei, T. R., de Korte, D. Quality of Platelets in Stored Whole Blood. *Transfus Med Rev.* **2020**, *34* (4), 234-241.

[231] Kobsar, A., Putz, E., Yilmaz, P., Weinig, E., Boeck, M.*, et al.* Decreasing phosphodiesterase 5A activity contributes to platelet cGMP accumulation during storage of apheresis-derived platelet concentrates. *Transfusion.* **2014**, *54* (4), 1008-1014.

[232] Nolte, C., Eigenthaler, M., Horstrup, K., Honig-Liedl, P., Walter, U. Synergistic phosphorylation of the focal adhesion-associated vasodilator-stimulated phosphoprotein in intact human platelets in response to cGMP- and cAMP-elevating platelet inhibitors. *Biochem Pharmacol.* **1994**, *48* (8), 1569-1575.

[233] Zangari, M., Guerrero, J., Cavallo, F., Prasad, H. K., Esseltine, D.*, et al.* Hemostatic effects of bortezomib treatment in patients with relapsed or refractory multiple myeloma. *Haematologica.* **2008**, *93* (6), 953-954.

[234] Rupa-Matysek, J., Gil, L., Wojtasinska, E., Nowicki, A., Dytfeld, D.*, et al.* Inhibitory effects of bortezomib on platelet aggregation in patients with multiple myeloma. *Thromb Res.* **2014**, *134* (2), 404-411.

[235] Shi, D. S., Smith, M. C., Campbell, R. A., Zimmerman, P. W., Franks, Z. B.*, et al.* Proteasome function is required for platelet production. *J Clin Invest.* **2014**, *124* (9), 3757-3766.

[236] Nguyen, M. N., Nayernama, A., Jones, S. C., Kanapuru, B., Gormley, N.*, et al.* Proteasome inhibitor-associated thrombotic microangiopathy: A review of cases reported to the FDA adverse event reporting system and published in the literature. *Am J Hematol.* **2020**, *95* (9), E218-E222.

[237] Hassan, S. A., Palaskas, N., Kim, P., Iliescu, C., Lopez-Mattei, J.*, et al.* Chemotherapeutic Agents and the Risk of Ischemia and Arterial Thrombosis. *Curr Atheroscler Rep.* **2018**, *20* (2), 10.

[238] Ng, M. S. Y., Tung, J. P., Fraser, J. F. Platelet Storage Lesions: What More Do We Know Now? *Transfus Med Rev.* **2018**.

[239] Colberg, L., Cammann, C., Wesche, J., Topfstedt, E., Seifert, U.*, et al.* The platelet proteasome and immunoproteasome are stable in buffy-coat derived platelet concentrates for up to 7 days. *Transfusion.* **2021**.

[240] Russo, G. L., Stampone, E., Cervellera, C., Borriello, A. Regulation of p27(Kip1) and p57(Kip2) Functions by Natural Polyphenols. *Biomolecules.* **2020**, *10* (9).

[241] Horii, K., Brooks, M. T., Herr, A. B. Convulxin forms a dimer in solution and can bind eight copies of glycoprotein VI: implications for platelet activation. *Biochemistry.* **2009**, *48* (13), 2907-2914.

[242] Borst, O., Gawaz, M. Glycoprotein VI - novel target in antiplatelet medication. *Pharmacol Ther.* **2021**, *217*, 107630.

[243] Wu, Y., Suzuki-Inoue, K., Satoh, K., Asazuma, N., Yatomi, Y.*, et al.* Role of Fc receptor gamma-chain in platelet glycoprotein Ib-mediated signaling. *Blood.* **2001**, *97* (12), 3836-3845.

[244] Manasanch, E. E., Orlowski, R. Z. Proteasome inhibitors in cancer therapy. *Nat Rev Clin Oncol.* **2017**, *14* (7), 417-433.

[245] Di, K., Lloyd, G. K., Abraham, V., MacLaren, A., Burrows, F. J.*, et al.* Marizomib activity as a single agent in malignant gliomas: ability to cross the blood-brain barrier. *Neuro Oncol.* **2016**, *18* (6), 840-848.

[246] Spinelli, S. L., Casey, A. E., Pollock, S. J., Gertz, J. M., McMillan, D. H.*, et al.* Platelets and megakaryocytes contain functional nuclear factor-kappaB. *Arterioscler Thromb Vasc Biol.* **2010**, *30* (3), 591-598.

7. Appendix

7.1. List of figures

7.2. List of tables

8. Abbreviations

° C	Degree Celsius
AC	Adenylyl cyclase
ADP	Adenosine diphosphate
Akt	Proteinkinase B
APS	Ammonium persulfate
ASS	Acetylsalicylic acid
ATP	Adenosine triphosphate
AU	Arbitrary unit
BCA	Bicinchoninic acid
BSA	Bovine serum albumin
Ca^{2+}	Calcium
$CaCl_2$	Calcium chloride
cAMP	Cyclic adenosine monophosphate
CD	Cluster of differentiation
cGMP	Cyclic guanosine monophosphate
citrate	Tri-Sodium citrate dihydrate
C-L	Caspase-like activity
CT-L	Chymotrypsin-like activity
Ctrl	Control
DAG	Diacylglycerol
DEA/NO	2-(N,N-Diethylamino)-diazenolate-2-oxide diethylammonium salt
dH_2O	Distilled water
DMSO	Dimethyl sulfoxide
DNA	Deoxyribonucleic acid
E1	Ubiquitin-activating enzyme
E2	Ubiquitin-conjugating enzyme
E3	Ubiquitin ligase
EDTA	Ethylenediamine tetraacetic acid

e.g.	*exempli gratia*
EGTA	Ethyleneglycol tetraacetic acid
ELISA	Enzyme-linked immunosorbent assay
EP receptor	Prostaglandin receptor
et al.	*et alia*
FA	Formaldehyde
FcRγ	Fc receptor γ-chain
FITC	Fluorescein isothiocyanate
GP	Glycoprotein
GPCR(s)	G protein-coupled receptor(s)
h	hour
HBSS	Hanks' Balanced Salt Solution
HCl	Hydrochloric acid
HEPES	4-(2-hydroxyethyl)-1-piperazineethanesulfonic acid
Ig	Immunoglobulin
IP_3	Inositol 1,4,5-trisphosphate
KCl	Potassium chloride
kDa	Kilodalton
MFI	Mean fluorescence intensity
MFIc	corrected mean fluorescence intensity
$MgCl_2$	Magnesium chloride
min	minute
MK(s)	Megakaryocyte(s)
mRNA	messenger RNA
NaCl	Sodium chloride
NaOH	Sodium hydroxide
NF-κB	nuclear factor kappa-light-chain-enhancer of activated B cells
NO	Nitric oxide
NOS	nitric oxide synthase
PAGE	Polyacrylamide gelelectrophoresis

PAR	Protease-activated receptor
PBS	Phosphate-buffered saline
PE	Phycoerythrin
PGE_1	Prostaglandin E_1
PI3K	Phosphoinositide 3-kinase
PIP_2	Phosphatidylinositol 4,5-bisphsphate
PIP_3	Phosphatidylinositol 3,4,5-trisphosphate
PKA	Proteinkinase A
PKC	Proteinkinase C
PKG	Proteinkinase G
PLC	Phospholipase C
PP	Polypropylene
PP2A	Protein phosphatase 2A
PPP	Platelet-poor plasma
PRI	Platelet reactivity index
PRP	Platelet-rich plasma
RFU	Relative fluorescence unit
ROCK	Rho-Kinase
Rpm	Revolutions per minute
Rpn	Regulatory particle non-ATPase
Rpt	regulatory particle triple A
RT	Room temperature
s	Second
SDS	Sodium dodecyl sulfate
SFK	Src family tyrosine kinase
sGC	Soluble guanylyl cyclase
TBS	TRIS-buffered saline
TBS-T	TRIS-buffered saline with Tween 20
TEMED	Tetramethylethylenediamine
T-L	Trypsin-like activity

TLR	Toll-like receptor
TRAP-6	Thrombin receptor-activating peptide 6
TRIS	Tris(hydroxymethyl)aminomethane
TRITC	Tetramethylrhodamine thiocyanate
TxA_2	Thromboxane A_2
Tyrode’s buffer	Tyrode’s Salt Solution
U	Unit
Ub	Ubiquitin
UPS	Ubiquitin-proteasome system
VASP	Vasodilator-stimulated phosphoprotein
vWF	Von Willebrand factor
WB	Whole blood
WP	Washed platelets

9. Affidavit

I hereby confirm that my thesis entitled "**Exploration of proteasome interactions with human platelet function**" is the result of my own work. I did not receive any help or support from commercial consultants. All sources and / or materials applied are listed and specified in the thesis.

Furthermore, I confirm that this thesis has not yet been submitted as part of another examination process neither in identical nor in similar form.

Place, Date Signature

10. Eidesstattliche Erklärung

Hiermit erkläre ich an Eides statt, die Dissertation „**Untersuchung von Proteasom-Wechselwirkungen mit der Funktion humaner Thrombozyten**" eigenständig, d.h. insbesondere selbständig und ohne Hilfe eines kommerziellen Promotionsberaters, angefertigt und keine anderen als die von mir angegebenen Quellen und Hilfsmittel verwendet zu haben.

Ich erkläre außerdem, dass die Dissertation weder in gleicher noch in ähnlicher Form bereits in einem anderen Prüfungsverfahren vorgelegen hat.

Ort, Datum Unterschrift

11. Publications

Klingler, P., Niklaus, M., Koessler, J., Weber, K., Koessler, A., Boeck, M., Kobsar, A. Influence of long-term proteasome inhibition on platelet responsiveness mediated by bortezomib. *Vascular Pharmacology*. **2021**, 138, 106830.

Schossee, N., Veit, G., Gittel, J., Viebahn, J., Niklaus, M., **Klingler, P.**, Uceyler, N., Klinker, E., Kobsar, A., Boeck, M., Koessler, J. Profile of the single-use, multiple-pass protein A adsorber column in immunoadsorption. *Vox Sanguinis*. **2021**, 117 (3). 393-398.

Koessler, J., **Klingler, P.**, Niklaus, M., Weber, K., Koessler, A., Boeck, M., Kobsar, A. The Impact of Cold Storage on Adenosine Diphosphate-Mediated Platelet Responsiveness. *TH Open.* **2020**, 4 (3), e163-e172.

Niklaus, M., **Klingler, P.**, Weber, K., Koessler, A., Boeck, M., Kobsar, A., Koessler, J. The involvement of toll-like receptors 2 and 4 in human platelet signalling pathways. *Cell Signal.* **2020**, 76, 109817.

Koessler, J., Schuepferling, A., **Klingler, P.**, Koessler, A., Weber, K., Boeck, M., Kobsar, A. The role of proteasome activity for activating and inhibitory signalling in human platelets. *Cell Signal*. **2019**, 62, 109351.

12. Curriculum vitae

13. Acknowledgement

I would like to thank all people, who were helping and supporting me during the preparation of this thesis (August 2018 – April 2022):

Prof. Dr. Markus Böck for giving me the great opportunity to draw up my PhD thesis at the Institute of Clinical Transfusion Medicine and Haemotherapy at the University Hospital of Würzburg.

Dr. Anna Kobsar for introducing and teaching me so many techniques to investigate human platelets with her outstanding knowledge and experience, for permanent mentoring in the lab, practical advice, solving problems, statistical review of my results and supervision of my entire doctoral process.

PD Dr. Jürgen Kößler for his untiring commitment for my colleague Marius and me, for medical expertise, many valuable discussions, suggestions and encouragements during the whole time of thesis preparation.

My colleague Marius Niklaus for the continuously exchange of experience, ideas, suggestions for improvement and methodical discussion, which made it all easier not to be alone with challenges or problems.

Katja Weber for her technical assistance and contribution of experimental expertise and the very nice time in our office.

Prof. Dr. Alexander Buchberger and Dr. Ingolf Berberich, who agreed to be part of my thesis committee, giving a lot of differentiated suggestions for the improvement of my experimental designs during our committee meetings.

The whole team of the Institute of Clinical Transfusion Medicine and Haemotherapy for the permanent support, especially the blood donation team as well as the team of physicians for always providing enough blood for our investigations. As well, thanks to all blood donors at our institute for their consent in using donated blood for my scientific purposes.

Frau Dagmar Ganz for the excellent management of almost every organizational task.

All proofreaders, especially Simon, for their time and suggestions for improvement.

My family, my mother, father and my sister and all my friends for their continuous support. Finally and most importantly, I want to give the biggest thank to my wonderful wife Silvana for her constant emotional support and encouragement and for our wonderful daughter.